

THE INTERSECTION OF FRAMEWORK GEOLOGY AND MINERAL POTENTIAL ASSESSMENT IN THE GOLD HILL MINING DISTRICT, UTAH

by Stephanie E. Mills



SPECIAL STUDY 175
UTAH GEOLOGICAL SURVEY
UTAH DEPARTMENT OF NATURAL RESOURCES
2025

Blank pages are intentional for printing purposes.

THE INTERSECTION OF FRAMEWORK GEOLOGY AND MINERAL POTENTIAL ASSESSMENT IN THE GOLD HILL MINING DISTRICT, UTAH

by
Stephanie E. Mills

Cover photo: UGS geologist looking north across the Gold Hill district towards Dutch Mountain.

Suggested citation:

Mills, S.E., 2025, The intersection of framework geology and mineral potential assessment in the Gold Hill mining district:
Utah Geological Survey Special Study 175, 54 p., 4 appendices, <https://doi.org/10.34191/SS-175>.



SPECIAL STUDY 175
UTAH GEOLOGICAL SURVEY
UTAH DEPARTMENT OF NATURAL RESOURCES
2025

STATE OF UTAH
Spencer J. Cox, Governor

DEPARTMENT OF NATURAL RESOURCES
Joel Ferry, Executive Director

UTAH GEOLOGICAL SURVEY
Darlene Batatian

PUBLICATIONS

contact

Natural Resources Map & Bookstore
1594 W. North Temple
Salt Lake City, UT 84116
telephone: 801-537-3320
toll-free: 1-888-UTAH MAP
website: utahmapstore.com
email: geostore@utah.gov

UTAH GEOLOGICAL SURVEY

contact

1594 W. North Temple, Suite 3110
Salt Lake City, UT 84116
telephone: 801-537-3300
website: geology.utah.gov

The Utah Department of Natural Resources, Utah Geological Survey, makes no warranty, expressed or implied, regarding the suitability of this product for a particular use, and does not guarantee accuracy or completeness of the data. The Utah Department of Natural Resources, Utah Geological Survey, shall not be liable under any circumstances for any direct, indirect, special, incidental, or consequential damages with respect to claims by users of this product.

CONTENTS

ABSTRACT.....	1
INTRODUCTION	1
Purpose and Scope.....	1
Mining History.....	2
Geological Setting	5
Overview	5
Development of the Gold Hill District.....	7
Mineralization in the Gold Hill District	13
METHODOLOGY.....	14
Literature Compilation and Field Observations	14
Geochemistry.....	14
Geophysics.....	15
RESULTS AND DISCUSSION.....	15
District Development.....	15
Jurassic Pluton Emplacement.....	15
Ferguson Detachment and Chainman Shale.....	17
Clifton Flat and the Gold Hill Wash Fault.....	18
Mineral Systems and Critical Mineral Potential.....	20
Skarns and Replacement Deposits	21
Skarn deposits	21
Replacement deposits.....	25
The Reaper group of deposits	26
Critical mineral potential	27
Vein Deposits.....	27
Polymetallic veins.....	27
Clifton vein swarm.....	29
Critical mineral potential	31
Low-Sulfidation Epithermal Deposits	32
Sediment-Hosted Gold Deposits	34
Iron-Oxide Copper Gold (IOCG) Deposits.....	36
Porphyry Molybdenum Deposits	38
Porphyry Copper Deposits	40
Supergene Processes.....	42
Exploration Considerations and Future Work.....	44
Research Questions	44
Exploration Considerations.....	44
SUMMARY AND CONCLUSIONS.....	45
ACKNOWLEDGMENTS	46
REFERENCES	47
APPENDICES	55
APPENDIX A—Historical Drilling Compilation	56
APPENDIX B—Surface Geochemistry	57
APPENDIX C—Drillhole Geochemistry.....	58
APPENDIX D—Geophysics Data	59

FIGURES

Figure 1. Regional overview of the Gold Hill district in northern Utah relevant to other important mining districts and the Uinta-Cortez Axis	2
Figure 2. Overview of notable mines and exploration areas in the Gold Hill district.....	6
Figure 3. Stratigraphic column of major Paleozoic bedrock units and intrusive units in the Gold Hill mining district.....	8
Figure 4. Geologic map and major geologic features of the Gold Hill mining district.....	9
Figure 5. Summary of geochronology locations for samples in Table 4	11

Figure 6. Whole-rock geochemistry of the Jurassic quartz monzonite and Eocene granite.....	12
Figure 7. Deformation in Paleozoic carbonates near the contact with the Jurassic pluton.....	16
Figure 8. Geophysical magnetic signature of the Jurassic pluton.....	17
Figure 9. Examples of bleaching in the Ochre Mountain and Ely Limestones	19
Figure 10. Total field reduced to pole (RTP) magnetic signature of Clifton Flat	20
Figure 11. Deposit type classification of historically producing mines and prospects in the Gold Hill district.....	22
Figure 12. Magnetite chemistry and alteration examples from Lucy L (LL) exoskarn and Yellow Hammer (YH) endoskarn deposits	23
Figure 13. Molybdenum concentration variation of zoned scheelite related to changes in cathodoluminescence (CL) response	23
Figure 14. Example of outcrop and alteration from W-bearing skarn around the Eocene granite	24
Figure 15. Ore minerals from the Gold Hill and U.S. mines.....	25
Figure 16. Large crystals from the Reaper mine.....	27
Figure 17. Examples of polymetallic veins in the Gold Hill district.....	28
Figure 18. Vein swarm size comparison at the same scale between the Clifton vein swarm at Gold Hill and the polymetallic veins at Bingham Canyon mine	30
Figure 19. Oxidized ore in veins from the Clifton vein swarm	31
Figure 20. Mapped extents and historical drilling of the low-sulfidation epithermal system.....	33
Figure 21. Textures from the low-sulfidation epithermal system	34
Figure 22. Au, Ag, and Be geochemistry from surface and drill hole samples around the Kiewit mine.....	35
Figure 23. Examples of jasperoid and silicification textures	36
Figure 24. Outcrop and handsample photos of IOCG-style alteration and mineralization	37
Figure 25. Map of the Goshute dike swarm and examples of dike textures.....	39
Figure 26. Examples of supergene oxidation at the Yellow Hammer mine.....	43

TABLES

Table 1. Gold Hill district annual production	3
Table 2. Select ore production by mine for the Gold Hill district.....	4
Table 3. Summary of significant exploration activity in the Gold Hill district, 1960s to present	5
Table 4. Summary of geochronological data in the Gold Hill district.....	10

THE INTERSECTION OF FRAMEWORK GEOLOGY AND MINERAL POTENTIAL ASSESSMENT IN THE GOLD HILL MINING DISTRICT, UTAH

by Stephanie E. Mills

ABSTRACT

The Gold Hill mining district (western Tooele County, Utah) was active from the late 1800s to the mid-1900s and is Utah's leading historical producer of tungsten and arsenic. The district was also a past producer of other base and precious metals such as lead and silver. In the modern era of intense focus on domestic sources for critical minerals, the historical tungsten and arsenic production in Gold Hill stimulated renewed research interest in this district. The multi-generational geological history of the district includes Cordilleran hinterland Paleozoic bedrock of carbonate shelf to basinal facies that underwent Jurassic contractional deformation and was subsequently dismembered through extensional deformation during the Cenozoic. Two large pulses of magmatism are recognized in the district: a Jurassic quartz monzonite pluton and an Eocene granite stock. Three distinct metallogenic events have been defined: (1) Jurassic skarn, replacement, and vein deposits associated with pluton emplacement; (2) Eocene skarn and vein deposits associated with stock emplacement; and (3) Miocene low-sulfidation epithermal deposits. Many other deposit types, such as sediment-hosted gold, have also been exploration targets within the district.

This study utilizes new field observations and new geochemical data supplemented by historical exploration documents plus geochemical and geophysical data from previous minerals exploration. A modern mineral system framework is applied to understand the interaction between the geological history of the district and the complex multi-generational mineralization.

Three main features of the framework geology were identified as highly relevant to the mineralization history and needing further research: emplacement of the Jurassic pluton, the Ferguson detachment fault, and development of Clifton Flat and the Gold Hill Wash fault. A re-evaluation of current thinking around the emplacement and crystallization of the Jurassic pluton calls into question the presumed Jurassic timing and provenance of the Clifton vein swarm, which historical exploration mapping shows to be a significant feature on par with the spatial extent of polymetallic veining at the Bingham Canyon porphyry deposit. The extent and metal endowment of the vein swarm suggests a connection with a deeper, unidentified magmatic-hydrothermal source, rather than the Jurassic pluton. The impact of the Ferguson detachment fault in Gold Hill has only recently been considered but has major

implications for disconnecting deep mineralization sources from shallow mineralization vectors, such as veining and alteration. The Clifton Flat basin to the west of the Clifton vein swarm has never been a target for minerals exploration, despite the prolific exploration history in the district, and may represent a covered target for a magmatic-hydrothermal system related to the Clifton vein swarm. Further investigation of all these features and the potential for a buried magmatic-hydrothermal system, particularly a porphyry copper system, is recommended.

INTRODUCTION

Purpose and Scope

The Gold Hill mining district is one of Utah's oldest and most diverse mining districts, located in western Tooele County north of the Deep Creek Range (Figure 1). The Gold Hill district is Utah's largest historical producer of both tungsten and arsenic, as well as a notable producer of lead, copper, gold, silver, and zinc. In addition to the overall historical production, Gold Hill is the most recent producer of tungsten in the United States (U.S. Geological Survey, 2017) due to a brief restart of artisanal mining at the Fraction mine in 2016. Although the production was short-lived and minor, it highlighted the remaining potential for mineralization in the district, and particularly the potential for critical minerals. Critical minerals are defined as non-fuel mineral commodities that are necessary to a country's economic or national security but that have vulnerabilities in the supply chain (Day, 2019). The increasing reliance of modern economies on mineral-intensive technologies in recent years has highlighted the importance of secure mineral supply chains and put emphasis on potential domestic production. As a result, the Gold Hill district was selected by the U.S. Geological Survey Earth Mapping Resources Initiative (EMRI) program for updated geological mapping and an assessment of the critical mineral potential in the district. A new map of the 7.5' Clifton quadrangle (Mills et al., 2023) covering the southern half of the district as well as a digital reproduction (GIS) of the Gold Hill 7.5' quadrangle covering the northern half of the district (Robinson, 2023) were undertaken to update the geologic mapping, and this report provides the assessment of critical mineral potential.

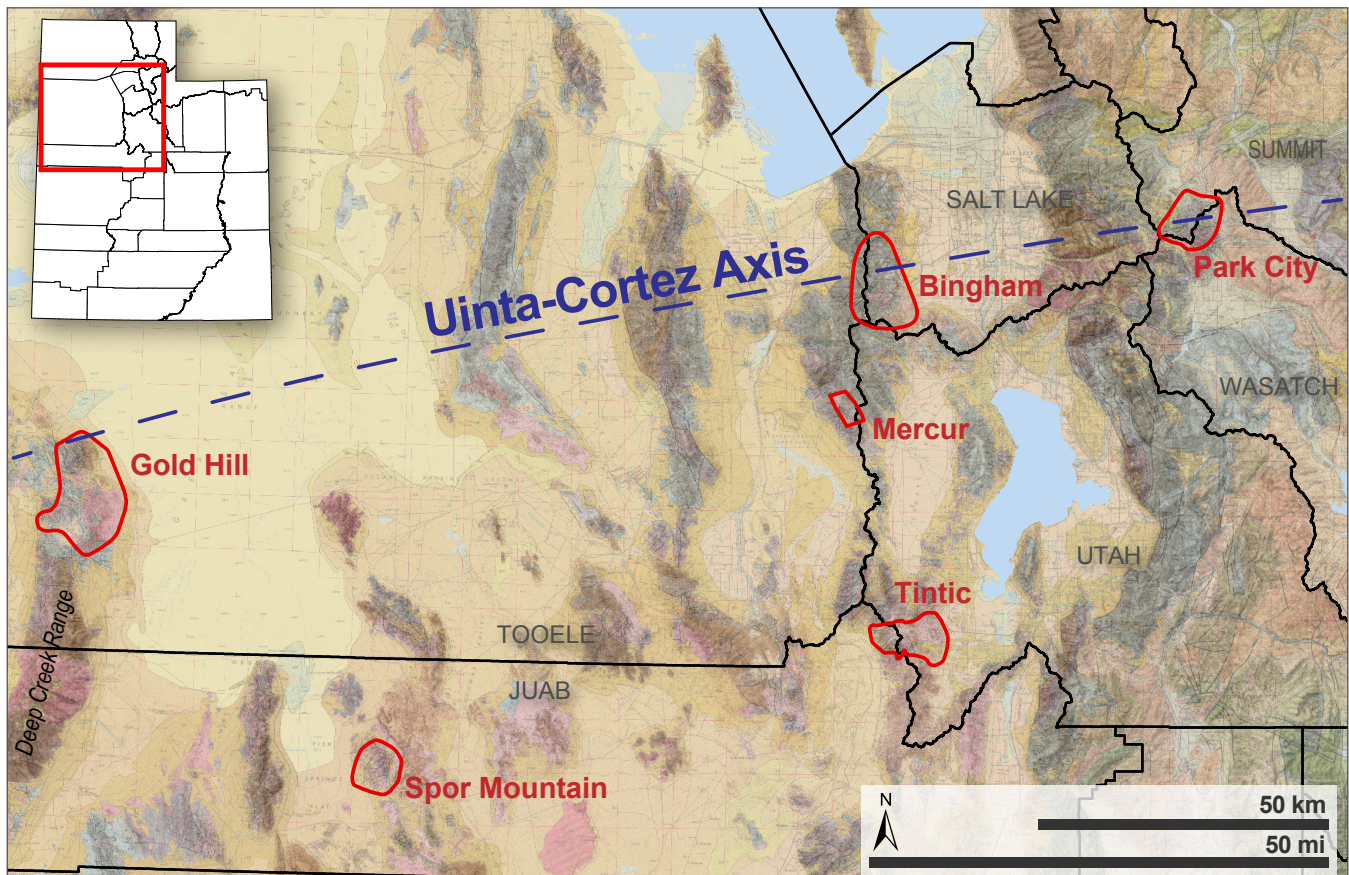


Figure 1. Regional overview of the Gold Hill district in northern Utah relevant to other important mining districts (red outlines) and the Uinta-Cortez Axis. Geologic basemap from Stokes et al. (1961–63).

The primary goals of this study were to build on the geologic mapping by identifying what aspects of the district's framework geology are particularly relevant for the development of economic mineral deposits, how the updated geological framework informs a modern interpretation of the known mineral deposits in the district, and any potential for new mineral systems that may not have been identified in previous exploration or mining. To accomplish these goals, geological mapping and field observations were supplemented with existing and new soil and rock chip geochemistry, airborne magnetic geophysics, and a robust review of historical exploration, mining data, and reports. Preliminary observations about district-scale geological controls on ore-forming processes were included in Mills et al. (2023); however, those observations are superseded by this report, which contains a more detailed evaluation of how the evolving geological history of the Gold Hill district impacted various stages of metallogeny.

Mining History

The first reported mineral discovery in the Gold Hill district was of gold in 1858, one of the earliest discoveries in Utah (Krahulec, 2017), and the district was organized as the Clifton (Gold Hill) district in 1867. Despite minor exploration and development over the following decades, it was not until the early 1900s that the district was developed in earnest. Develop-

ment resulted in a railroad line to the Gold Hill townsite that allowed a significant increase in production and for the district to become known more generally as Gold Hill. Early mining focused on gold, silver, lead and copper, whereas arsenic became the main economic driver from 1924 to 1925 and 1943 to 1945 due to wartime demand (Table 1). Zinc, bismuth, and tungsten were produced sporadically (El-Shatoury and Whelan, 1970; Krahulec, 2017), and production of several other commodities including molybdenum, antimony, vanadium, fluorite, beryllium, tin, and cobalt have been reported (Lee, 2004; Krahulec, 2017), though no reliable production records for these commodities could be located. Despite the sporadic production of tungsten, typically regarded as a byproduct of gold and copper mining, Gold Hill is Utah's largest tungsten producing district (Krahulec, 2018). Tungsten was produced starting in 1912 from Lucy L mine, and significant tungsten production came from Reaper, Yellow Hammer, and Fraction (Timm) mines among others (Table 2). Historical mining in Gold Hill decreased substantially after WWII and ended completely in 1958. Despite having over 200 recognized mines and prospects, by far the most mineral occurrences of any mining district in Utah, Gold Hill ranks as Utah's 28th most productive mining district (Krahulec, 2018).

Modern minerals exploration in the district was intermittent from the 1960s to the early 2000s and mainly focused on gold

Table 1. Gold Hill district annual production. The annual production of tungsten is not available. Modified from Krahulec (2017).

Year	Ore Tons	Gold (oz)	Silver (oz)	Copper (lbs)	Lead (lbs)	Zinc (lbs)	Arsenic (lbs) ^e	Value ¹	Reference
1871 ^e	7	-	-	-	5400	-	-	5022	Nolan (1935)
1872 ^e	68	-	2790	-	54,000	-	-	\$122,760	Nolan (1935)
1873–1891	-	-	-	-	-	-	-	\$-	
1892–1895	19,000	9772	-	-	-	-	-	\$24,430,000	Nolan (1935)
1896-1900	-	-	-	-	-	-	-	\$-	
1901	18	-	68	-	666	-	-	2387	Nolan (1935)
1902	651	482	641	-	6000	-	-	\$1,227,246	Nolan (1935)
1903	-	-	-	-	-	-	-	\$-	
1904	1660	969	92	-	-	-	-	\$2,424,892	Nolan (1935)
1905–1913	-	-	-	-	-	-	-	\$-	
1914	66	57	146	5054	-	-	-	\$166,512	Nolan (1935)
1915	16	5	149	1470	1924	-	-	\$24,043	Nolan (1935)
1916	67	9	645	10,547	4782	-	-	\$85,905	Nolan (1935)
1917	33,960	564	161,204	1,894,731	513,929	-	-	\$13,658,182	Nolan (1935)
1918	19,714	450	97,241	828,658	1,204,472	-	-	\$8,088,057	Nolan (1935)
1919	14,257	234	53,706	194,476	778,869	-	-	\$3,483,608	Nolan (1935)
1920	39,656	77	89,578	92,913	1,010,833	-	-	\$3,833,255	Nolan (1935)
1921	11,627	266	23,208	3194	336,292	-	-	\$1,593,936	Nolan (1935)
1922	211	279	2974	4521	16,524	-	-	\$808,275	Nolan (1935)
1923	13,237	861	41,195	33,040	291,554	-	-	\$3,626,875	Nolan (1935)
1924 ^e	66,094	511	147,786	3615	1,840,453	-	16,576,000	\$39,998,017	Nolan, 1935; USBM ²
1925 ^e	16,721	809	111,372	54,459	1,960,853	-	1,424,000	\$9,807,601	Nolan, 1935; USBM ²
1926	1382	1129	13,772	13,826	267,083	2243	-	\$3,487,179	Nolan (1935)
1927	526	926	4413	2396	53,701	14,754	-	\$2,508,444	Nolan (1935)
1928	195	3	1578	2995	50,233	-	-	\$107,225	Nolan (1935)
1929	415	480	1229	40,001	1237	-	-	\$1,393,108	Nolan (1935)
1930	1009	78	3704	47,885	280,480	-	-	\$743,690	Nolan (1935)
1931	2259	1142	2384	22,046	458,723	-	-	\$3,431,780	Nolan (1935)
1932	2915	2361	1207	6473	174,084	-	-	\$6,121,672	Nolan (1935)
1933	3249	2023	10,199	14,714	213,959	-	-	\$5,580,512	Nolan (1935)
1934	2609	458	7747	23,625	297,486	-	-	\$1,717,584	Perry and McCarthy (1977)
1935–1936	2114	343	9215	30,848	215,391	-	-	\$1,420,796	Perry and McCarthy (1977)
1937	1348	235	5382	43,000	78,000	-	-	\$971,972	Perry and McCarthy (1977)
1938	659	207	7210	3816	89,370	-	-	\$803,338	Perry and McCarthy (1977)
1939	186	128	2092	1029	17,596	-	-	\$394,872	Perry and McCarthy (1977)
1940	15	1	142	-	9220	-	-	\$14,767	Perry and McCarthy (1977)
1941	16	1	308	3100	300	-	-	\$23,187	Perry and McCarthy (1977)
1942	8	4	59	-	2400	-	-	\$13,766	Perry and McCarthy (1977)
1943 ^e	15,363	-	3292	600	29,800	-	4,159,660	\$8,435,026	USBM ²
1944 ^e	87,835	241	7349	10,800	43,500	-	22,693,940	\$46,265,109	USBM ²
1945 ^e	24,000	-	-	-	-	-	7,092,330	\$14,184,660	USBM ²
1946	28	-	208	1500	2000	-	-	\$13,268	Perry and McCarthy (1977)
1947	518	12	1147	2700	143,300	6800	-	\$212,731	Perry and McCarthy (1977)
1948	310	10	674	800	72,300	5000	-	\$119,463	Perry and McCarthy (1977)
1949	4	-	42	-	600	100	-	1780	Perry and McCarthy (1977)
1950	175	31	1696	15,500	11,800	-	-	\$194,570	Perry and McCarthy (1977)
1951	128	3	1022	9400	8000	-	-	\$79,112	Perry and McCarthy (1977)
1952–1953	-	-	-	-	-	-	-	\$-	
1954	9	1	61	-	1700	-	-	5667	Perry and McCarthy (1977)
1955	25	1	168	3200	3000	200	-	\$22,718	Perry and McCarthy (1977)
1955–1956	156	31	-	51,900	-	-	-	\$285,100	UGS Files
1956	101	6	1036	4500	16,800	200	-	\$75,820	Perry and McCarthy (1977)
1957	3938	44	2514	30,200	87,500	362,100	-	\$848,269	Perry and McCarthy (1977)
1957–1958	158	-	-	11,100	-	-	-	\$44,400	UGS Files
1959–2009	-	-	-	-	-	-	-	\$-	
2010 ^e	4,000	64	1500	30,000	-	-	-	\$319,000	UGS Files
2011 ^e	14,000	225	5255	105,100	-	-	-	\$1,119,530	UGS Files
2012–2013	-	-	-	-	-	-	-	\$-	
2014 ^e	200,000	1000	910	-	-	-	-	\$2,523,660	UGS Files
2015 ^e	430,000	2820	2570	-	-	-	-	\$7,116,820	UGS Files
2016 ^e	505,000	1028	1378	-	-	-	-	\$2,605,828	UGS Files
2017	-	-	-	-	-	-	-	\$-	
2018 ^e	14,057	205	-	-	-	-	-	\$512,500	UGS Files
2019 ^e	58,972	860	-	-	-	-	-	\$2,150,000	UGS Files
2020 ^e	263,522	3843	3470	-	-	-	-	\$9,697,720	UGS Files
2021 ^e	260,574	3800	-	-	-	-	-	\$9,500,000	UGS Files
2022 ^e	171,224	2497	2738	-	-	-	-	\$6,313,688	UGS Files
2023 ^e	14,606	213	234	-	-	-	-	\$538,584	UGS Files
Total	2,324,638	41,799	840,700	3,659,732	10,656,114	391,397	51,945,930	\$255,305,490	

¹Value is given in 2024 dollars based on current metal prices and does not represent the actual historical value of production in a given year.²U.S. Bureau of Mines Mineral Yearbook for the given year.^e Estimated

Table 2. Select ore production by mine for the Gold Hill district. Modified from Krahulec (2017).

Mine	Tons ¹	Ag g/t	As %	Au g/t	Bi %	Cu %	Pb %	Zn %	WO ₃ %	Year(s)
Albert	5	25.7		2.7		8.0				1912–1925
Alvarado ⁴	95			21.9						1893–1895
B. Estelle ⁴	1								0.75	1940–1945
Cane Springs ⁴	8			14.7						1893–1895
Cane Springs	46	12.9		36.7		5.5				1914
Cane Springs	2			17.1						1932–1933
Cash boy	4	891.4		0.7		0.1	13.0			1915
Centennial	47	54.9		1.7		5.4				1917
Christmas	11	644.6		2.7		0.5	4.4			1917
Climax	1	994.3					27.0			1917
Copper Queen ^{4,5}	1500	596.6				0.6	15.4			1916–1919
Copperopolis	55	188.6		3.8		5.6	0.6			1917
Cyclone	5	25.7		1.3		0.9	3.0	2.8		1926
Doctor ⁴	2								0.75	1917
E.H.B.5	2374								1.3	1953
Fraction (Timm) ⁵	1843								1.65	1942–1955
Fraction (Timm) ^{4,5}	275								1.65	2016
Frankie	353	51.4		2.7		4.8	0.7			1917
Garrison Monster	7	82.3				0.6	15.3			1917
Gold Hill ⁴	15			12.1						1893–1895
Gold Hill	28,718		4.3			3.0				1917
Gold Hill ⁴	171,638	137.1	4.7	0.3		0.7	2.1			1917–1929
Herat	156	38.6		1.3		0.3	7.4			1920
Herat	47	548.6		0.7		0.2	11.4			1923
Herat	1	342.9	13.0	9.9			7.9			1923
Kiewit ³	63			0.3						2014–2015
Kiewit ⁵	782,955	0.5		0.5						2018–2023
Lucy L ^{4,5}	500								1	1944
Midas	95			92.9						1896
Midas ³	622			24.7						1902
Monocco	786	12.1				1.2	0.9			1917–1920
Napoleon	135	89.1		3.8		6.4				1917
New Baltimore	22	1,817.2		0.7			47.0			1923
Ozark	12	174.9		3.8		3.2				1917
Pole Star	313	126.9		32.9	14.5	3.0				1917
Reaper ⁴	1200								0.75	1916–1918
Rube Gold	692			249.6						1921–1929
Rube Gold	37			342.9						1931
Silver Hill	78	86.6		1.4			18.1			1917
Silver King	132	62.6		1.4		2.8	5.2			1922–1923
Southern C	3	128.6					3.0			1918–1926
Star Dust Group ^{4,5}	1500								1.3	1937–1957
Success Group	94	117.4				1.6	9.0			1920
U.S. Mine	1	41.1	25.7					0.1		1923
U.S. Mine	12,153	54.9	25.8	1.3		0.2	0.9	0.4		1924–1925
U.S. Mine	98,784		15.2							1943–1945
Undine	5	198.9		1.3		3.1	1.0			1918
Western Utah Extension	2	185.1		1.3		4.1				1917
Wilson Consolidated	150								1	1915–1917
Wilson Consolidated ²	4			14.4	12.4					1917
Yellow Hammer ²	2								69.5	1917
Yellow Hammer	400								0.97	1954–1955
Yellow Hammer ^{4,5}	1500			8.2		2.1			2.07	1958
Yellow Hammer ^{3,5}	18,000	51.4		1.7		2.3			0.5	2010–2011

¹Tons of select ore shipments, unless otherwise noted.²Tons and grade of concentrate.³Grade recovered from mill.⁴Estimated tons and/or grade.⁵Mined tons and grade.

or base metals such as copper, lead, and/or zinc (Table 3). Beryllium enrichment was discovered in 1965 (Griffitts, 1965) but did not convert to mining production due to the discovery of the much higher grade Spor Mountain district to the southeast (Figure 1). The main exploration program targeting porphyry mineralization was by Kennecott over the IBX target area in the late 1990s (Figure 2). Revived interest in the Clifton Shears Pb-Ag area failed to convert to active mining, also in the late 1990s, but in 2010 minor production at the Yellow Hammer mine restarted for a short period, producing gold, silver, and copper. In 2016, artisanal-scale mining at the Fraction (Timm) tungsten skarn produced 275 tons of tungsten ore. Although the total contained tungsten was not reported, based on an estimated historical grade at the Fraction mine of 1.7% WO₃ (Everett, 1961), the ore is estimated to have contained roughly 7500 lbs tungsten metal. While this is a very minor amount of tungsten (the U.S. has imported an average of 2300 tons of tungsten annually over the past four years; U.S. Geological Survey, 2023), the

Fraction mine is the most recent domestic producer of tungsten in the U.S. (U.S. Geological Survey, 2017). Newmont launched a substantial gold exploration program over the entire Gold Hill district in 2013; however, all work and claims were dropped in 2018. The Kiewit low-sulfidation epithermal gold deposit was first targeted in the early 1990s but did not start production until 2014. Production at Kiewit was put on standby from 2016 to 2019, was revived from 2019 to 2023 due to increased gold prices, but returned to standby in 2023.

Geological Setting

Overview

The Gold Hill district is located on the Uinta-Cortez axis (Figure 1), a roughly east-west-trending structural zone known by several other names (see, for example, Roberts et al., 1965;

Table 3. Summary of significant exploration activity in the Gold Hill district, 1960s to present.

Year(s)	Company	Area	Target	Activity
1962	Vanguard Research Company	Kiewit	Vein and stockwork low sulfidation epithermal Au	Discovery of anomalous gold grades at surface
1973–1980	AMAX Exploration	Goshute Wash	Porphyry Mo	Geochemical reconnaissance, 3 rotary drill holes with diamond core at depth.
1980–1997	American Consolidated Mining Company (ACMC)	Clifton Shears	Base metal veins	Geophysical surveys, 28 reverse circulation holes
1982–1985	Superior Oil Company/ Gulf Resources Corporation	Ochre Springs	Sediment hosted Au	Initial mapping and drilling
1983–1985	Hunt, Ware and Proffett/Freeport McMoRan	Ochre Springs	Sediment hosted Au	Shallow drilling
1984–1985	Battle Mountain Gold (previously Duval Corp.)	Trail Gulch	Sediment hosted Au	6 widely spaced drill holes
1987–1990	Atlas Precious Metals	Trail Gulch	Sediment hosted Au	20–40 drill holes
1988–1990	ASARCO	Ochre Springs	Sediment hosted Au	31 rotary drill holes
1991–1992	Coeur Mining	Ochre Springs	Sediment hosted Au	3 diamond-core drill holes
1992–1993	Goldstack Resources	Kiewit	Vein and stockwork low sulfidation epithermal Au	16 reverse circulation drill holes, 1 diamond core drill hole
1993–2002	Clifton Mining	Clifton Shears	Base metal veins	Geochemical reconnaissance, test mining, 12 diamond core drill holes
1994–1997	Kennecott Utah Copper	Ibapah	Skarn/porphyry	Geophysical survey, 10 reverse circulation drill holes
2002	Clifton Mining Company/ New Centennial Mining	Cane Springs	Cu and/or Au bearing skarn	Drill planning but no execution
2003–2004	Dumont Nickel Inc.	Ibapah	Skarn/porphyry	Soil sampling and geochemical reconnaissance, 1 diamond core drill hole
2003–2008	Dumont Nickel Inc.	Cane Springs	Cu and/or Au bearing skarn	3 diamond core drill holes
2003–2008	Dumont Nickel Inc.	Clifton Shears	Base metal veins	7 diamond core drill holes, geochemical reconnaissance
2003–2008	Dumont Nickel Inc.	Kiewit	Vein and stockwork low sulfidation epithermal Au	5 diamond core drill holes, channel sampling and mapping
2013–2015	Newmont Gold Corp	Trail Gulch, Ochre Springs	Sediment hosted Au	5 drill holes, soil geochemistry
2015–2016	Newmont Gold Corp	Yellow Hammer	Cu and/or Au bearing skarn	6 diamond core drill holes, reconnaissance geochemistry
2016–2017	Newmont Gold Corp	Kiewit	Vein and stockwork low sulfidation epithermal Au	10 diamond core drill holes, geophysical survey

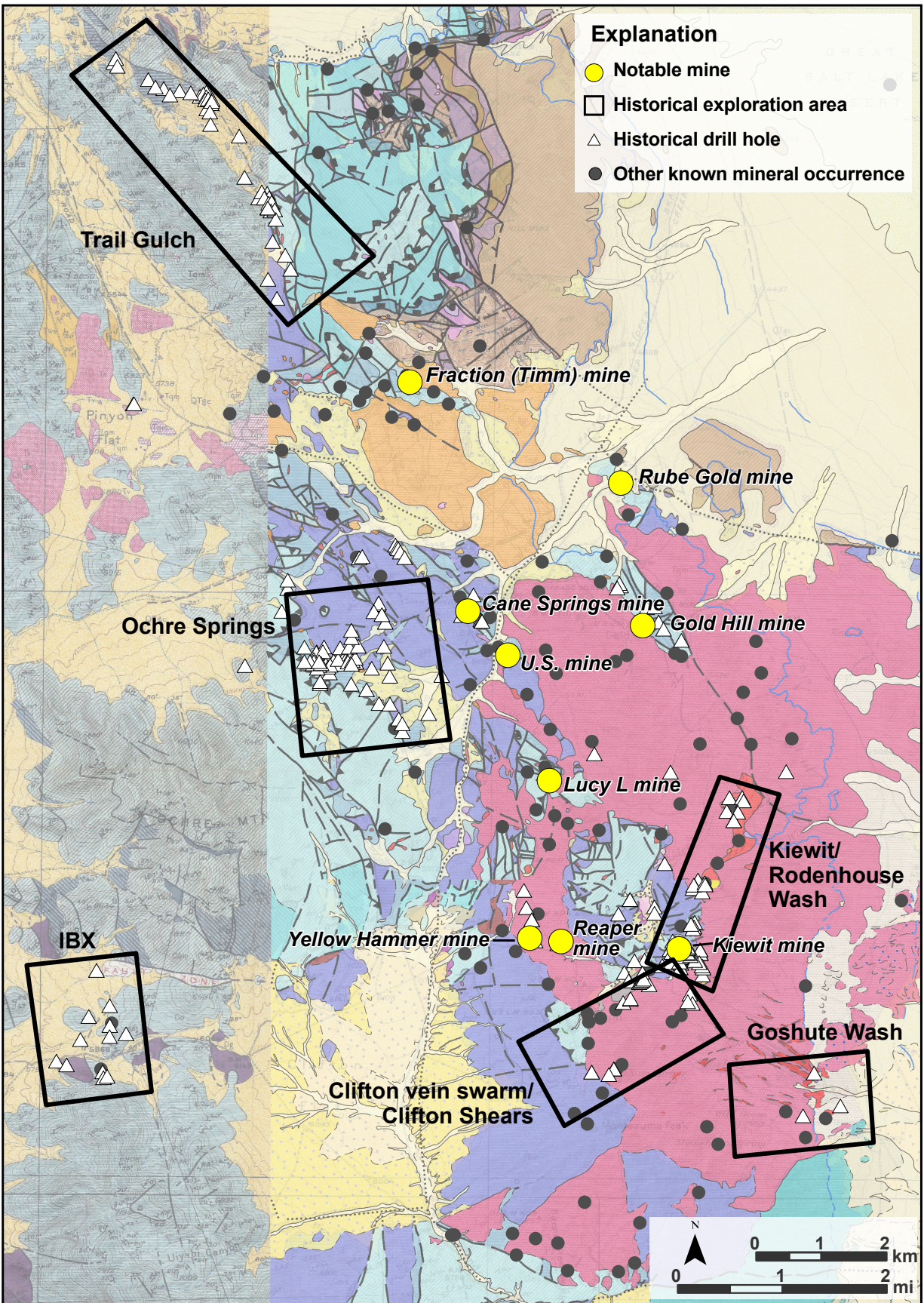


Figure 2. Overview of notable mines and exploration areas in the Gold Hill district. Geologic basemap as in Figure 4.

Armstrong, 1968; Erikson, 1974; Vogel, 2001; Yonkee and Weil, 2015; Clark, 2020), and is considered to represent the western extension of the Bingham-Park City mineral belt (Butler et al., 1920; John and Ballentyne, 1997). The Uinta-Cortez axis is defined by the contact between the northern Archean Wyoming Province-Grouse Creek block and the southern Proterozoic Mojave and Yavapai Provinces which collided ~1.7 Ga (Whitmeyer and Karlstrom, 2007; Yonkee et al., 2014). The resulting east-west suture is a deep-seated basement zone of structural weakness that has played a role in subsequent formation of multiple uplifts (e.g., Uinta Mountains, Tooele arch, Stansbury uplift, etc.) and rotation of Sevier orogenic belt thrust sheets. Importantly for magmatic-hydrothermal ore deposits, the deep-seated crustal weakness also created a zone of preferential emplacement of metal-enriched igneous rocks, particularly during the Eocene. The Park City, Cottonwood, Bingham, Stockton, and Gold Hill mining districts are the best examples of large magmatic-hydrothermal systems located along the axis, but there are a number of intrusive and extrusive expressions of magmatic localization along the axis. The Uinta-Cortez axis is also recognized as a patchy magnetic high in airborne geophysical data, interpreted to be related to the localization of deep magmatic activity (Stewart et al., 1977; Mabey et al., 1978). Most of the defining features of the Uinta-Cortez axis are best recognized in Utah; however, some authors (Roberts et al., 1965; Presnell, 1998) interpret the cratonic suture zone to continue westward into central Nevada where it is obscured by thrust sheets.

In addition to being located along the Uinta-Cortez axis, the Gold Hill district is considered part of the north-south-trending retroarc hinterland of the North American Cordilleran orogenic system, also known as the Cordilleran or Sevier hinterland (Camillari and Chamberlain, 1997; DeCelles, 2004; Smith et al., 2013; Yonkee and Weil, 2015). The hinterland is characterized by accumulation of thick, Paleozoic passive margin carbonate sequences affected by Jurassic thin-skinned deformation and magmatic emplacement. This period of deformation is often referred to as the Sevier orogeny, though the term “Sevier” or “Sevier-age” is more appropriately applied to the Sevier fold and thrust belt that formed east of the Gold Hill district (e.g., Yonkee and Weil, 2015). The Jurassic deformation in the hinterland is generally considered to have been active from pre-165 Ma to ~150 Ma, based on deformation in Jurassic strata and intrusive units, and younger intrusive units cross-cutting deformation (Camillari and Chamberlain, 1997; Smith et al., 2013; Zuza et al., 2020; Di Fiori et al., 2021). Magmatism initiated in eastern Nevada by ~167 Ma, though the most intense phase of magmatic emplacement occurred between roughly 160 and 153 Ma (White, 2023). Crustal thickening through the Cretaceous and Paleogene created an over-thickened orogenic plateau known as the Nevadaplano (Allmendinger, 1981; DeCelles, 2004; Zuza et al., 2020) that is estimated to have been ~25–35 mi (~45–60 km) thick and represented a paleoelevation of ~1–2 mi (~2–3 km). Metamorphic core complexes formed in the hinterland during this

period either through deep burial or tectonic overpressure (Dickinson, 2006; DeCelles and Coogan, 2006; Long, 2015; Zuza et al., 2020; Di Fiori 2021; Long et al., 2024). The Nevadaplano destabilized during the Cenozoic and the hinterland experienced renewed magmatism. The magmatic upwelling resulted in Eocene to Miocene stock emplacement, volcanism, and extensional faulting, followed by Miocene volcanism and extensional faulting during formation of the Basin and Range physiographic province (Jones et al., 1998; Colgan and Henry, 2009; Long, 2019).

On the district scale, the multistage geological history of the region has resulted in complex faulting of the Paleozoic bedrock. Paleozoic lithologies in the district developed in passive-margin marine basinal to carbonate platform environments, all of which are intruded by Jurassic to Miocene-age intrusive and extrusive igneous rocks. Due to the intense structural dismemberment, there is no intact Paleozoic stratigraphic section anywhere in the Gold Hill district (Chamberlain, 1981; Mills et al., 2023), which makes mapping challenging. Geologic units exposed in outcrops are Mississippian to Pennsylvanian carbonates that are not prone to forming foliation or other kinematic indicators that help interpret deformation of the district. Faults are poorly exposed and are typically interpreted by lithologic offsets rather than discrete fault surfaces, and very few places exist where fault dips or shear sense can be discerned (Robinson, 1990).

Development of the Gold Hill District

Leading up to the Late Devonian and Early Mississippian, the stratigraphic section of the Great Basin was dominated by a long-lived early Paleozoic carbonate platform setting. The Late Devonian-Early Mississippian Antler orogeny in Nevada, which caused early Paleozoic deep-water strata to be thrust over mid to late Paleozoic carbonate platform strata, created an exposed highland that shed sediment eastward into western Utah (Cook and Corboy 2004; Beranek et al., 2016; Jones et al., 2021; Cashman and Sturmer, 2021). These marine rocks dominate the stratigraphic section at Gold Hill. Details on the stratigraphy and unit descriptions for Gold Hill can be found in Nolan (1935), Robinson (1993), and Mills et al. (2023). In this study, the formations most frequently encountered are the Woodman Formation, the Ochre Mountain Limestone, the Chainman Shale, and the Ely Limestone (Figure 3), for which brief descriptions are provided below from stratigraphically oldest to youngest.

The Mississippian Woodman Formation is largely equivalent to the Deseret Limestone and Humbug Formation of central Utah. The Woodman is composed of basal phosphatic siltstone/shale (Delle Phosphatic Member) and silty shales in the northern part of the Gold Hill district, whereas in the southern area the Woodman consists of siltstone and limestone that are distinctive due to the light brown color and silty composition resulting in distinct weathering to platy subcrop.

The Mississippian Ochre Mountain Limestone is largely a stratigraphic and lithologic equivalent to the Great Blue Limestone of central Utah. In the Gold Hill district the Ochre Mountain is a thick-bedded, finely crystalline limestone commonly forming cliffs and ledges with local fossiliferous (coral) beds and nodules of chert. The Ochre Mountain is often described as dark blue to blue-gray in color; however, the intense hydrothermal activity and bleaching in Gold Hill makes color an unreliable indicator in many areas. Likewise, fracturing with low to moderate density calcite veining and/or tectonic brecciation are often cited as features of the Ochre Mountain. However, calcite veining can be locally abundant in the

Ely Limestone as well, particularly in proximity to intrusive units. An informal shale member of the Ochre Mountain was mapped in Mills et al. (2023) which looks very similar to the Chainman Shale, particularly around Clifton Shears, and is likely the same unit referred to as the Herat shale in previous mapping (Nolan, 1935).

The Mississippian Chainman Shale is a highly recessive unit in the Gold Hill district and fresh outcrop is rarely observed, typically forming highly weathered slopes or valleys. Where exposed by road cuts or mining trenches the shale is black to brick red, variably carbonaceous, and fissile. Some authors (e.g., Christensen, 1975) report chialstolite-bearing hornfels in the Chainman, presumably where in proximity to the Jurassic or Eocene intrusive units; however, the hornfels observed in this project was in the thick limestone units (Ochre Mountain or Ely) adjacent to the Jurassic pluton. The Chainman is regionally estimated to be 1000–2500 ft (300–800 m) thick (Bereskin et al., 2015), but, especially in the southern part of the Gold Hill district, this thickness is drastically reduced. Mills et al. (2023) hypothesized this may be due to attenuation in the unit due to partitioning much of the stress of deformation into the Chainman, as it is a soft and platy unit bracketed by two resistant limestone units.

The Pennsylvanian Ely Limestone is a cyclic, thick limestone-dominant carbonate unit with minor siliciclastic input. In the Gold Hill district the Ely is thick bedded, resistant, coarsely crystalline limestone. Color is reported as light to dark gray but as mentioned, the hydrothermal alteration in the district makes color an unreliable indicator when discriminating between Ochre Mountain and Ely limestones. Locally, the Ely limestone is fossiliferous (e.g., brachiopods and fusulinids), cherty, and contains wispy sandstone lenses. Dolomite-rich areas of the Ely are reported in the district (e.g., Robinson, 1993) but were not recognized in the field during this study. The Permian Ferguson Mountain Formation was first separated from the Ely Limestone by Mills et al. (2023), having previously all been mapped as a single unit known as the Oquirrh Formation. The Ferguson Mountain Formation forms a large outcrop in the southeastern part of the district but was not considered further in this study.

Jurassic compressional deformation in the Gold Hill district resulted in localized thrust faulting and minor folding, the most notable expression of which is the Ochre Mountain thrust (OMT) that places Mississippian over Pennsylvanian strata (Figure 4). Displacement on the OMT is estimated to be 6 mi (10 km), and previous researchers have theorized that there may be duplex structures associated with the main OMT (Robinson, 1993). At Gold Hill, the Jurassic pluton that comprises the eastern side of the district is dated at 156–154 Ma (Table 4; Figure 5) and is interpreted to have emplaced rapidly at shallow depths, though the regional stress regime at the time of emplacement is debated (Stacey and Zartman, 1978; Allmendinger and Jordan, 1984; Miller and Hoisch, 1995; Burwell, 2018; Zuza et al., 2020; White, 2023).

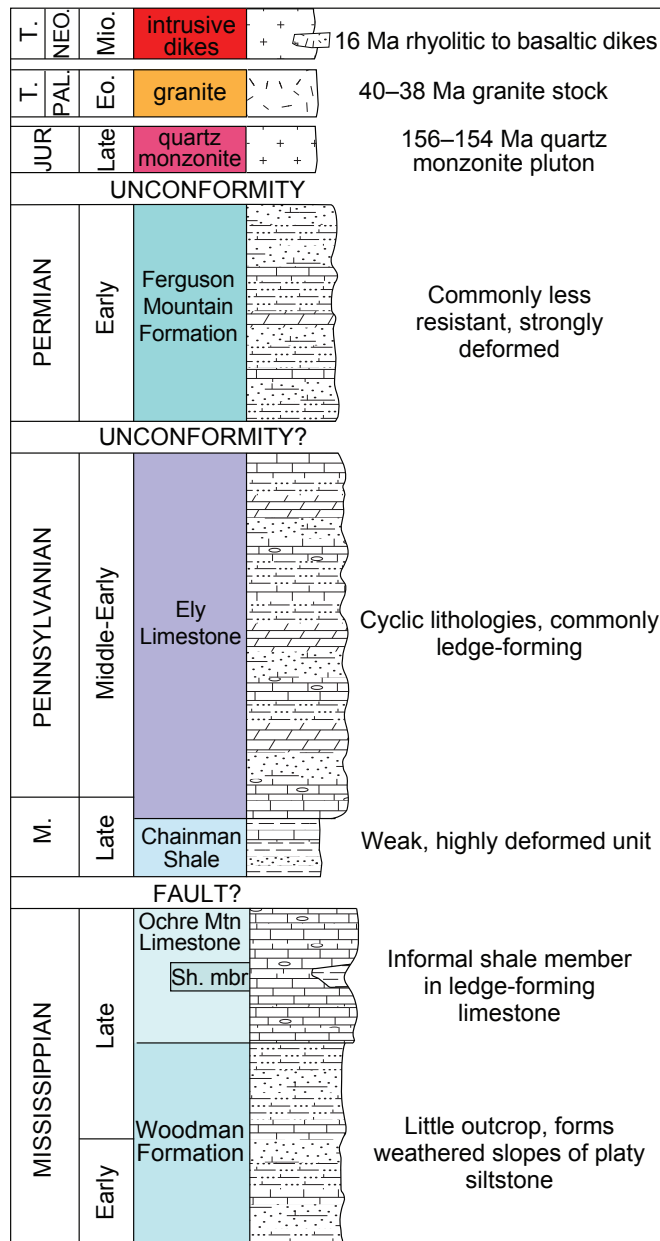


Figure 3. Stratigraphic column of major Paleozoic bedrock units and intrusive units in the Gold Hill mining district. Modified from Mills et al. (2023). Complete stratigraphy and descriptions of all units in the Gold Hill district can be found in Nolan (1935), Robinson (1993), and Mills et al. (2023).

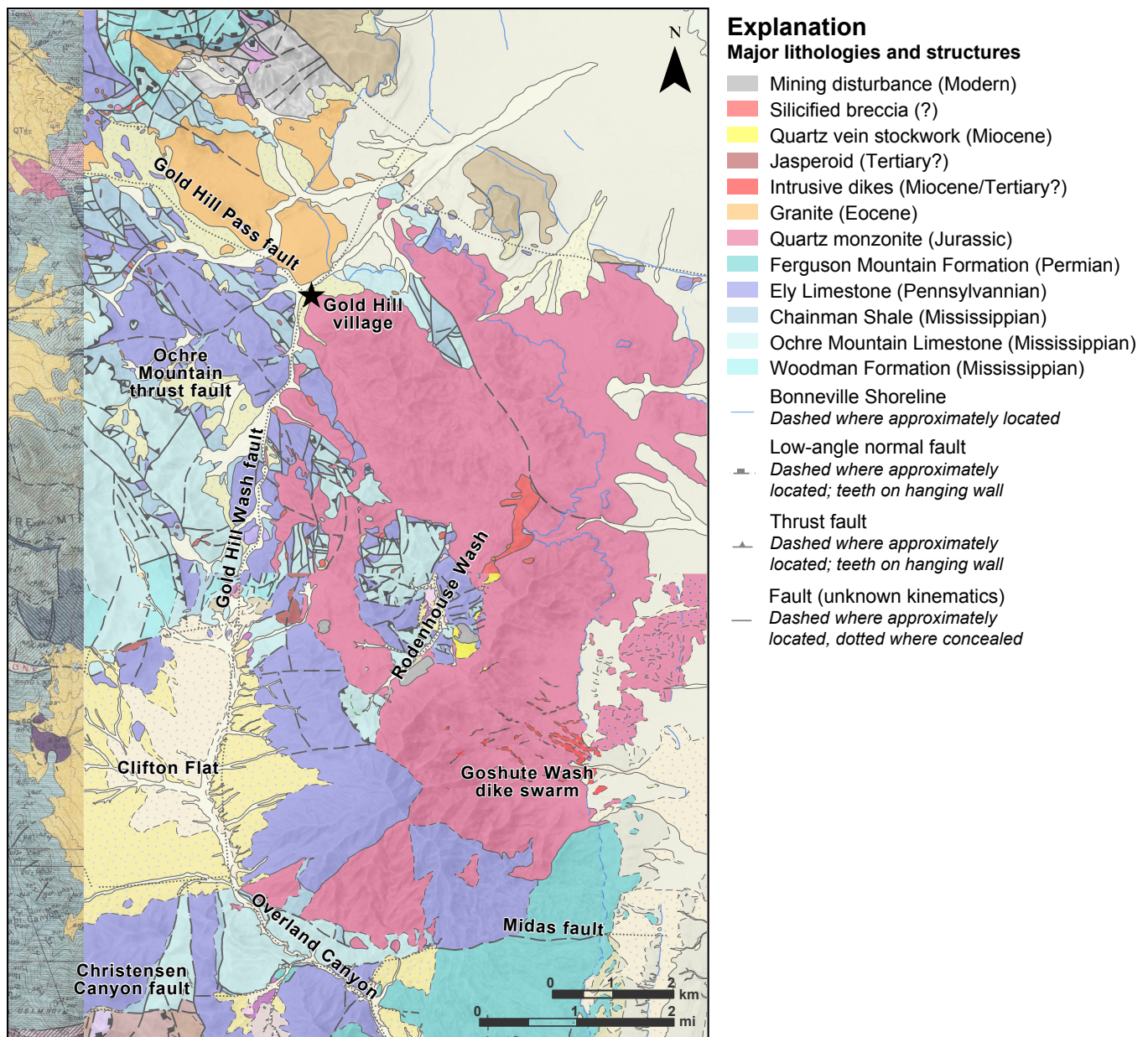


Figure 4. Geologic map and major geologic features of the Gold Hill mining district. Map based on 1:24,000-scale mapping by Robinson (2023) and Mills et al. (2023) where available, otherwise on 1:62,500 mapping by Nolan (1935). Major geologic units are shown in the explanation. Brown, pink, and purple units are Cambrian to Devonian units that do not constitute a significant portion of the exposed geology in the mining district. Pale yellow to tan units are Quaternary cover. Refer to referenced publications for full unit descriptions.

The Jurassic pluton is one of the most distinct geologic features of the Gold Hill district. The 156–154 Ma pluton is exposed over roughly 30 mi² (85 km²) and forms the eastern margin of the district (Figure 5). The pluton is most commonly observed as a biotite-hornblende quartz monzonite that includes minor magnetite, titanite, zircon, and apatite, and is oxidized (Burwell, 2018; Mills et al., 2023). It is typically medium to coarse grained and equigranular to locally porphyritic, and often has pink potassium feldspar phenocrysts. Mafic enclaves are common throughout the pluton. Existing mapping shows the pluton as a single cohesive unit, though detailed studies evaluating the potential for internal magmatic heterogeneity are lacking. Roof pendants of Paleozoic bedrock and mag-

matic-hydrothermal textures suggest that the current level of exposure is near the top of the pluton chamber (Nolan, 1935; Chorney, 1943). Burwell (2018) conducted geobarometry and thermometry that suggest a shallow emplacement depth (<2 mi [<3 km]) and a temperature of $\sim 750^{\circ}\text{C}$, though the barometry is poorly constrained.

Following Jurassic deformation, the hinterland was part of an overthickened crustal zone known as the Nevadaplano, which caused some Paleozoic units to be buried rapidly and undergo metamorphism before being exhumed as metamorphic core complexes, though the timing and mechanism of exhumation is an area of active research (Allmendinger, 1992; DeCelles,

Table 4. Summary of geochronological data in the Gold Hill district.

Sample ID	Eastings	Northing	Datum	Sample Type (as defined in this study)	Sample Type (Original study)	Age	Error	Mineral	Method	Source
Unk	262305	4446524	NAD83, zone 12N	Low sulfidation epithermal system	qtz-adu-cal (Be) vein	7.85	0.8	Adularia	K-Ar	Whelan (1970)
GHC22-010	263556	4442284	NAD83, zone 12N	Rhyolite porphyry dike	Felsic dike (unit Tid)	16.23	0.26	Zircon	U-Pb	Mills et al. (2023)
GXJ256085	263675	4446959	NAD83, zone 12N		Monzonite dike	17.14	0.4	Zircon	U-Pb	Burwell (2018)
NV21-007GLD	257912	4451274	NAD83, zone 12N	Granite	Granite	38	0.83	Zircon	U-Pb	White (2023)
GH-002	257986	4451361	NAD83, zone 12N	Eocene granite stock	Granite	38.16	0.45	Zircon	U-Pb	King and Burwell (2016)
70-2	255754	4452145	NAD83, zone 12N	Eocene granite stock	Granite	38.23	1.3	Biotite	K-Ar	Stacey and Zartman (1978)
74-KA-15	247472	4453714	NAD83, zone 12N		Latite	39.2	0.6	Biotite	K-Ar	Moore and Mckee (1983)
GXJ256081	261612	4447769	NAD83, zone 12N		Granite porphyry dike	39.95	0.47	Zircon	U-Pb	Burwell (2018)
GH-001	257972	4451168	NAD83, zone 12N		Mafic dike	40.08	0.56	Zircon	U-Pb	King and Burwell (2016)
GH-006	256815	4454054	NAD83, zone 12N		Diorite	40.08	0.56	Zircon	U-Pb	King and Burwell (2016)
6	258568	4452055	NAD83, zone 12N	Eocene granite stock	Granite	40.62	1.4	Biotite	K-Ar	Stacey and Zartman (1978)
8	259192	4450090	NAD83, zone 12N	Quartz monzonite*	Adamellite	42.5	0.8	Biotite, hornblende	K-Ar	Armstrong (1970)
74-KA-16	259429	4450083	NAD83, zone 12N	Quartz monzonite*	Hornblende biotite	43.9	0.8	Biotite	K-Ar	Moore and Mckee (1983)
74-KA-9	260297	4447585	NAD83, zone 12N	Quartz monzonite	Quartz monzonite	134.9	4	Hornblende	K-Ar	Moore and Mckee (1983)
NV21-006GLD	259131	4449509	NAD83, zone 12N	Quartz monzonite	Quartz monzonite	152.29	1.4	Zircon	U-Pb	White (2023)
15A	259673	4439116	NAD83, zone 12N	Quartz monzonite	Granite	154.32	5	Biotite	K-Ar	Stacey and Zartman (1978)
GXJ256076	260301	4447703	NAD83, zone 12N	Quartz monzonite	Quartz monzonite (pyroxene rich)	155.4	1.8	Zircon	U-Pb	Burwell (2018)
GXJ256084	263686	4447042	NAD83, zone 12N	Quartz monzonite	Quartz monzonite	156.1	1.8	Zircon	U-Pb	Burwell (2018)
18	259886	4442845	NAD83, zone 12N	Quartz monzonite	Granite	156.46	5	Biotite	K-Ar	Stacey and Zartman (1978)

*Age is interpreted to represent resetting due to proximity to emplacement of the Eocene stock.

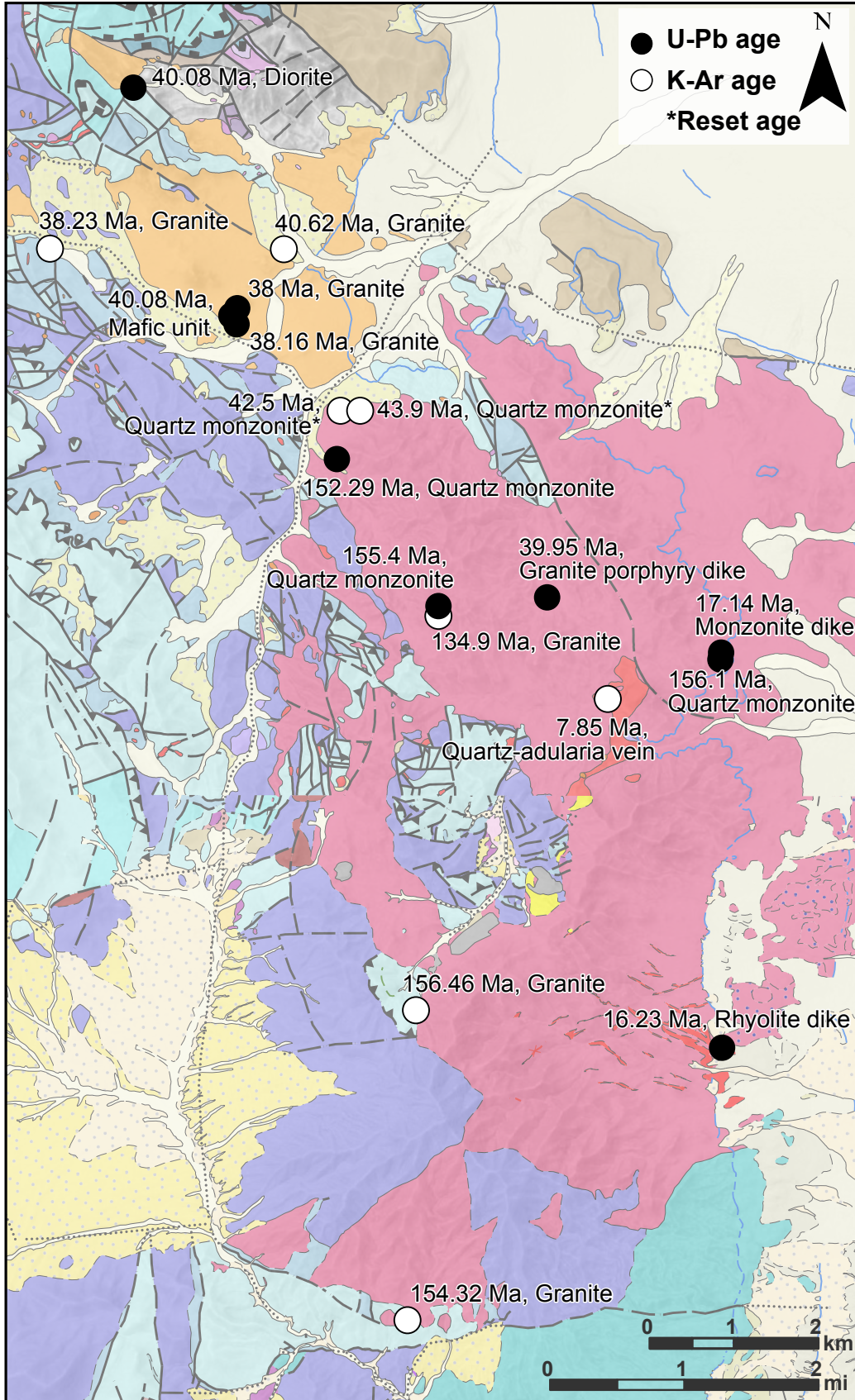


Figure 5. Summary of geochronology locations for samples in Table 4. Geology as in Figure 4.

2004; Dickinson, 2006; DeCelles and Coogan, 2006; Long, 2015; Zuza et al., 2020; Di Fiori et al., 2021). A voluminous regional magmatic flare-up occurred across eastern Nevada and western Utah from approximately 40–35 Ma. These magmas resulted from crustal interaction with mantle-derived basaltic melts reflecting crustal underplating from slab removal (Best et al., 2016; White, 2023). In Utah, this magmatic event initiated in the north at 40 Ma and swept south in a prolonged magmatic event to 25 Ma; this era of magmatism generated several of the largest magmatic-hydrothermal districts in Utah, such as Bingham Canyon, Park City, and Tintic (Presnell, 1998; Krahulec, 2015).

In Gold Hill, the Eocene granite stock, dated to 40–38 Ma (Stacey and Zartman, 1978; King and Burwell, 2016; White, 2023), is exposed over roughly 5 mi² (15 km²) in the north-west of the district and was emplaced during this period (Table 4; Figure 5). Originally described as a quartz monzonite (Stacey and Zartman, 1978; Robinson, 1993), whole rock geochemistry from Mills et al. (2023) showed the composition is granitic (Figure 6A). The stock is a smaller intrusive body than the Jurassic pluton and is coarse grained and equigranular, commonly hosting phenocrysts of potassium feldspar up to 0.75 in (2 cm). Magnetite, apatite, and titanite are common accessory minerals. Although the Eocene intrusion is typically

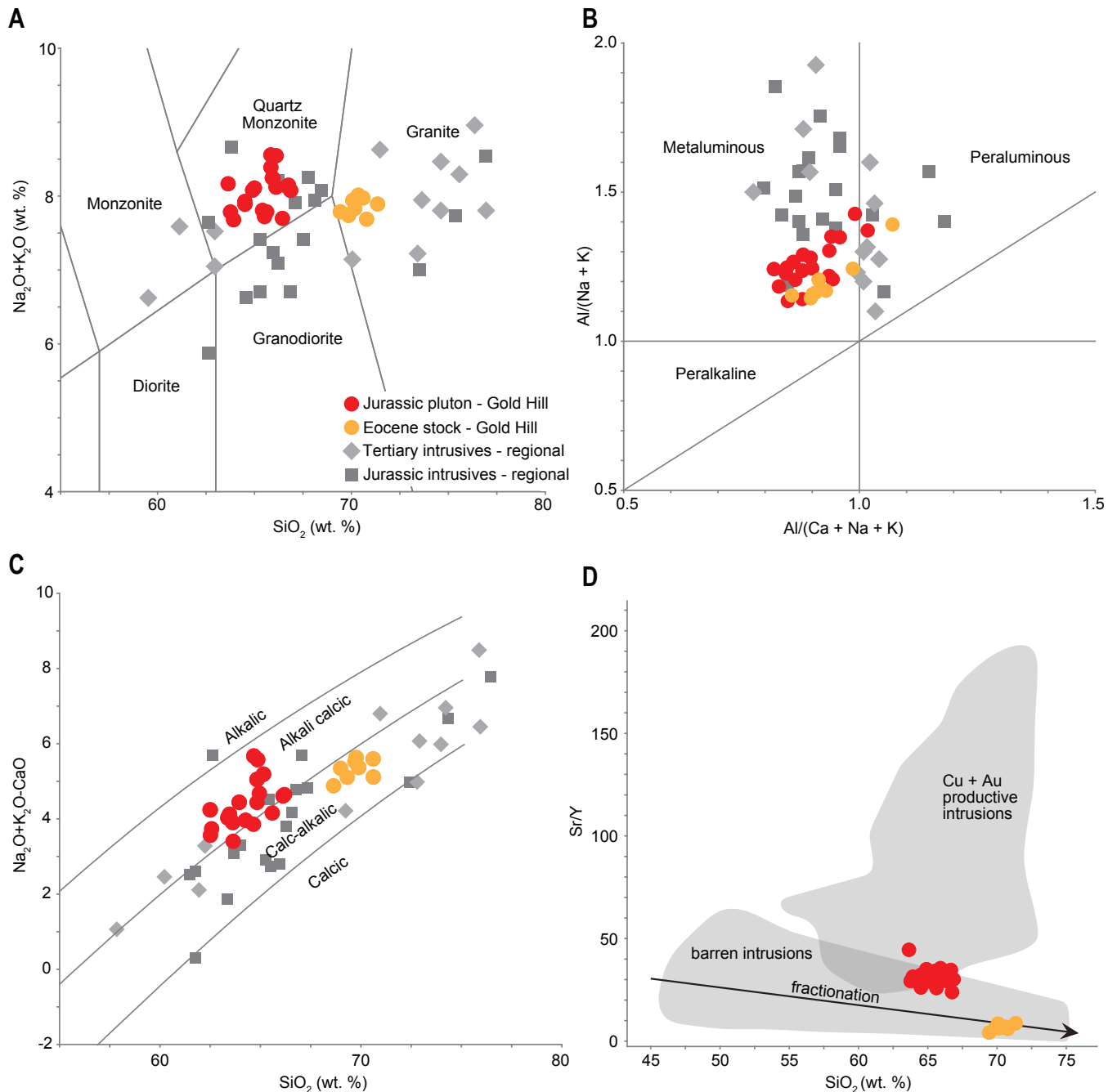


Figure 6. Whole-rock geochemistry of the Jurassic quartz monzonite and Eocene granite, with background data on regional Jurassic and Tertiary intrusives from eastern Nevada and western Utah for reference (White, 2023). Gold Hill data from Mills et al. (2023).

referred to as a stock in the singular, Robinson (1993) interpreted it to be a swarm of small intrusive stock-like bodies that formed within the juxtaposition of the north-south Gold Hill Wash fault and the west-northwest–east-southeast Gold Hill Pass fault. It is unclear what evidence was used to support this interpretation. The Gold Hill Wash fault is interpreted as the contact between the Jurassic and Eocene intrusive bodies, though no explicit contact has been defined. Both the Jurassic quartz monzonite and the Eocene granite are meta-luminous, though the granite is slightly more peraluminous (Figure 6B). The Eocene granite is of the same age range as other major productive porphyries such as Bingham Canyon. Skarn mineralization associated with the stock trends towards W-enriched, as opposed to Cu(-Au).

A small mafic exposure was mapped within the Eocene stock (Robinson 1993; Mills et al., 2023). Dates from King and Burwell, 2016 yield an age of 40 Ma for the mafic body and 38 Ma for the granite stock, which raises the question as to whether the mafic body is some sort of enclave within the stock or a dike, as it has generally been described (King and Burwell, 2016; Mills et al., 2023). A mafic enclave could explain the older age for the mafic body; if the mafic unit is a dike, further investigation into the dating veracity or age relationship between the mafic unit and the granite stock is required. Burwell (2018) mapped a 40-Ma granite dike cutting the northern extent of the Jurassic pluton. Additionally, a variety of volcanic rocks are described in the Gold Hill district (Robinson, 1993; Mills et al., 2023) and preliminary dating shows the trachytic to latitic welded tuff unit (very limited extent) of Mills et al. (2023) is Eocene in age, roughly coeval with the granite stock (Don Clark, Utah Geological Survey, verbal communication, 2024). Also, the more extensive intermediate lava flow unit overlying the welded tuff unit is likely of Eocene or Oligocene age (Don Clark, Utah Geological Survey, verbal communication, 2024). Preliminary dating on the volcanoclastic sandstone and tuff (Mills et al., 2023) exposed in Rodenhouse Wash and Blood Canyon yielded a Miocene age of 19 Ma (Don Clark, Utah Geological Survey, verbal communication, 2024).

Cenozoic extension caused significant structural dismemberment and possible rotation of parts of the Gold Hill district (Robinson, 1993, 2005; Mills et al., 2023). Much of the extension is interpreted to have occurred on pre-existing faults, overprinting previous events and making interpretation of the structural history of the district extremely difficult. Additionally, Gold Hill may be part of the regional Ferguson detachment (Ketner et al., 1998; Silberling and Nichols, 2002; Clark et al., in progress), further adding to the complex deformation. Magmatism accompanied Miocene extension, most demonstrably observed in the Goshute Wash dike swarm hosted on the east side of the Jurassic pluton (Figure 4). These dikes trend distinctly northwest-southeast and at least three compositions of dike are recognized in this area: a gray to pale green rhyolite porphyry dike, a black porphyritic andesite dike that hosts phenocrysts of feldspar up to 4 cm, and a black aphanitic basalt

dike. Mapping by Mills et al. (2023) and by exploration geologists in the late 1970s and early 1980s could not define the chronological relationship between these dike compositions; for example, exposures of the rhyolite dike cross-cutting the andesite dike suggest the rhyolite dike to be younger, whereas outcrop of andesite dike containing clasts of the rhyolite dike suggest the andesite dike to be younger. The andesite and basalt dikes may be transitional phenocryst-rich and phenocryst-poor endmembers of the same unit. Overall, field relationships suggest a coeval emplacement of all dike compositions, and an age of 16 Ma on the rhyolite dike obtained by Mills et al. (2023) suggests a Miocene age for the entire Goshute Wash dike swarm (Figure 5). Basalt dike exposures in Gold Hill Wash were too altered for reliable geochronology.

Mineralization in the Gold Hill District

Given the multi-stage formation of the Gold Hill district described above, it follows that the mineralization history at Gold Hill is also complex. Detailed write-ups of individual deposits are available in previous studies on the district (e.g., Nolan, 1935; Chorney, 1943; El-Shatoury and Whelan, 1970; Krahulec, 2017). A summary of the best-defined mineralization events is provided below; however, many questions remain about the mineralization history at Gold Hill.

The earliest known mineralizing event in the district manifests as replacement, skarn, and vein deposits associated with emplacement of the Jurassic pluton. These deposits occur both in the Jurassic pluton itself and within the Paleozoic bedrock, and are typically concentrated along the western margin of the pluton and in the Paleozoic bedrock block, often interpreted as a roof pendant. Yellow Hammer and Reaper deposits, both located on the margin of the Paleozoic bedrock block, have been dated by Re-Os on molybdenum, yielding ages of roughly 156–154 Ma and demonstrating a direct genetic link with the Jurassic pluton (Carey, 2022). Other deposits such as the U.S. mine and Gold Hill mine, which occur on the northern end of the Jurassic pluton in proximity to the Eocene stock, are assumed to be genetically associated with the Jurassic pluton but no explicit age relationship has been established (Figure 2).

The Eocene stock was the magmatic driver for the next era of mineralization, which formed as skarn and vein deposits around the stock and to the north. As opposed to the Jurassic skarns which have a complex Cu(-Au-W-Mo)-rich metallogeny (Krahulec, 2017; Carey, 2022), the Eocene skarns are W-Pb(-Zn-Ba) rich. Deposits such as the Rube Gold mine are located at the contact zone between the Jurassic pluton and Eocene stock and it is unclear which magmatic-hydrothermal events these deposits are related to, particularly since the contact between the two intrusive units is not exposed.

The third well-defined mineralizing event is the low-sulfidation epithermal gold system in the east of the district which

hosts the Kiewit mine and was the subject of intense exploration by Newmont in the late 2010s. This system has a K-Ar adularia age of 8 Ma (Whelan, 1970), younger than any other known event in the district. Epithermal veins grading to zones of stockwork that have low-grade gold mineralization and intense silicification \pm calcite veining define the system, along with anomalous beryllium enrichment (Griffitts, 1965).

Other types and ages of mineralization such as sediment-hosted gold and porphyry molybdenum deposits have been proposed in Gold Hill and are considered in more detail below, but currently lack enough information to be defined as a distinct mineralizing event. However, there is extensive jasperoid development throughout the Gold Hill district. Although jasperoid is not known to be metal-bearing in the district, it is often considered a significant regional indicator for potential mineralization (e.g., Bailey, 1974). Jasperoid is defined here as pervasive silica and iron-rich replacement alteration that is protolith destructive. The nature of the jasperoids in Gold Hill vary, and though they are often treated as a uniform feature, field relationships strongly suggest that there is more than one generation of jasperoid, or possibly that some jasperoid has been tectonically modified post-formation. The jasperoids are distinctively dark red to black and form large ledges, typically in a broadly linear architecture either mantling bedding or controlled by faulting. Some jasperoids are internally brecciated but have been cemented with silica whereas others are massive and textureless. The jasperoids exist on a spectrum from early stages of silicification and iron oxidation to completely replaced. In the early stages of jasperoid formation there may be unaltered clasts of protolith (typically Paleozoic bedrock) within the matrix; in the most well developed jasperoids all clasts are pervasively altered and replaced.

Although not counted as a separate mineralizing event due to the lack of forming new orebodies (e.g., supergene blanket), oxidation of the previous mineralization events is pervasive throughout the district. Oxidation created in situ supergene minerals, though the oxidation profile is uneven across the district and likely reflects structural controls on meteoric fluids. Exact age for oxidation/supergene mineral formation is not known, but is presumed to be younger than the 8 Ma low-sulfidation event given these rocks are also oxidized.

METHODOLOGY

Literature Compilation and Field Observations

Gold Hill is one of the oldest districts in Utah and has a long-lived and diverse exploration history. As a result, a wealth of exploration data and files have been contributed to the UGS by previous explorers and geologists, particularly from the 1980s onwards. These files provide much information about various exploration models and projects across the district as well as detailed mapping and interpretation of notable mineral

localities throughout the district. Historical and modern exploration data were also taken from Utah Division of Oil, Gas and Mining (OGM) mineral files; unpublished work carried out by previous UGS geologists, most notably Ken Krahulec, was also utilized. These sources of data were combined with publications on the district to create the historical drillhole database (Appendix A), and were used as context for the mineral potential research carried out in this study.

Fieldwork in the Gold Hill district has been ongoing since 2020. Fieldwork served a dual purpose of mapping for Mills et al. (2023) and for this mineral potential investigation. Field areas in the Clifton quadrangle were visited more frequently and field observations were made with greater density; however, significant mineral sites and geological features across the district were visited. The Utah Mineral Occurrence System (UMOS; Utah Geological Survey, 2023) and the USGS topo mine symbols (Horton and San Juan, 2016) were used to guide visits to mineralized features of the district. Additional site selection was based on information in reports (Nolan, 1935; El-Shatoury and Whelan, 1970; Robinson, 1993; Krahulec, 2017; Burwell, 2018) and personal communication with people knowledgeable about mineralization in the area (industry geologists, permit managers, landowners, etc.). Several transects were made across the district to evaluate the nature of the geology away from known mineralized features.

Geochemistry

As part of the EMRI funding for this project, 250 whole-rock geochemistry samples were taken during the fieldwork and involved the effort and help of several UGS geologists, including Kayla Smith, Taylor Boden, Wil Hurlbut, Bear Jordan, and the author of this report (Appendix B). These samples were taken in two grids over the Eocene stock and the western margin of the Jurassic pluton, focused on areas of known tungsten mineralization around both intrusive centers. Samples were taken on a 350 m (1150 ft) spacing in order to simulate exploration conditions in similar geological settings. The spacing was planned to be close enough to pick up anomalous geochemical signals associated with mineralization that may be buffered by carbonate stratigraphy or strongly fracture/fault controlled in a brittle deformation setting, but spaced out enough so that a large area could be assessed by the fewest necessary samples. Sampling on a grid also ensured a range of the various rock compositions in both areas and that samples with unaltered signatures, i.e., “background” geochemistry, were included in the sample set. Infill samples were taken at areas of interest, i.e., sites that host mineralization or significant alteration, to ensure the chemistry of mineralization was also captured. Whole-rock geochemistry for these samples was coordinated by the USGS laboratory in Denver. Major elements were analyzed by wavelength dispersive X-ray fluorescence (WDXRF). Pulped sample material was fused with lithium metaborate/lithium tetraborate flux and the resultant glass disk was introduced into the WDXRF and irradiated by

an x-ray tube. The method also provided a gravimetric loss on ignition (LOI). For trace elements, pulped sample material was fused at 750°C with sodium peroxide and the fusion cake dissolved in a dilute nitric acid. The resulting solution was analyzed by inductively coupled plasma-optical emission spectroscopy-mass spectroscopy (ICP-OES-MS).

In addition to the samples collected as part of this study, a database of surface rock and soil geochemistry was contributed to this study by Newmont Gold Corporation (Appendix B), as was location, survey, and geochemical data for 21 drillholes (Appendix C). Newmont had a large exploration program in the Gold Hill district from roughly 2013 to 2017. The geochemical and drillhole data are included in this study as-is, as information on methodology is not available, though it is the opinion of the author that these results meet a high level of technical and analytical rigor.

Geophysics

Aeromagnetic and aeroradiometric data over the Gold Hill district and surrounding region supported mapping and mineral resource assessment (Appendix D). The geophysical data were contributed to this study by Newmont, who flew the survey in 2015 as part of a research and development test of a new in-house airborne system during their exploration in Gold Hill. Line spacing for the survey was 650 ft (200 m) and the lines were flown east-west, perpendicular to the prevailing structural fabric of the district. Aeromagnetic data was flown at a clearance of 200 ft (60 m) and aeroradiometrics were flown at 275 ft (85 m) clearance. Further information on instrumentation and database fields is provided in Appendix D; base station location is not known, nor are details of any specific calibrations. The data are presented as-is since further technical details of the surveys are not available.

RESULTS AND DISCUSSION

District Development

“...one of the most geologically complex mining districts in Utah.” -Krahulec, 2017

Jurassic Pluton Emplacement

The Jurassic pluton (156–152 Ma; Stacey and Zartman, 1978; Burwell, 2018; White, 2023) in the Gold Hill district is one of the major geological features of the district, as well as one of the only absolute age constraints on the early evolution of the district. Compressional deformation and tectonic setting of Jurassic magmatism in eastern Nevada and western Utah has long been a topic of research and multiple models exist. The onset of compressional deformation in the hinterland is regionally estimated to have been Middle to Late Jurassic

(Camillari and Chamberlain, 1997; Smith et al., 2013; Zuza et al., 2020; Di Fiori et al., 2021). Shortening is interpreted to have ended, or relaxed, as magmatism ramped up ~160 Ma due to regional observations of Jurassic plutons cutting strike-slip and normal faults (Stacey and Zartman, 1978; Allmendinger and Jordan, 1984; Miller and Allmendinger, 1991; Miller and Hoisch, 1995). Accordingly, the Jurassic plutons in eastern Nevada and western Utah are interpreted to have been emplaced in this low stress field induced by subdued regional deformation (White, 2023). However, consensus on the cause of the change in stress regime has not been reached, and some studies suggest possible continuous compressional deformation from the Middle-Late Jurassic to the Late Cretaceous (Long, 2019; Zuza et al., 2020). The relationship between Jurassic plutons and normal faults has generated a range of models relating to Jurassic magmatic emplacement, such as intrusion through thermally thinned crust, transtensional pull-aparts, presence of back-arc setting during the Jurassic, or broad strike-slip shear zones (Miller et al., 1989; Wright and Wooden, 1991; Miller and Allmendinger, 1991; Elison, 1995; Miller and Hoisch, 1995; Rowley, 1998; Robinson, 2005; Barton et al., 2011). However, there has been no direct research on the stress regime or emplacement mechanism of the Gold Hill pluton.

Jurassic pluton emplacement occurred at shallow depths both regionally (2.5–7.5 mi [4–12 km]; Miller and Hoisch, 1995) and at Gold Hill (2–3 mi [3–5 km]; Burwell, 2018), suggesting accommodation of the plutonic volume was accomplished through uplift of the overlying rock. Plutons are typically thought to emplace through methods such as diapirism and stoping, and emplacement is known to be influenced by pre-existing structures, i.e., structural inheritance (Liu et al., 2020; Langenheim et al., 2021). Given that the pre-existing structures in the Gold Hill district were dominated by compressional deformation, compressional structures such as thrust faults are a candidate to control pluton emplacement, particularly if compressional deformation was ongoing during pluton emplacement; hence, synkinematic (i.e., during active compression) emplacement of plutons along thrust faults is considered a possibility in Gold Hill. Analog modeling studies on granitic emplacement in shallow compressive regimes demonstrate that thrust ramps can act as conduits for magma ascent and flats or flexures in faults serve as sites for emplacement (e.g., Mohammad and El Kazzaz, 2022). Field-based structural studies delineate a thrust ramp model for emplacement in fold and thrust belts (e.g., Kalakay et al. 2001). Features of synkinematic pluton emplacement include elongation parallel to the main thrust, a sharp thrust-side margin, and intense thrust-side deformation of country rock (Musumesci et al., 2005; Montanari et al., 2010; Ferre et al., 2012).

At Gold Hill, the Ochre Mountain thrust (OMT) is the most significant thrust feature in the district. The Jurassic pluton has a general north-south elongation, roughly parallel to the OMT, which has a northwest-southeast to north-south orientation. However, since the Gold Hill area is interpreted to sit

on the thrust flat above the ramp of the OMT, which would occur somewhere to the west, the mapped trace of the OMT is not necessarily the structure that would have controlled emplacement of the pluton. A duplex structure on the OMT, as suggested in Robinson (1993), could provide the structural architecture needed proximal to the observed location of the Jurassic pluton, although an imbricate thrust system may be more appropriate for the intensity and depth of deformation in Gold Hill. It is worth noting that Jurassic plutons at the nearby Newfoundland Mountains cut thrust faults (Allmendinger and Jordan, 1984), so pre-existing structures do not always exert controls on emplacement.

Unlike the synkinematic model, the Jurassic pluton in Gold Hill does not have a sharp thrust-side margin at the current exposure level. The western margin of the pluton is irregular and embayed by Paleozoic bedrock units. This pattern possibly indicates the pluton is thinning to the west, which would negate a synkinematic emplacement model. Intense deformation of the Paleozoic bedrock on the western margin of the pluton is some of the strongest carbonate deformation observed in the district, manifesting as tight folds, small scale thrust, and locally penetrative strain (Figure 7). This deformation could be interpreted as thrust-side deformation, although it may also be related to younger deformation from the Ferguson detachment (Silberling and Nichols, 2002).

Analog modeling of basement architectures similar to Gold Hill, i.e., hosting thicker rheologically competent strata separated by thin viscous strata (analogous to limestones separated by shales), suggests the potential for the viscous strata to act as a lubricant during thrusting and magma emplacement, re-

sulting in the uprooting of a basement block (Musumeci et al., 2005). In Gold Hill, the block of Paleozoic basement in the Jurassic pluton has traditionally been interpreted as a roof pendant (Robinson, 1993; Robinson, 2006); an alternate interpretation is uprooted basement strata detached along the easily deformed Chainman Shale. Current mapping does not support basement uprooting since much of the roof pendant is mapped as Ochre Mountain Limestone (Mills et al., 2023), which underlies the Chainman Shale. However, much of the roof pendant is metasomatized and bleached leading to difficulty in formation identification during mapping (see following section).

Geophysical data over the district delineates a notable change in the magnetic signature of the Jurassic pluton from south to north, adding another layer of complexity to understanding the pluton's architecture (Figure 8). There is a distinct shift in reduced-to-pole (RTP) magnetic data from magnetic high to magnetic low along a broadly east-west trend that cuts the pluton, roughly coincident with Rodenhouse Wash and the northern extent of the low-sulfidation epithermal system. This magnetic shift is not shown in the analytic signal derivation of the data, suggesting it is a remnant magnetic feature, and is notable for being perpendicular to the general structural fabric of the district. Previous exploration in Gold Hill noted east-west faulting in the Rodenhouse Wash, as well as arcuate north-south structures cutting through the pluton that host the low-sulfidation epithermal system. These structures were not confirmed during this study nor were maps from previous exploration showing these features available. It is unclear if these observations relate to an emplacement model; further study on the emplacement of and structural controls on the Jurassic pluton is needed.

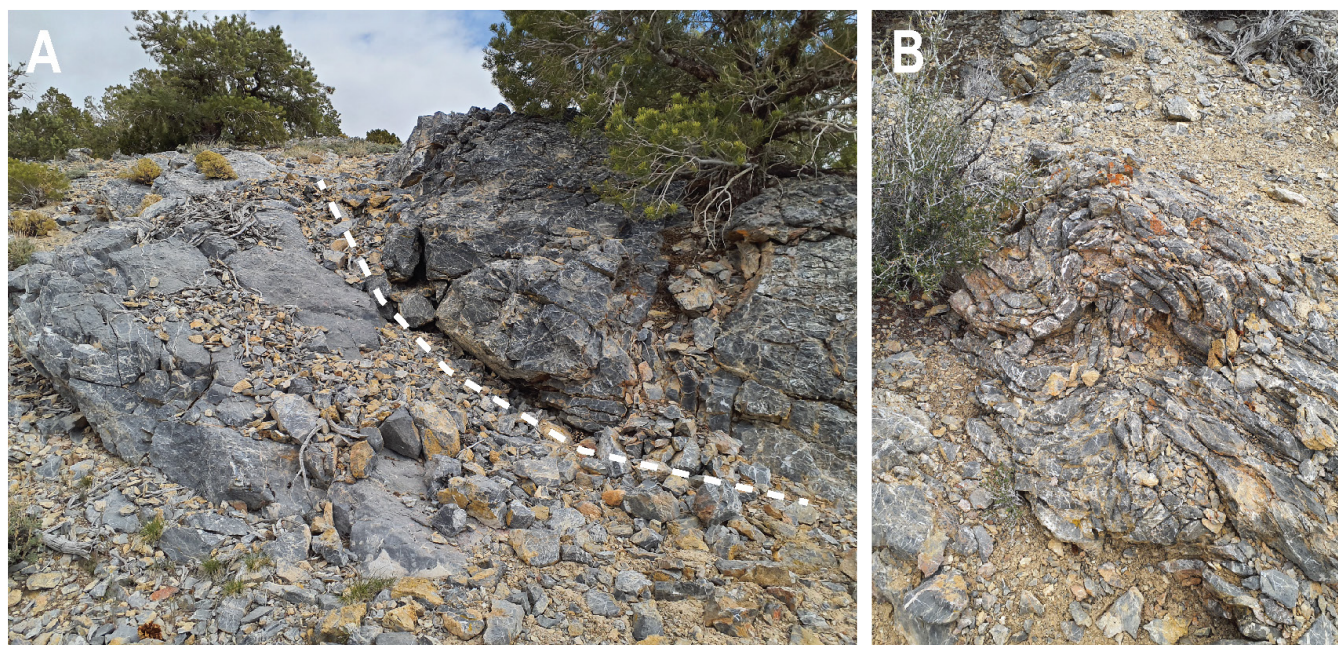


Figure 7. Deformation in Paleozoic carbonates near the contact with the Jurassic pluton. **A)** Dark gray Mississippian Ochre Mountain Limestone is locally thrust over lighter gray Pennsylvanian Ely Limestone (white dashed line showing faulted contact). **B)** Tight folding in a thinly bedded horizon of the Ely Limestone.

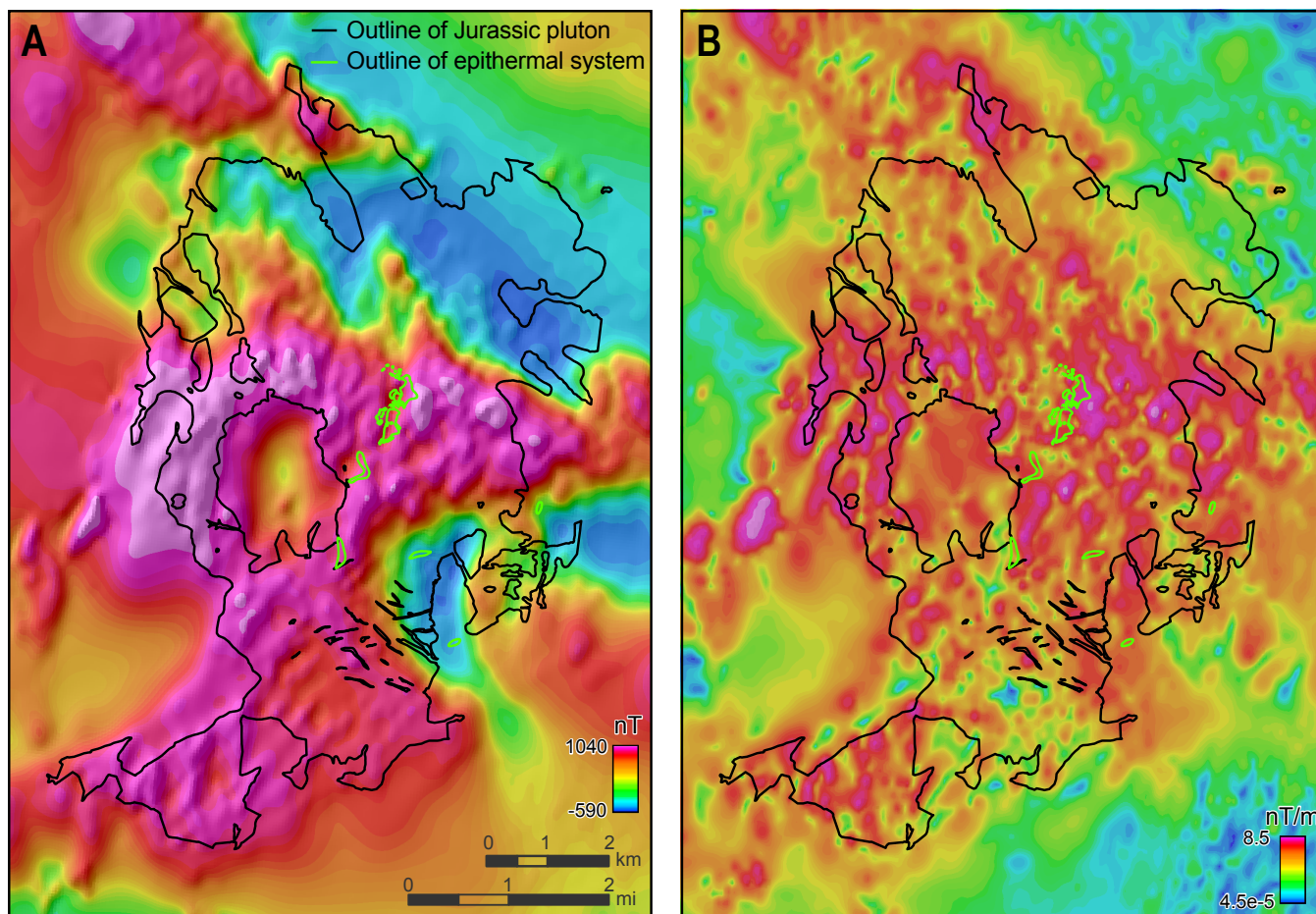


Figure 8. Geophysical magnetic signature of the Jurassic pluton. Black outline shows mapped extent of the Jurassic pluton at surface, green outline shows the mapped extent of the low-sulfidation epithermal system at surface. **A)** Total field reduced to pole (RTP) magnetic signature in units of nanoTesla (nT). **B)** Calculated magnetic analytic signal (ASIG) signature in units of nanoTesla per meter (nT/m).

Ferguson Detachment and Chainman Shale

The Chainman Shale is a well-known stratigraphic unit in the Basin and Range. The Chainman is a Mississippian unit (Osagean to late Chesterian) and stratigraphically overlies the Mississippian Ochre Mountain Limestone and underlies the Pennsylvanian Ely Limestone in the Gold Hill district (Mills et al., 2023). Regionally, the Chainman is a transitional slope facies shallowing from moderate to shallow depths and comprises carbonaceous fissile shale with minor interbedded fine quartz-rich sandstone and micritic limestone (Robinson, 1993; Cook and Corboy, 2004). In western Utah, the thickness of the Chainmain Shale is generally between 1000 and 2600 ft (300–800 m; Bereskin et al., 2015). At Gold Hill, the unit is estimated at only 450 ft (140 m) thickness, and in some areas the Chainman is mapped as completely faulted out, i.e., Ochre Mountain and Ely Limestones in direct contact, absent along a mapped thrust fault.

Multiple studies at Gold Hill have cited the Chainman as a rheologically weak unit that accommodated deformation and was attenuated through multiple deformation events (Nolan, 1935; Welsh and Bissell, 1979; Robinson, 1993; Mills et al.,

2023). Welsh and Bissell (1979) described a regional reduction of thickness in Mississippian strata due to thrust faulting, describing the result as a “grandiose chaos of nappes.” Hence, the concept of shale-rich units acting as lubricant strata in a compressional thrust setting during Jurassic compression has been common for many decades. However, the mechanism through which the Chainman is proposed to have attenuated so drastically, i.e., from ~1300 to 450 ft (~400–140 m), is not discussed. There is an abundance of research on shale deformation in fold and thrust belts (e.g., Morley et al., 2017, and references therein) that show shale accommodating deformation and acting as a viscous unit, particularly in a basal thrust setting. Analog and field examples do not demonstrate the wholesale removal of a shale unit, rather that the shale “flows” to another part of the deforming system. Shale often accumulates at the base of a thrust ramp, along the ramp itself, or, in extreme examples, the shale flows around and envelopes dismembered blocks of rheologically stiffer units (sandstones, limestones). None of these examples are a directly translatable example to explain the loss of the Chainman Shale at Gold Hill.

Recent work by the UGS mapping the Wildcat 30' x 60' quadrangle has highlighted the importance of the Ferguson

detachment (Silberling and Nichols, 2002) in the Gold Hill area (Don Clark, Utah Geological Survey, verbal communication, 2025). The Ferguson detachment extends from Nevada in the west and possibly terminates near Gold Hill, where the Jurassic and Eocene plutons may have played a role as a rigid body stopping or deforming the detachment sheet. The hanging wall of the Ferguson detachment is interpreted to have slipped eastward along the Chainman Shale, and this type of regional detachment faulting could account for the thickness loss in Gold Hill, particularly given the massive thicknesses of Chainman accumulated on either side of Sugarloaf Peak and Whitehorse Mountain in Nevada (Silberling and Nichols, 2002). The Ferguson detachment is a modern interpretation of Welsh and Bissell (1979)'s "grandiose chaos of nappes," where large sheets are mobilized along the Chainman but in a detachment rather than thrust setting. The timing of the Ferguson detachment is broadly Cenozoic, but the hanging wall of the detachment is cut by high-angle Basin and Range era structures in the Ferguson Flat area bracketing the detachment to pre-Basin and Range extension (Ketner et al., 1998; Silberling and Nichols, 2002).

In Gold Hill, an interesting piece of Chainman Shale history is found in the block of Paleozoic strata within the Jurassic pluton (traditionally interpreted as a roof pendant, e.g., Nolan [1935]). In this block, heavily faulted Ochre Mountain Limestone is mapped in direct contact with Ely Limestone, suggesting that the Chainman Shale is faulted out between these two layers. Because the block is hosted in the Jurassic pluton, the Ochre Mountain-Ely faulted contact has implications for the timing of Chainman attenuation. If dominantly removed through compressional deformation, the Ochre Mountain and Ely would be in contact prior to emplacement of the Jurassic pluton and the block could be "frozen" within the pluton, not requiring further deformation. However, if the Chainman was dominantly removed through detachment faulting, this would require extreme deformation of the Jurassic intrusion surrounding the Paleozoic block during the Cenozoic. Currently there is not enough detailed mapping to delineate whether Cenozoic removal of the Chainman is possible in the Paleozoic block, but defining this relationship could present a key piece of evidence for interpreting the structural evolution of Gold Hill.

A factor influencing attempts to define the structural history associated with the Chainman Shale is the difficulty differentiating between Ochre Mountain and Ely Limestones, particularly where bleached and/or silicified in proximity to intrusive units. Because of the intense faulting in the district, helpful contextual stratigraphic relationships are rare to assist in unit identification, and the few differentiating features between the Ochre Mountain and the Ely are often obscured in later bleaching or marbleization (Figure 9). Much of the proposed fault architecture in the Gold Hill area is based on the relationship between lithologic units due to the poor exposure of actual fault traces, and if units are incorrectly identified, structural interpretations would need to be revisited.

The main takeaway from the absence of the Chainman within large parts of the district is that the structural deformation is complex, multi-generational, remains to be fully understood, and may be able to accommodate alternative structural histories. Recent recognition of the potential role of the Ferguson detachment fault in the history of Gold Hill has significant implications for mineral exploration, as detachment faulting may displace shallow, traditional mineral vectors (e.g., alteration, veining, etc.) from their source at depth.

Clifton Flat and the Gold Hill Wash Fault

Despite being a significant geologic feature within the district, there is very little discussion on the formation of the Clifton Flat basin in previous literature. It is cited more commonly as a geographic feature. However, the formation of Clifton Flat warrants further consideration, as it is regionally somewhat unique to have a smaller basin internal to an area of consistent geology, e.g., the same Paleozoic units on all sides of the basin. In contrast, many basins in the hinterland formed as a result of Basin and Range extension and geology changes significantly between margins of the basin, indicating major structural boundaries.

Clifton Flat basin is surrounded dominantly by the Ochre Mountain and Ely Limestone on all sides. The south side of Clifton Flat is nearly adjacent to the Blood Canyon fault of Nolan (1935). The Blood Canyon fault was separated into the Christiansen Canyon and Midas faults in Mills et al. (2023). The Christiansen Canyon and Midas faults are regionally significant features that represent a major tectonic transition from the moderately west-dipping Cambrian sequence of the Deep Creeks to the intensely faulted Mississippian-Permian sequence of Gold Hill (Figure 4). Over 1 mi (1.5 km) of Ochre Mountain/Ely Limestone outcrops between the fault traces and the southern margin of Clifton Flat. The northern end of Clifton Flat is partially bounded by the Skinner Spring fault (Mills et al., 2023), a steep oblique-slip fault.

The Gold Hill Wash (GHW) fault, like Clifton Flat, is a notable geological feature in the Gold Hill district that has received relatively little study. The fault was first identified in Robinson (1987) and included in Robinson (1993). In these studies the fault is identified as having strike-slip motion on the order of 2500 ft (750 m) based on offset in other faults. The age of the youngest movement on the fault is constrained to 10 Ma by Robinson (1993), who also notes that the fault was likely a major zone of weakness since the Mesozoic. The GHW fault is interpreted as the boundary between the Jurassic and Eocene pluton and as a structural control on the emplacement of the Eocene stock(s). The Ochre Mountain thrust (OMT) is northwest-southeast trending and is considered to represent the earliest stages of Jurassic deformation. Current mapping suggests the GHW fault cuts the OMT, offsetting the eastern extent of the exposed fault trace to the south. Hence the only age control on the GHW fault currently is that it is post-Late Jurassic, when the OMT was formed, and pre-Eocene, when

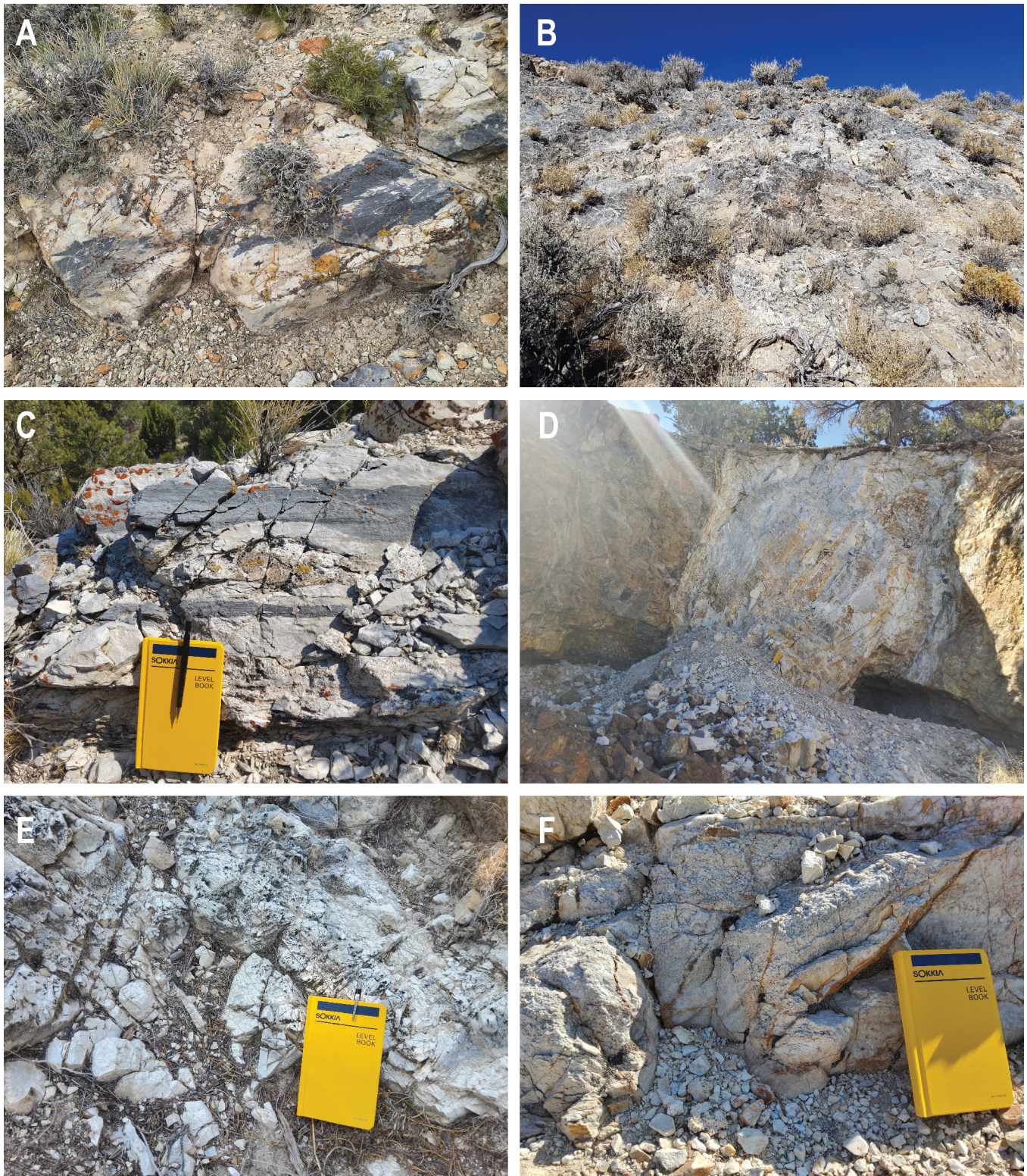


Figure 9. Examples of bleaching in the Ochre Mountain and Ely Limestones. **A)** and **B)** Partial bleaching of the Ely Limestone. **C)** Partial bleaching of the Ochre Mountain Limestone. **D)** Pervasive bleaching of a carbonate unit in contact with the Jurassic quartz monzonite, unit unidentifiable. **E)** and **F)** Pervasive bleaching and incipient recrystallization of carbonate lithologies, units unidentifiable. Photos C through F courtesy of Kayla Smith.

the granite stock emplaced. Some authors suggest Gold Hill was part of a transverse zone during Cenozoic extension (e.g., Rowley, 1998; Robinson, 2005), which would suggest the formation of the GHW fault was roughly contemporaneous with emplacement of the Eocene granite stock, given the close association of transverse zones and magmatism proposed for the eastern Great Basin. The GHW fault is roughly north-south trending and is mapped from north of the Eocene stock to the southeast corner of Clifton Flat, where several faults join.

The GHW fault forms the eastern margin of Clifton Flat. Aeromagnetic data show a continuation of the structure through the eastern margin of Clifton Flat, including an offset magnetic high, though the kinematics remain unclear (Figure 10). The magnetic high in the eastern part of the basin may represent volcanic deposits continuing under cover, as volcanics can be seen to follow the paleodrainage on the GHW fault to the north of the basin. Alternatively, the magnetic high may represent a buried intrusive unit, either part of one of the recognized systems or an unknown unit. Further investigation of the geophysical signature in the basin is warranted and more work is needed to fully understand the architecture, timing, and formation of Clifton Flat. The basin is a reasonable target for covered (“blind”) mineralization and because of the lack of exploration to date still represents a viable exploration target, which is discussed in more detail below.

Mineral Systems and Critical Mineral Potential

“It is possible that the existence of so many small ore deposits instead of a smaller number of large deposits is to be ascribed to recurrent fracturing.” Nolan, 1935

The Gold Hill district is characterized by multiple eras of ore generation. The earliest known mineralizing event was associated with the Jurassic quartz monzonite pluton, which created a variety of contact metamorphic and magmatic-hydrothermal deposits, such as skarn, replacement, possible iron-oxide copper gold (IOCG)-style, and vein deposits at the contact with the Paleozoic basement. The next known mineralizing event was associated with emplacement of the Eocene stock, which had a similar style of contact metamorphic and magmatic-hydrothermal mineralization but was less Cu-enriched and more W-enriched. A number of deposits are demonstrably magmatic-hydrothermal in nature but are located in the contact zone between the Jurassic and Eocene intrusions with no clear criteria for determining which was the causative intrusion (e.g., the Rube gold mine). The third clearly identified mineralizing event is a low-sulfidation epithermal gold system in the east of the district which hosts the Kiewit mine and was the subject of intense exploration by Newmont in the late 2010s. This system has an adularia K-Ar age of 8 Ma (Whelan, 1970).

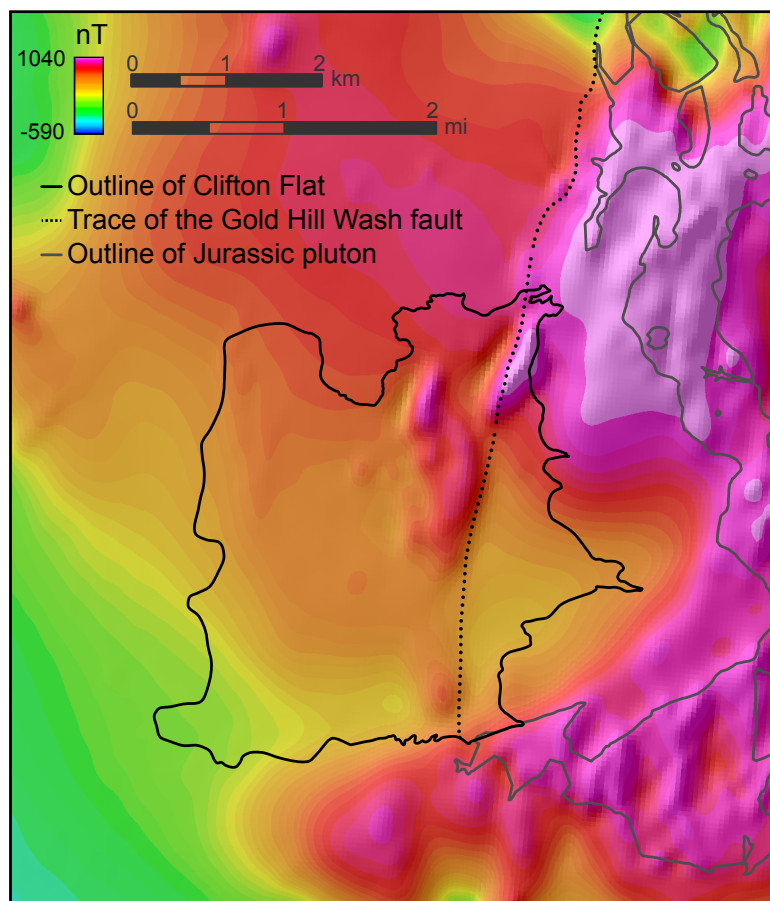


Figure 10. Total field reduced to pole (RTP) magnetic signature of Clifton Flat in units of nanoTeslas (nT).

The above deposit types have been well-defined within the district; however, a number of other deposit types have been the subject of exploration but not clearly delineated as a significant ore-forming event. Much of the exploration since the 1980s in Gold Hill has focused on the potential for sediment-hosted gold deposits, given the favorable carbonate stratigraphy and widespread jasperoid development. The dike swarm in Goshute Wash was another focus of exploration for the potential of a deeper Climax-type porphyry molybdenum deposit. Perhaps most compelling is the vein swarm at Clifton Shears, which has not been a significant focus of modern exploration.

Some of the earliest explorers in Gold Hill noted that the widespread faulting in the district may have surpassed the optimal point for transporting but also concentrating ore fluids, instead letting fluids leak out in multiple directions to form multiple small deposits instead of fewer larger deposits (Nolan, 1935; Chorney, 1943). Although Gold Hill has the most identified mineral occurrences of any mining district in Utah (Utah Geological Survey, 2023), this is in part due to the multi-generation history of the district, rather than a single event of ore fluid dispersion. However, despite the significant number of mineral occurrences, a mineral system at depth could remain and contain enough hydrothermal fluid and metal content to form a porphyry deposit, e.g., Chiaradia and Caricchi (2022).

The geological basis, potential, and critical mineral endowment of the mineral systems identified by this study are discussed below. The discussion centers around the genetic formation of these deposits and how they fit into the overall geological framework of the district; descriptions of individual deposits can be found in previous studies (e.g., Nolan, 1935; El-Shatoury and Whelan, 1970; Robinson, 2005; Krahulec, 2017).

Skarns and Replacement Deposits

Skarn deposits: Skarn deposits were one of the earliest recognized mineral deposits at Gold Hill and one of the most extensively mined (e.g., Alvarado, Cane Springs mines) (Figure 11). They have historically been called different names such as tactite, contact, and contact metasomatic deposits and have a range of mineralization and alteration styles within the district. Skarns form by the interaction of magmatic-hydrothermal fluids with carbonate host rock and are broadly broken into endoskarn (mineralization and alteration within the intrusive body) and exoskarn (mineralization and alteration present outside of the intrusive body, typically within limestone or dolomite), though these terms can be overly simplistic on an individual deposit scale (e.g., Xu et al., 2023). Skarns can form in both porphyry (e.g., Sillitoe, 2010) and IOCG (e.g., Groves et al., 2010) mineral systems, both of which are discussed in more detail below.

The metallic suite associated with skarns can vary greatly. At Gold Hill, the skarn suites have been separated by previous researchers into various categories based on metallogenic profile, e.g., Au-Cu, W, Au-W, W-Cu-Mo, Au(-Cu-Mo-Pb), and

Cu-Au-Ag-W-Mo skarns (Robinson, 2005; Krahulec, 2017; Burwell, 2018). This variety of classifications stems from early work on global skarn classifications that divided skarns based on their principal commodities (Einaudi et al., 1981; Meinert, 1992; Newberry, et al., 1997). With increasing research on skarn deposits, it has become more evident that rarely do skarns fit into primary or single commodity classifications (e.g., Chang et al., 2019). Additionally, the order in which researchers list the commodities of a skarn are not always related to the genetic formation of a deposit, but rather relate to economic importance. As a result, Au is often emphasized despite often being one of the least common metallic components.

Due to the first-order relationship between skarns and an intrusive body, it is more informative to separate the skarns of Gold Hill based on their association with either the Jurassic pluton or the Eocene stock. The skarns associated with the Jurassic pluton have a diverse metallogenic assemblage including Au, Cu, Mo, W, Ag, Pb, Zn, and Bi; however, the expression of these elements and associated gangue mineralogy can vary distinctly between deposits. The Alvarado deposit, for example, is generally referred to as an Au-Cu deposit and is considered a different class of skarn compared to the Rustler deposit, which is dominated by Mo mineralization. Yellow Hammer also has been considered a separate class of skarn to Alvarado and Cane Springs due to the presence of Mo and W. However, an extensive body of literature details the zoned nature of skarns (e.g., Einaudi et al., 1981; Bowman, 1998; Nakano and Ishihara, 2003; Chang and Meinert, 2008; Beinlich et al., 2019; Chang, 2021; Shu et al., 2024), and the Cu, Mo, W, Zn, Pb, Au, Ag metallogenic signature has been shown to be relatively common on an intrusion scale. The giant Jiama skarn in China, for example, contains Cu, Mo, Au, Ag, Pb, and Zn within the skarn system, along with local W occurrences (Shu et al., 2024). The Jiama system is zoned both vertically and laterally: Mo occurs dominantly in the endoskarn, Cu and Au occur within the exoskarn most proximal to the intrusion, Zn-Pb-Ag occur as the most distal exoskarn, and W mineralization is found in the deepest part of the system.

In the context of Gold Hill, which has a multi-generational structural network, complex contacts between multiple Paleozoic units, and potential post-mineral dismemberment, it is reasonable to conclude that any skarn zonation is fragmented. Additionally, hydrothermal fluid interaction with the Paleozoic basement versus the Jurassic pluton has distinct effects on the expression of a skarn deposit. The control on host rock can be seen in magnetite chemistry from the Lucy L deposit, hosted in Paleozoic basement, and the Yellow Hammer deposit, hosted in the Jurassic pluton (Figure 12), where the two populations have distinct chemistries despite both deposits occurring on the western margin of the Jurassic pluton (Carey, 2022). Evolution of ore fluids through time also plays a significant role in variable expressions of skarn deposits, demonstrated through scheelite chemistry in multiple deposits associated with both the Jurassic pluton and the Paleozoic basement (Reaper, Doctor, and Yellow Hammer; Figure 13). Early high-Mo cores in

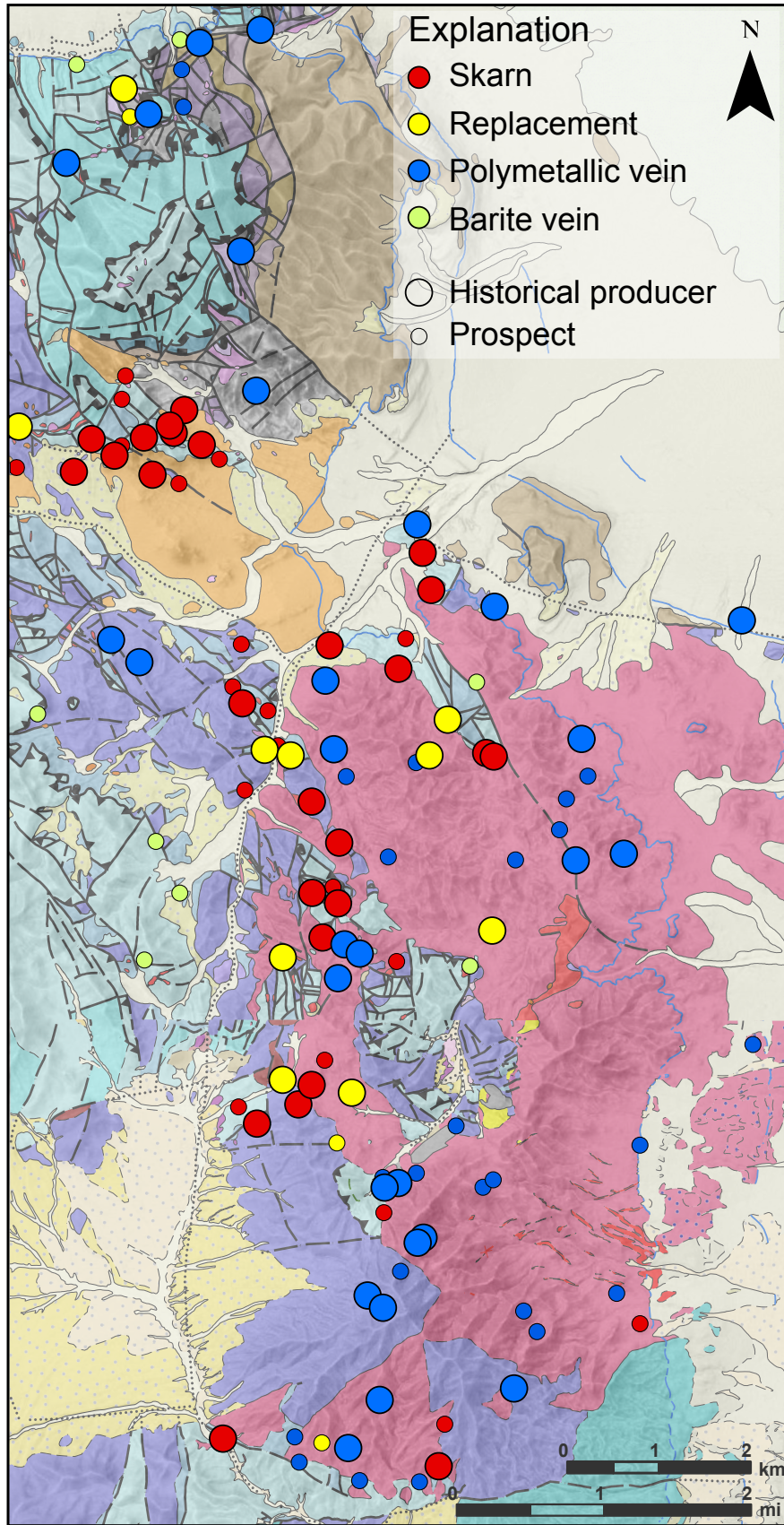


Figure 11. Deposit type classification of historically producing mines and prospects in the Gold Hill district. Geology as in Figure 4.

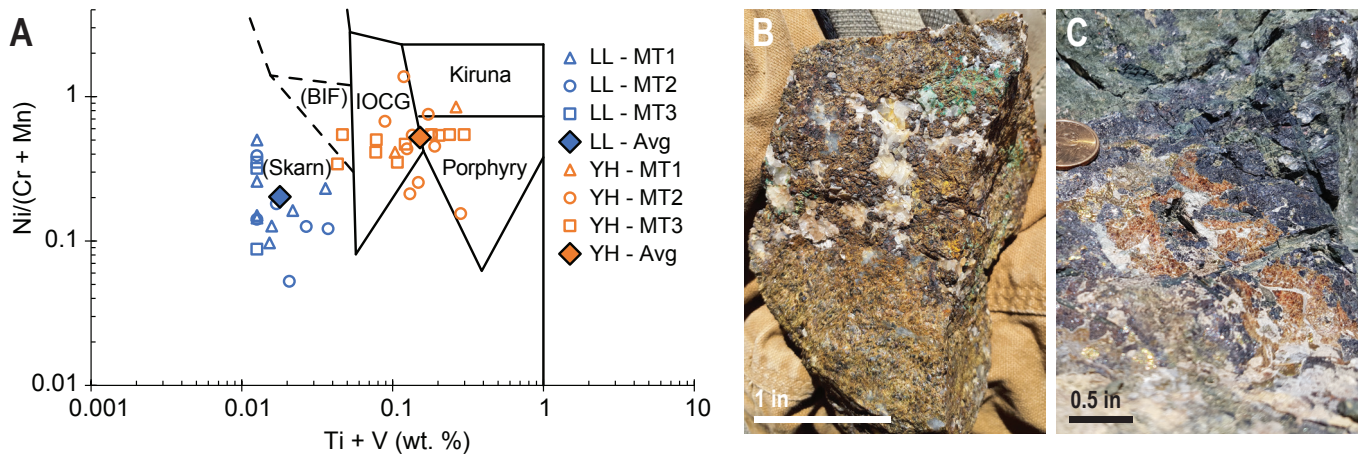


Figure 12. Magnetite chemistry and alteration examples from Lucy L (LL) exoskarn and Yellow Hammer (YH) endoskarn deposits. Modified after Carey (2022). **A)** Ni / (Cr + Mn) vs. Ti + V plot with discriminatory boundaries for deposit types proposed by Dupuis and Beaudoin (2011). Values are all in weight percent. All values below the detection limit were reported as half of the lower detection limit. **B)** An example of garnet-bearing exoskarn alteration from the Lucy L deposit. **C)** An example of garnet-bearing endoskarn alteration from the Yellow Hammer deposit.

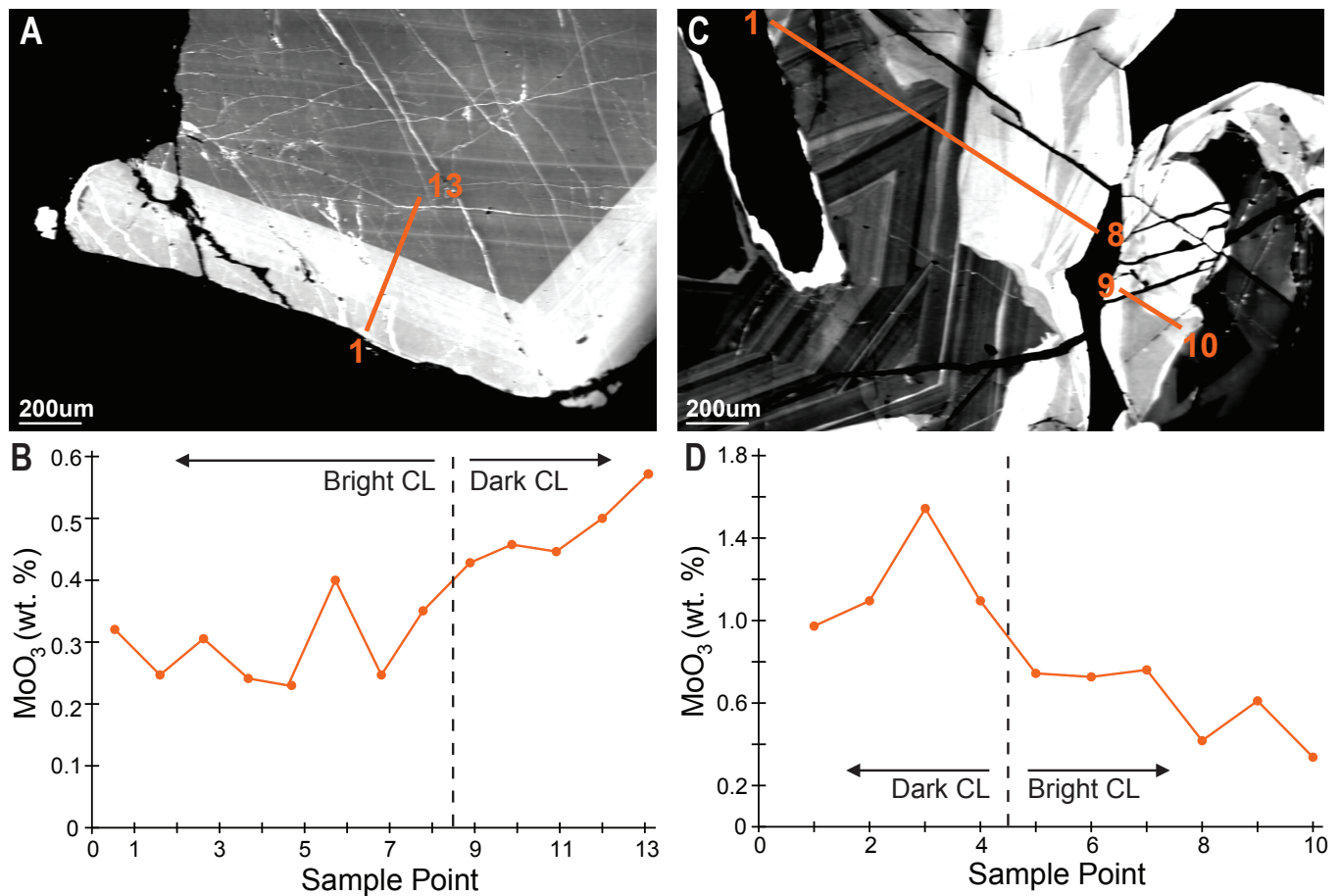


Figure 13. Molybdenum concentration variation of zoned scheelite related to changes in cathodoluminescence (CL) response. Modified after Carey (2022). **A)** CL image of a scheelite grain from sample RU001 (Rustler deposit) showing the electron microprobe transect measuring molybdenum concentration, with results shown in **B)**. **C)** CL image of a scheelite grain from sample YH044a (Yellow Hammer deposit) showing the electron microprobe transect measuring molybdenum concentration, with results shown in **D)**.

scheelite crystals demonstrate evidence for dissolution prior to the precipitation of low-Mo rims, which are associated with the ore-forming stage (Carey, 2022). The occurrence of high-Mo cores and low-Mo rims in scheelite has been observed at many deposits and is hypothesized to represent different ore-forming processes, such as early reduced ore-forming fluids that gradually oxidize (Meinert, 1995), initiation of molybdenite precipitation removing Mo from the ore fluid (Su et al., 2019), or leaching of Mo from the scheelite rim to form molybdenite (Zhan et al., 2021). Initiation of molybdenite precipitation removing Mo from the ore fluid is favored by Carey (2022), though the evidence for dissolution on the original Mo-cores suggests there may have been some degree of leaching due to either Mo scavenging or ore fluid chemistry changes, thus demonstrating another avenue for variation between the Jurassic skarn deposits, while still all being driven by the same Jurassic magmatic-hydrothermal system.

The term polymetallic skarns is preferred when referring to the Jurassic skarns, particularly in discussion of genetic formation over economic exploitation. Though an imperfect solution, the general term “polymetallic” avoids deeper entrenchment of artificial model-driven differences between the deposits.

The W-only skarns are reasonable to classify separately from the polymetallic skarns, because they are spatially associated with the Eocene stock as opposed to the Jurassic pluton, and hence have a different magmatic-hydrothermal source. The Eocene intrusion is also oxidized; both the Jurassic pluton and the Eocene stock host magnetite-titanite-quartz assemblages suggesting a relatively oxidized composition (Wones, 1989), but the Eocene has a stronger crustal signature (Stacey and Zartman, 1978). Tungsten skarns can form from both reduced or oxidized magmas because tungsten behaves incompatibly regardless of oxidation state (Candela and Bouton, 1990; Meinert, 1995), though oxidized systems tend to be smaller. Very little work has focused on the Eocene stock since the Pb and Sr isotopic study of Stacey and Zartman (1978), which

was the first to identify the northern stock as a different magmatic unit than the Jurassic pluton and assigned an upper crustal source to the Jurassic pluton and a metamorphosed lower crustal source to the Eocene stock. Stacey and Zartman (1978) identified a consistent Pb isotopic signature in the Jurassic intrusion and associated ore deposits, supporting the genetic relationship described above. However, the deposits sampled around the Eocene stock did not have a collinear relationship with the Pb isotopes of the stock itself, leading the authors to suggest that a genetic relationship between the deposits and stock cannot be established. This assertion has been repeated by subsequent researchers as a generalized statement for deposits around the Eocene stock (e.g., Robinson, 2005). However, the deposits sampled for the study were Garrison, Rube Lead mine, Spotted Fawn, and Dutch Mountain, all of which are classed as polymetallic replacement veins and none of which occur within the cluster of W skarns on the northern margin of the Eocene stock. The implications for the source of the polymetallic veins is discussed in the following section, but for the purposes of the W skarns there is no evidence to suggest they are not genetically related to the Eocene stock.

The lack of attention to the W skarns associated with the Eocene stock is nowhere more clear than in their omission from the most comprehensive mineral reports on the district, such as Nolan (1935) and El Shatoury and Whelan (1970). Instead, brief descriptions of the major workings of the Eocene W skarns are contained in Everett (1961), and Lemmon (1969) notes that the majority of the 250,000 lbs of WO_3 produced from the Gold Hill district was from the E.H.B., B. Estelle, and Fraction Lode mines, all of which are associated with the Eocene granite. Despite the fact that these Eocene-associated mines are the reason Gold Hill is the top tungsten producing district in Utah, there is a dearth of detailed descriptions, paragenetic study, or genetic interpretation. The deposits are associated with a prograde assemblage of andradite to grossular garnet, epidote, quartz and calcite (Figure 14). Scheelite is the tungsten ore mineral and occurs in massive calc-silicate veins with very little sulfide content (Krahulec, 2017).

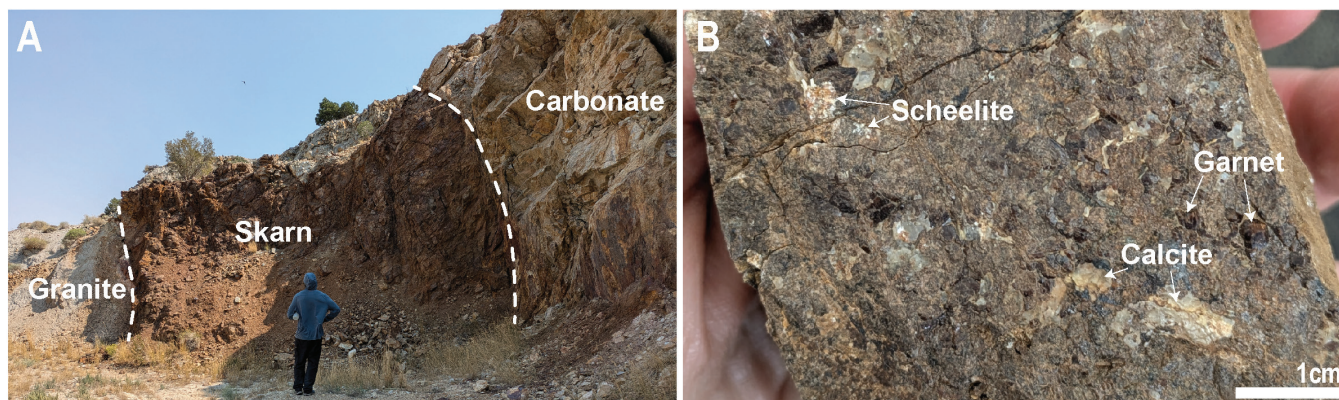


Figure 14. Example of outcrop and alteration from W-bearing skarn around the Eocene granite. **A)** Outcrop of the skarn at the Fraction W mine (location on Figure 2) showing sharp fault-bounded contacts with the Eocene granite and the Paleozoic carbonate. **B)** Hand sample of skarn alteration and mineralization from the Fraction W mine showing garnet, calcite, and scheelite.

Replacement deposits: Previous researchers noted the occurrence of replacement deposits in the Gold Hill district (Figure 11). Often, replacement deposits are lumped in with polymetallic veins, or called replacement veins. However, given the character and spatial distribution of replacement deposits versus polymetallic veins at Gold Hill it is deemed appropriate to classify replacement deposits more similarly to the skarn deposits. In the classic model for replacement deposits in carbonate terranes (e.g., Megaw et al., 1988; Titley, 1996), replacement deposits are a distal expression of skarn systems, occurring as chimneys, pods, and tabular bodies (often referred to as blankets or mantos) away from the main contact with the intrusion or associated with secondary intrusive bodies (sills and dikes) as opposed to a central stock or pluton. Replacement deposits may still be characterized by calc-silicate alteration assemblages; however, an important difference to skarns is that mineralization occurs as zones of massive sulfide that are interpreted to completely replace, rather than alter, the host rock. Structural features such as faults and fracture networks are the main control on the formation of chimney and pod deposits. Stratigraphy is a strong control on tabular bodies, which are stratigraphically discordant but can be continuous along specific horizons, or can form beneath impermeable shale units (fluid ponding). As with many ore deposit models in magmatic-hydrothermal settings, skarn deposits and replacement deposits exist on a continuum and may grade into one another.

The Gold Hill mine (Gold Hill mine of the Western Utah Copper Co.) and the U.S. mine (Gold Hill mine of the United States Smelting, Refining, and Mining Co.), the two major producers of arsenic in the district, are classified as arsenic replacement deposits. Ore from these deposits contains in excess of 20% arsenic and these mines account for nearly 80% of the total historical value for the Gold Hill district. The arsenic orebodies occur within the Ochre Mountain Limestone and it is noted that arsenic mineralization does not occur within calc-silicate altered limestone, rather it replaces unaltered limestone (Nolan, 1935). In both mines, arsenic ores occur as massive zones controlled by the intersection of a fault cutting the beds perpendicular to strike and bedding-parallel fractures, thereby creating a network for fluids to reach the site of deposition with relatively little wallrock interaction and then penetrate along bedding. The orezone is oxidized to scorodite at the Gold Hill mine (Figure 15A), but at U.S. mine, ore occurs as a ~30 ft (10 m) zone of massive sulfide dominated by arsenopyrite. Arsenopyrite from the massive sulfide zone was rarely observed to have a bladed habit; however, the majority of the arsenopyrite has been brecciated (Figure 15B). The paragenesis interpreted by Nolan (1935) is early bladed arsenopyrite, followed by brecciation and introduction of pyrite, followed by further brecciation and introduction of quartz and base metal sulfides (galena, sphalerite, and chalcopyrite). Both Gold Hill and U.S. mines produced minor Ag and Pb from ore shoots that occurred on the margins of or distal to the massive sulfide zone, and are paragenetically older than the arsenic ore. Cobaltite also occurs as well formed crystals

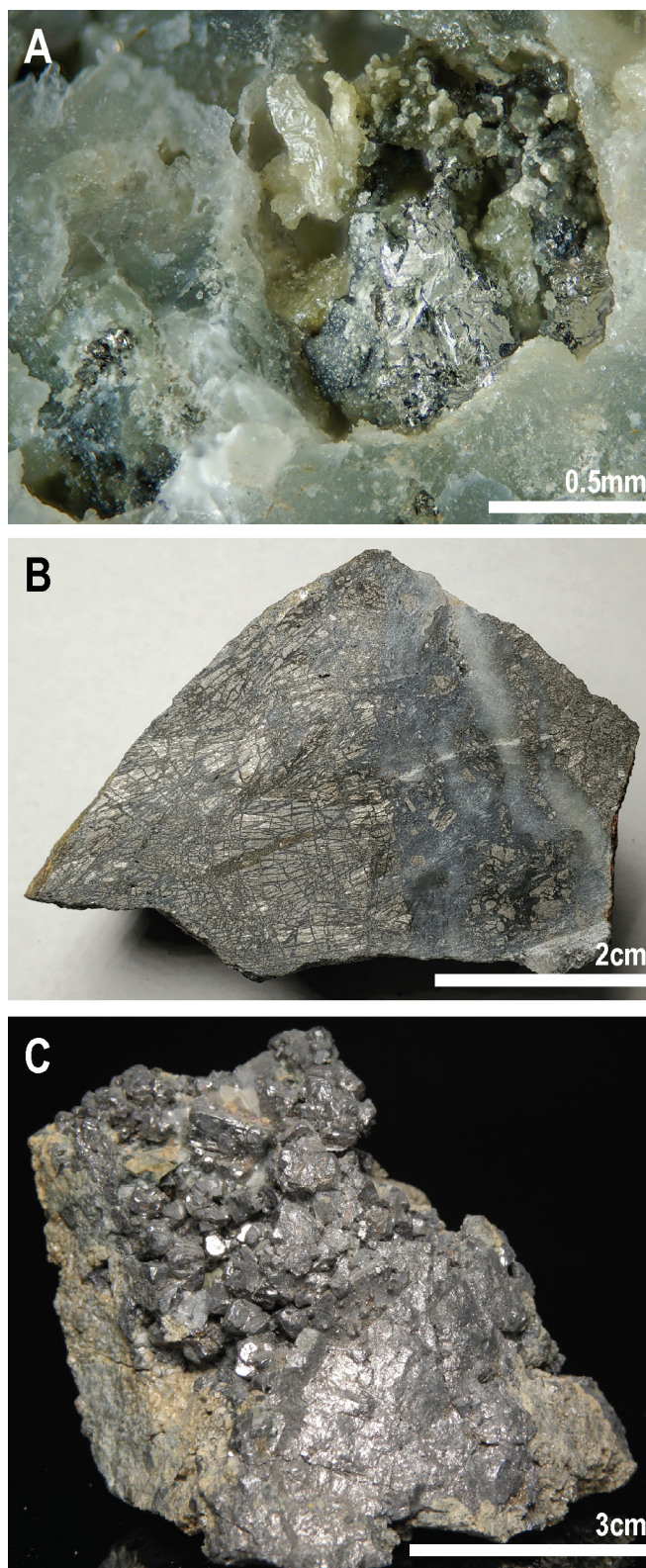


Figure 15. Ore minerals from the Gold Hill and U.S. mines. **A)** Metallic arsenopyrite oxidizing to green scorodite in a vug of quartz and scorodite from the 300-ft (90 m) level of the Gold Hill mine. Photo credit Alex Earl. **B)** Shattered metallic arsenopyrite and quartz from the U.S. mine. Photo credit Bob Werner, provided by Gabe Cangelosi. **C)** Euhedral cobaltite crystals from U.S. mine, associated with erythrite, arsenopyrite, and native silver. Specimen credit Rick Dalrymple Collection, photo credit Adrienne McElwain.

at Gold Hill mine, though the paragenesis is unknown (Figure 15C). Quartz-tetrahedrite veins are present at the Gold Hill mine and also postdate the arsenic mineralization. The limited high-grade Cu ore from the Gold Hill mine was also enriched in arsenic, and Nolan (1935) proposed supergene leaching of copper from the quartz-tetrahedrite veins to account for the copper enrichment.

Arsenic is a common element in various hydrothermal systems (e.g., Ballantyne and Moore 1988; Aehart et al., 1993; Large et al., 2009; Wu et al., 2020). Examples of extreme arsenic-enriched ore systems exist within orogenic (Baccu Locci [Zucchetti, 1958], Czarnów [Mochnacka, 2009]), epithermal (AntaKori [Eggleston et al., 2019]), and polymetallic vein (Odenwald, [Burisch et al., 2017]) ore deposits. Very little literature and research on arsenic replacement or skarn deposits exists. The lack of arsenian skarn/replacement research is likely due less to the rarity and more to the lower economic importance, negative environmental associations, and/or relatively new focus on skarns as an independent deposit type (e.g., Chang et al., 2019). Recent literature on the arsenic-enriched Yiliu skarn in China (Wang et al., 2024) details the occurrence of arsenopyrite as the dominant sulfide phase rimmed or replaced by other base metal sulfides, suggesting it forms as an early paragenetic phase, similar to Gold Hill. The arsenic orebodies at Yiliu form both in limestone and skarn (interpreted as endoskarn), and the limestone-hosted bodies are the larger, higher grade deposits (Wang et al., 2024). Given the early formation of arsenopyrite in both deposits and arsenic mineralization under reduced conditions (e.g., Scharrer et al., 2020), it is possible that the Gold Hill and U.S. mines represent an early reduced ore fluid pulse that evolved to more oxidizing fluid as the magma crystallized (Bell and Simon, 2011). It seems unlikely that wallrock interactions were a significant contributor to such As-enriched mineralogy given that multiple other deposits in the district are hosted in the Ochre Mountain Limestone with no evidence of significant arsenopyrite formation.

The Reaper group of deposits: Previous researchers at Gold Hill have suggested the occurrence of a third class of deposit in the skarn-replacement deposit spectrum. Particularly Reaper, but also Yellow Hammer, Rustler, Centennial, and Enterprise mines have been variously described as pegmatite veins, pipe-like deposits, replacement pegmatite, pegmatite dike, or pegmatite pipes (Butler et al., 1920; Nolan, 1935; Chorney, 1943; Everett, 1961; Krahulec, 2017; Burwell, 2018). Pegmatites are texturally defined as a magmatic rock comprising coarse (>0.5 in [>1 cm]), well-formed, interlocking crystals. Compositionally, pegmatite typically refers to silica-rich, highly evolved, late stage magma that is enriched in volatiles and incompatible elements such as Li, B, and Nb. It is important to define the two different applications of the term pegmatite given the extraordinary increase in focus on pegmatite exploration for a variety of critical minerals, e.g., the Plumbago North pegmatite in Maine (Simmons et al., 2020).

The description of the Gold Hill deposits as pegmatites or similar originated with Butler et al. (1920) and Hess (1924) due to the large size of crystals at these deposits. Nolan (1935), which is generally accepted as the most complete reference on Gold Hill mineral deposits, questioned the propriety of using the term pegmatitic, as did El-Shatoury and Whelan (1970). Both Nolan (1935) and El-Shatoury and Whelan (1970) instead suggest classification as replacement deposits because of the confusion around genetic implications with the term pegmatite.

The description of the deposits as pipes or pipelike appears to originate in Nolan (1935) particularly with respect to the Reaper deposit, which is elliptical (30 by 60 ft [9 by 18 m]) at surface before narrowing to circular (20 ft diameter [6 m]) at 50 ft (15 m) depth, before becoming lenticular at 100 ft (30 m) depth. Nolan (1935) notes that the Reaper “pipe” clearly occurs at the intersection of two orientations of fractures, that veins of the same composition are associated with the deposits, that the pipes likely transition to a vein system at depth, and that the rounded pipe shape may be due to formation in the shallowest part of the quartz monzonite and potential fluid ponding at the contact to Paleozoic basement. These points suggest Nolan (1935) was describing a chimney-style replacement deposit before the term had been coined. The term pipe is problematic in current economic geology terms due to potential for confusion with other important ore features such as breccia pipes.

Despite disagreement with the term pegmatite and classification as replacement deposits by Nolan (1935) and El-Shatoury and Whelan (1970), and despite a clear structural explanation for the pipe-like shape of the deposits by Nolan (1935), both terms pegmatite and pipe-like have persisted into later literature (e.g., Chorney, 1943; Everett, 1961; Krahulec, 2017; Burwell, 2018; Carey, 2022) and reinforced a narrative that these deposits are “extremely unusual” (Crawford and Chorney, 1944). The large size of the crystals in the deposit is striking (Figure 16), but this has been inaccurately reported through time: Everett (1961) states that scheelite crystals at Reaper reach up to 24 in (60 cm). This statement is a misreport of information in Butler et al. (1920) which states that zones of massive scheelite mineralization were as thick as 24 in (60 cm), but that individual crystals were a maximum of 4 in (10 cm). Skarns, by definition, are coarse-grained deposits (Einaudi et al., 1981), and calc-silicate alteration is a mass loss reaction which creates space for the growth of large, euhedral crystals (Lentz, 2005).

The Reaper, Yellow Hammer, Rustler, Centennial, and Enterprise deposits are not genetically unique from the other deposits associated with the Jurassic pluton and are expressions of the same skarn-replacement spectrum of mineralization and alteration processes under variable local structural and lithological controls. Although local variations in mineralization can be significant on a deposit scale and should not be discounted, it is important to emphasize that the overall mineral system driving these deposits was the same. The terms

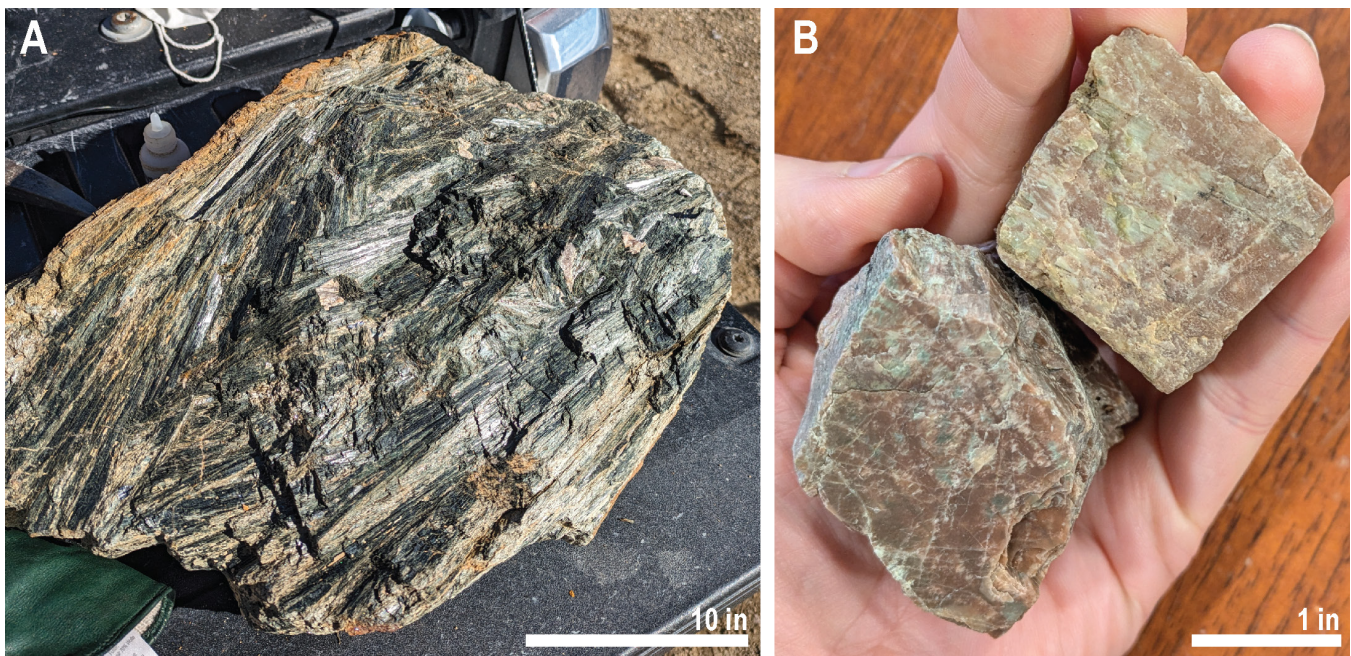


Figure 16. Large crystals from the Reaper mine. **A)** Large blades of actinolite. Individual blades up to 20 in (50 cm). **B)** Large orthoclase crystals (single crystal face shown).

pegmatite, pegmatitic, pipe, and pipe-like should be retired for the Gold Hill deposits. Without further detailed study it is difficult to determine if these deposits trend more towards the skarn or replacement model endmembers, a classification which should take place on a deposit-by-deposit basis rather than as a group.

Critical mineral potential: The arsenic replacement deposits are the highest potential critical mineral deposits at Gold Hill, since large As reserves are reported to remain at both the Gold Hill and U.S. mine (Dasch, 1969). Additionally, the presence of cobalt in these deposits is understudied. Cobalt enrichment is not discussed in any geological report on these deposits, but the presence of cobaltite is well known by mineral collectors. Further research on potential for accessory cobalt would be an important aspect of prospectivity in the arsenic replacement deposits. The presumed Eocene-age W skarns are also prospective given the relatively simple ore mineralogy and likely underexplored extents. The Jurassic polymetallic skarn deposits are demonstrated to host W and Bi as secondary commodities, e.g., Bi was a reported focus of mining at the Wilson Consolidated deposit (Everett, 1961), although it is unclear if any ore was ever shipped. Carey (2022) completed the first modern SEM-enabled mineralogical study of the Jurassic polymetallic skarn deposits, showing, for the first time, deportment of critical minerals such as Bi and Te in minerals such as bismuthinite, aikinite, and an unnamed Bi-Te-Se phase. Additionally, micron-scale Au in electrum was shown to occur both during the hypogene phase as inclusions in arsenopyrite and in the supergene phase hosted in anhydrite-calcite-iron oxide veins. This work highlights the complexity of sulfide ore in the polymetallic skarns and the difficulty of economic extraction of minor inclusion-hosted phases.

Vein Deposits

The variety of vein types described at Gold Hill over nearly a century of research and exploration is staggering. Replacement veins, polymetallic veins, fissure veins, pneumatolytic veins, shear veins, quartz veins, quartz-sulfide veins, beryllium veins, carbonate veins, barite veins, quartz-carbonate-adularia veins, quartz carbonate veins, and veins with silicate gangue are just some of the variety of vein descriptions that exist in literature. The variety, expression, and importance of polymetallic veins in Gold Hill are discussed below, as is the area defined as the Clifton vein swarm. Beryllium-bearing veins and quartz-calcite-adularia veins are discussed separately in the low-sulfidation epithermal section.

Polymetallic veins: The term polymetallic vein can refer to many types of veins in different mineral systems (e.g., Cox, 1986). At Gold Hill, the term generally refers to originally sulfide-rich Pb-Ag-Zn(-Cu-Au-As)-bearing veins (Figure 11) that occur as a distal expression of a magmatic-hydrothermal system, typically observed in the upper porphyry to epithermal environment, such as intermediate sulfidation veins with quartz-calcite gangue mineralogy (Einaudi et al., 2003). These veins are paragenetically late features that cut earlier alteration (potassic, sericite) and mineralization (disseminated Cu and Mo) assemblages (Fontboté and BendeZú, 2009). Although the overarching model for polymetallic veins suggests a relatively simple mineralization context, deposit-scale studies of these veins demonstrate complex multistage formation and a range of ore and gangue minerals on the meter to 10s of meters scale (e.g., Tomlinson et al., 2021). Examples of these veins and their context in a larger magmatic-hydrothermal system setting can be seen at Butte (Meyer et al., 1968),

Bingham Canyon (Tomlinson et al., 2021), and Resolution (Manske and Paul, 2002). Polymetallic veins have come under recent exploration focus due to their shallow, late expression and therefore their potential to indicate deeper magmatic-hydrothermal activity. Polymetallic vein assemblages, zoning, and orientation supported vectoring to the blind Stockton porphyry Cu deposit in the Oquirrh Mountains (Krahulec, 2014). Polymetallic veins are often lumped with replacement deposits because where the controlling structures intersect carbonate host-rock, the veins may transition to replacement-style orebodies. The variation between polymetallic veins and replacement deposits can be seen in mining districts such as Park City, Utah, which arguably has some of the most famous polymetallic vein and replacement deposits in the U.S. Polymetallic veins contain the highest Ag concentrations in the district, even though replacement deposits were typically larger and hosted more Pb and Zn (John, 2006).

At Gold Hill, polymetallic veins occur in association with both the Jurassic pluton and the Eocene stock, though the association to one or the other intrusive suite is based on spatial

proximity since direct age dating is lacking. Previously mined polymetallic veins associated with the Jurassic pluton (Walla Walla and Copper Hill in the north, Bonanza and Cyclone in the south) are small and share a common Pb-Ag-Zn(-Cu-Au-As) metallogenic profile (Figure 17). The main sulfide minerals in these deposits are galena, sphalerite, and pyrite, with lesser arsenopyrite and chalcopyrite. Many of the veins have been variably oxidized to plumbojarosite, cerussite, scorodite, chalcocite, and other lead, zinc, and copper oxides. Cyclone is noted as having aikinite occurrences, indicating the presence of Bi. The Rube Lead mine was genetically assigned to the Eocene stock in Stacey and Zartman (1978); however, the unique Pb isotope signature in the findings and reports by El-Shatoury and Whelan (1970) that identify quartz monzonite in the 200 ft (60 m) mine level suggest it is more likely genetically associated with the most distal extent of the Jurassic pluton. The Rube Lead mine produced Ag-enriched ore that has been oxidized to plumbojarosite and cerussite.

Polymetallic veins in the north spatially associated with the Eocene stock (Evans, Garrison, Silver Hill/Spotted Fawn, and

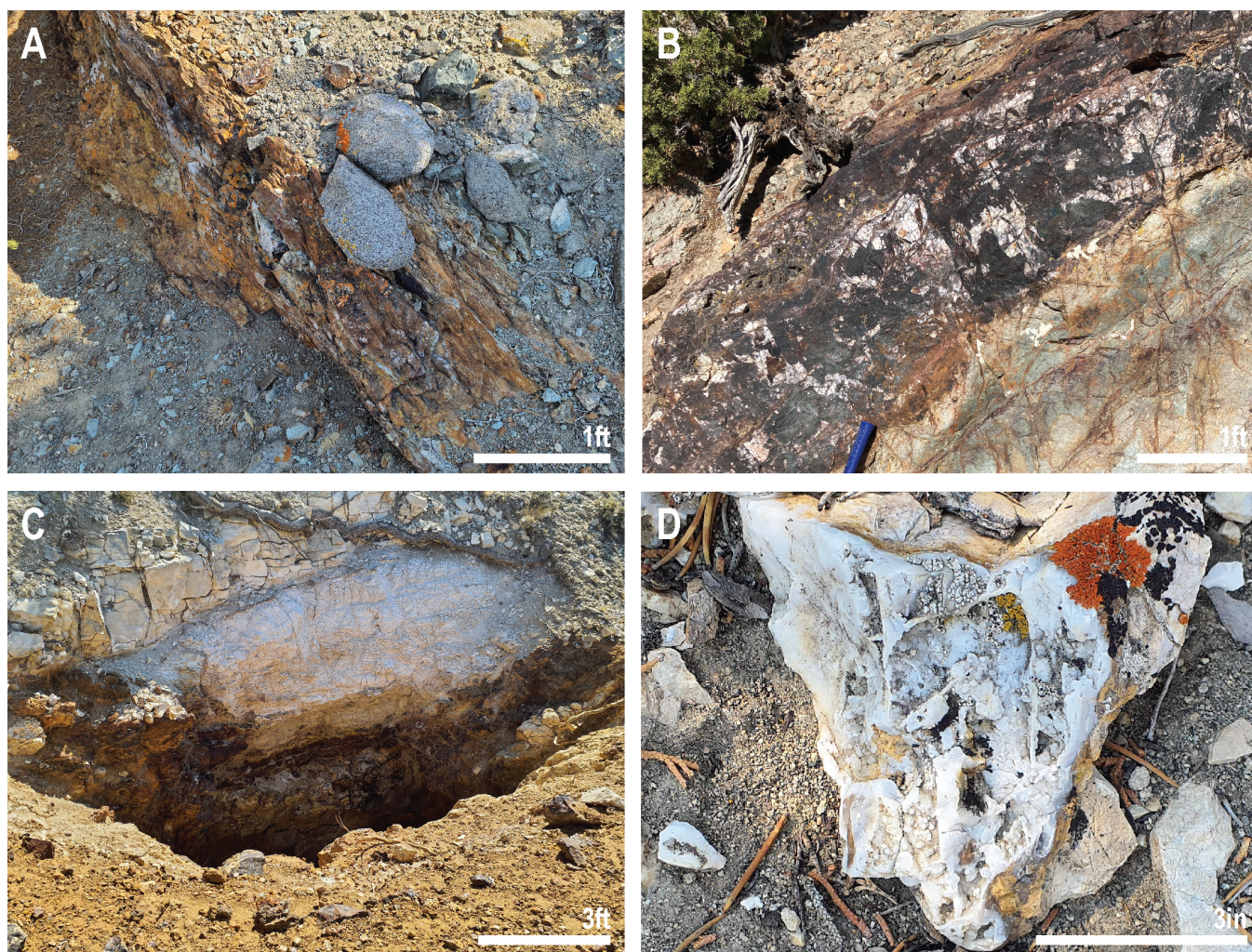


Figure 17. Examples of polymetallic veins in the Gold Hill district. **A)** Structurally controlled “fissure” vein in quartz monzonite. **B)** Vein with sharp contacts to the quartz monzonite exhibiting propylitic to argillic alteration haloes. Photo courtesy of Jim McVey. **C)** Irregular to massive vein in prospect pit. **D)** Complex silicification textures in a polymetallic vein.

Uncle Sam mines) are also Pb-Ag(-Zn) enriched but notably are associated with barite and minor Sn and W. This metallogenic profile is in agreement with the stronger crustal signature in the Eocene stock and the W skarns farther south. The Evans, Garrison, and Uncle Sam mines are ~2 mi (~3 km) from the closest outcrop of Eocene stock. That distance is farther from the intrusive source than the Jurassic-associated polymetallic veins, which is notable because the Eocene stock is a relatively small intrusion with a limited thermal aureole. There is no evidence for another mineralizing source for the northern polymetallic veins

in outcrop or geophysics, so a tentative link to the Eocene stock is assumed, though further investigation would be warranted. As noted above, though it is easy to apply a generalized Pb-Ag(-Zn-Ba) classification to these vein deposits, there remains significant variation on a deposit scale for polymetallic veins (e.g., Subías et al., 2010). The Garrison deposit is notable for having Cu and Au enrichment as well as trace tennantite associated with pyrite, and ore from the Silver Hill/Spotted Fawn mine averaged just over 1 g/t Au.

A number of barite-only vein occurrences are mapped just to the north of the Eocene polymetallic veins, as well as around the Cane Springs area and in the Paleozoic basement block in the Jurassic pluton. Barite veins are not considered a separate class of deposits here because field investigations showed that the barite veins are generally small and occur along faults or in association with jasperoid. Barite veins and barite enrichment can be characteristic of sediment-hosted gold deposits (e.g., Radtke, 1985), and the focus on barite veins as an exploration vector during multiple exploration campaigns for sediment-hosted gold deposits has perhaps led to an overstatement of their density, size, or importance in terms of an ore phase.

Clifton vein swarm: The area around and to the southwest of the old Clifton townsite is characterized by a vein swarm mapped in previous literature as roughly 4500 by 6500 ft (1.5 by 2 km) extending along a distinct northeast-southwest trend (Lee, 2004), which is roughly the same footprint as the late polymetallic vein extents at the Bingham Canyon mine, i.e., the same footprint as a vein system that is genetically related to one of the largest porphyry copper deposits in the world (Tomlinson et al., 2021) (Figure 18). The area has, in previous literature, been known as Clifton Shears; however, the veins formed through fracturing and faulting, referred to as “fissure” veins in previous literature, so the name Clifton Shears is genetically misleading. An individual mine is also named Clifton Shears, adding to the confusion. The area is referred to as the Clifton vein swarm in this report for clarity.

The vein swarm is hosted in both Paleozoic basement and Jurassic pluton and is made up of ~40 sub-parallel steeply dipping veins. Previous reports have interpreted the steep dip,

which varies from northwest to southeast dipping, to reflect possible formation in an anticlinal nose but no field evidence was observed to support this hypothesis. As mapped in literature, individual veins range from 1 to 10 ft (0.3–3 m) in width and extend over 1000 ft (300 m) along strike (Lee, 2004). Historical descriptions suggest that large veins can continue more than 6000 ft (1800 m) along strike, but detailed mapping in the center of the vein swarm in the early 2000s suggests that the veins are offset by a number of small northwest-southeast-trending jogs, hence may not be as laterally continuous as has been historically suggested. A “silica flood zone” was mapped in an area of this cross-faulting (Lee, 2004).

The veins are generally Pb-Ag enriched, though those hosted in the Paleozoic basement are reported as more enriched in Cu and/or As. Almost all of the ore in the vein swarm has been oxidized with only minor pods of sulfide reported (Figure 19). Ore from the Ely Limestone-hosted Monocco mine had a reported average grade of 10.2% Cu, 0.9% Pb, and 120 ppm Ag, whereas the Herat mine hosted in Ochre Mountain Limestone averaged 380 ppm Ag and 7.4% Pb with scorodite common in the ore zone (Nolan, 1935; Lee, 2004). Particularly in the Herat mine, replacement bodies formed where the veins intersect favorable limestone beds, extending a maximum of 15 ft (5 m) from the vein. The Southern C¹ mine, which contains one of the largest veins hosted in the Jurassic pluton, produced ore averaging 30% Pb and over 1000 g/t Ag, and is also reported to have had minor Cu, As, and Zn (Nolan, 1935; Lee, 2004). A selvage of sericite and chlorite alteration forms in the quartz monzonite around the vein no more than 10 ft (3 m) wide and typically ~3 ft (1 m).

Several historical mining operations exploited the mineralization in the veins, and attempts have been made at modern exploration. A 1996 Behre Dolbear & Company resource estimate for the Clifton Shears deposit cited 580,000 tons at approximately 275 g/t Ag, but that estimate was revised by Clifton Mining in 1999 to an underground resource of 100,000 tons at approximately 285 g/t Ag. In 2003 to 2004 Dumont Nickel drilled seven holes totaling 4200 ft (1280 m) diamond core around the Southern C vein to test the dip extent of the veins. Despite previous models suggesting veins widen at depth or transition to a mineralized stockwork zone, drilling demonstrated the veins narrow and no mineralization formed between the veins. Interpretations from the time note that the veins are strongly “structurally disturbed” (Dumont Nickel Inc., 2005), providing further evidence that a likely unrecognized structural complexity affects the vein swarm. In addition to the Dumont drilling, a small exploration program focused around the Atlantis vein drilled over 4000 ft (1200 m) of diamond core in the 1980s. Reports indicate that the deepest hole, over 2000 ft (600 m), intersected quartz-carbonate veins and a zone of propylitic alteration down to approximately 1700 ft (500 m) depth. Little else is known about this program and the core reportedly was never assayed (Lee, 2004).

¹The original name for this mine is Southern Confederate (Utah Geological Survey, 2023). The name has been updated to Southern C in this report.

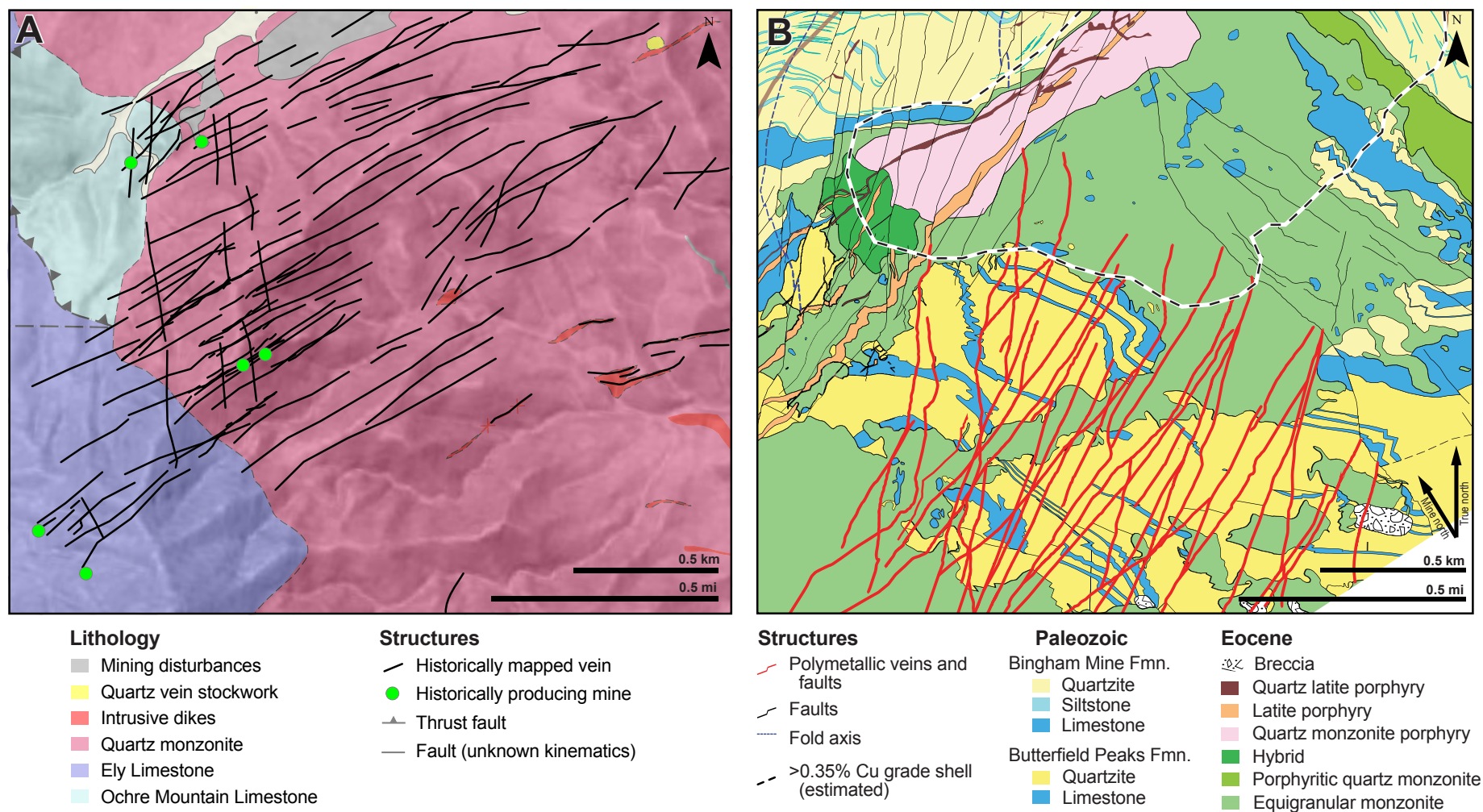


Figure 18. Vein swarm size comparison at the same scale between **A)** the Clifton vein swarm at Gold Hill and **B)** the polymetallic veins at Bingham Canyon mine. Bingham Canyon map modified from Tomlinson et al. (2021); copper grade shell modified from Brodbeck et al. (2022). Location of Clifton vein swarm as shown in Figure 2.

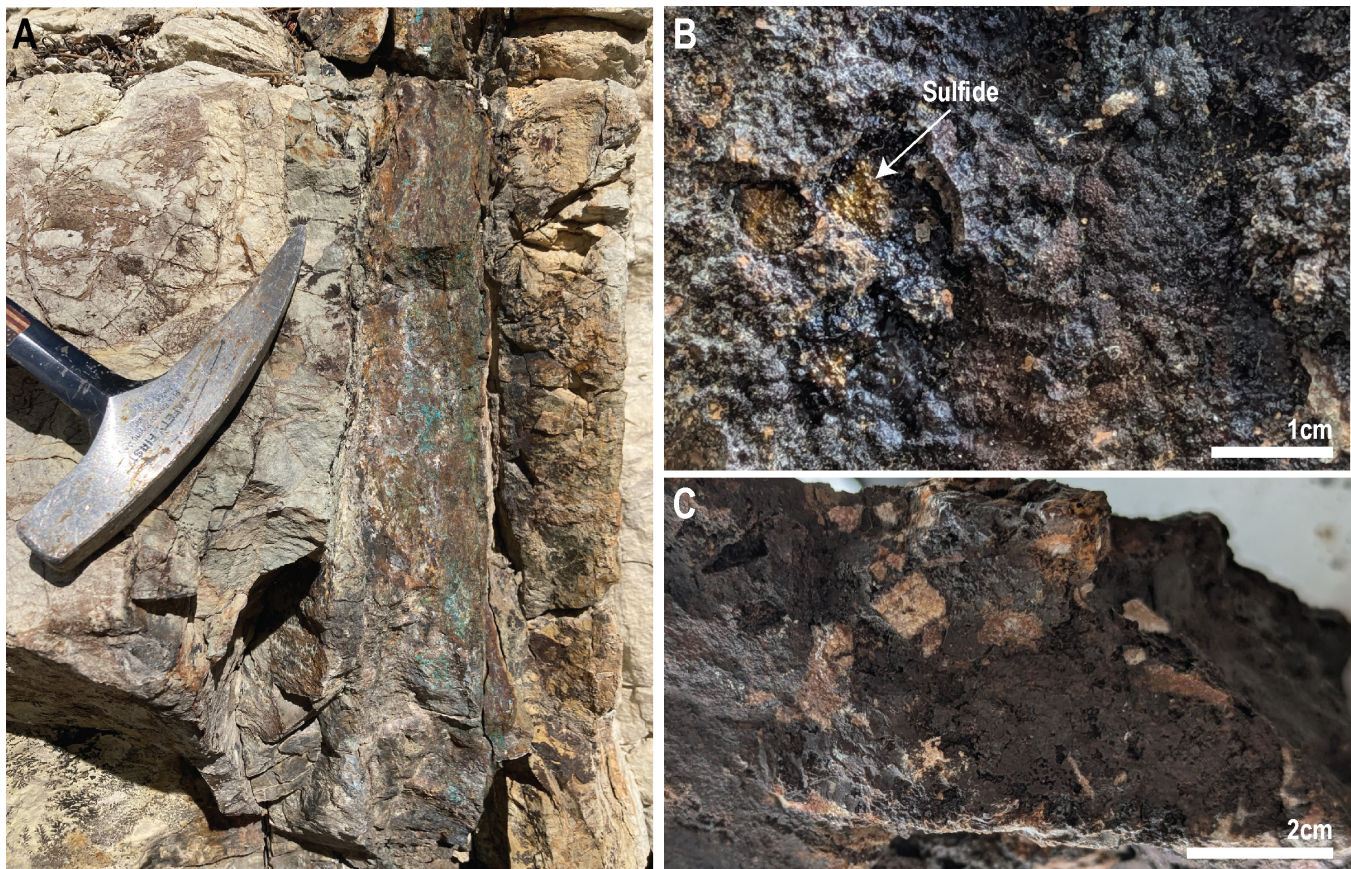


Figure 19. Oxidized ore in veins from the Clifton vein swarm. **A)** Outcrop showing vein with sharp contacts to wall rock and green copper oxidation from the Monocco mine. Photo courtesy of Jim McVey. **B)** Small residual sulfide bleb in otherwise oxidized ore from the Southern C mine. **C)** Oxidized ore with brecciated clasts of quartz monzonite from the Southern C mine.

The Clifton vein swarm has been singled out in this study due to the unique and considerable density of historically mapped veining and the consistency of orientation across two different host rocks, all of which have received relatively little consideration in terms of genetic implications for a source system. Although the Gold Hill district is known to contain an abundance of vein deposits, nowhere else in the district is known to contain a comparable density of subparallel veining. The Clifton vein swarm has no age constraints and has been interpreted by previous explorers to be Jurassic because the swarm is partially hosted in the Jurassic pluton (e.g., Lee, 2004). The polymetallic veins could represent fracturing during the lattermost stage of crystallization in the Jurassic pluton, particularly given assumptions by Nolan (1935) that the exposed level of the pluton is very close to the roof of the intrusion, which would allow a combination of pressure driven roof extension and hydraulic fracturing from exsolving magmatic-hydrothermal fluids (Gruen et al., 2010). However, it is not clear if a shallow pluton setting is able to account for the large expanse of veins extending from a crystallizing pluton into the host Paleozoic basement, maintaining a strikingly consistent orientation and relatively consistent spacing throughout. An alternative explanation is that the veins are related to a younger magmatic-hydrothermal event not currently exposed. The consistent structural fabric of the veins, as currently mapped, may suggest rapid emplacement during a major magmatic devolatilization event; for ex-

ample, the veins at Bingham formed within 1 myr of the onset of intrusive activity (Seo et al., 2012; Large, 2018; Tomlinson et al., 2021). The Clifton vein swarm is one of the most poorly understood aspects of the Gold Hill district metallogeny while also being one of the highest potential areas for vectoring to a blind magmatic-hydrothermal system(s). See the Exploration considerations section for further discussion.

Critical mineral potential: The polymetallic veins at Gold Hill have been a historical source of small-tonnage, high-grade ore. Main commodities from these veins have been Ag and Pb, as well as Cu to a lesser extent, but notable enrichment in As and Zn has been noted in individual veins. Barite is also a constituent in several of the polymetallic veins associated with the Eocene stock. However, vein deposits are extremely difficult to exploit under the economics of modern mining because of the small tonnage and the potential for complex and variable metallurgy. None of the veins at Gold Hill are dominated by a critical mineral commodity, meaning critical minerals would be produced as a byproduct, which further decreases the potential for significant development of the polymetallic veins as a critical mineral source. Vein deposits need to occur in high density in order to be economic, and past exploration at the Clifton vein swarm has yielded little potential for development as a vein deposit due to the lack of down dip continuity.

Low-Sulfidation Epithermal Deposits

Quartz-calcite-adularia veins and stockwork zones were documented in the eastern part of the Gold Hill district as early as the 1960s, initially due to interest in the beryllium enrichment (Griffitts, 1965). The network of veins grading into zones of stockwork is located on the western side of Rodenhouse Wash and can be characterized as a low-sulfidation epithermal system (Figure 20). This type of mineralization is characterized by low temperature (<200°C), near neutral pH ore fluids, typically ascribed to a dominantly meteoric fluid system with varying input from magmatic-hydrothermal fluids. Low-sulfidation epithermal deposits are also referred to as adularia-sericite (White and Hedenquist, 1990) or hot-spring deposits and are akin to geothermal systems, both fossil and modern (Simmons et al., 2005). Common gangue mineralogy includes chalcedonic quartz, adularia (low temperature K-feldspar), pyrite, and illite. In economic deposits in the Great Basin, gold and silver form as native elements and electrum (e.g., Round Mountain, Sleeper). Common textures include crustiform (visible crystals) and colloform (cryptocrystalline) banding, bladed calcite, massive chalcedony, and other features indicative of repeated cycles of open-space filling crystal growth.

At Gold Hill, the low-sulfidation epithermal system manifests as a narrow north-northeast-trending zone of intermittent vein swarms, stockwork zones, faulting, and alteration. A roughly north-south-trending normal fault system that cuts the Jurassic pluton exerts a first-order control on the low-sulfidation system, and east-west faulting in the Rodenhouse Wash area may contribute to the degree of fracturing (i.e., veins versus stockwork), though detailed mapping on these structures was not undertaken in this study. The age of the north-south normal fault is not well constrained other than that it formed prior to the low-sulfidation mineralization. The low-sulfidation system has been dated at 8 Ma by K-Ar on adularia (Whelan 1970); however, the location of the sample is very poorly constrained and is interpreted to be taken from a vein in the Climax mine. Modern dating is underway to confirm this age (Nathan Carey, Arizona Geological Survey, written communication, 2024). Despite classification as a low-sulfidation epithermal system, there are several unique aspects to the system at Gold Hill. Cryptocrystalline amethyst occurs as a late vein stage cutting the earlier colloform quartz veins (Figure 21). Economic low-sulfidation epithermal deposits in the Great Basin are generally associated with volcanic activity and/or geothermal activity, but aside from minor undated volcanic deposits in Rodenhouse Wash, very few volcanic rocks exist in the district and no evidence for geothermal activity is present outside of the epithermal system. The veins and stockwork are mainly hosted in the Jurassic pluton with associated argillic-pyritic alteration.

Neither pyrite nor any other sulfide has been observed in any of the outcrops. Geochemical sampling by the UGS did not cover this area. Newmont's extensive surface sampling included 136 samples over the system and drill holes GHN-

008, 009, 010, 011, 013, 014, 016, 020, and 021 all targeted the low-sulfidation system and included 2059 assay samples (Appendix C). The highest gold value reported in Newmont's drilling results is <2.5 g/t Au; surface sampling yielded one >20 g/t Au sample but all other results <6 g/t Au. Ag is slightly more enriched; one anomalous surface sample yielded over 950 ppm Ag and several others were >50 ppm Ag, whereas results from drilling were <15 ppm Ag. Beryllium was the most consistent between surface and drilling samples, both yielding values up to ~550 ppm Be with a few high outliers in drilling. It has been suggested that gold and beryllium are directly proportional in the deposit (Robinson, 2016), but the geochemical data do not support any sort of correlation or proportionality (Figure 22). Geochemistry does support the lack of correlation between gold and silver, unlike other mineralized low-sulfidation systems, though Ag correlates to As, Pb, Sb, and Zn in surface samples. In drilling, the correlation is more specific to As, Pb, and Zn. The description of the system as "gold-only" (e.g., Robinson, 2005) and low in other metals ignores the fact that the system is low in gold as well, so it would be more accurate to describe the entire system as metal-poor.

The lack of significant gold grade is perhaps why the potential of the low-sulfidation system beyond beryllium did not become a focal point for exploration until relatively late in the district's history. After beryllium interest died in the mid 1960s due to the discovery of the higher grade Spor Mountain deposit, the system in Gold Hill remained unexplored until the 1990s. Robinson (2016) reports early surface sampling yielded up to 35 g/t Au which encouraged exploration and drilling by Goldstack Resources and Dumont Nickel Incorporated on the Kiewit zone of the system and led to Desert Hawk Gold Corporation entering into a Mining Venture Agreement and commencing limited mining production in 2014 at Kiewit. Desert Hawk continued mining sporadically until gold prices rose in 2019, then remained in operation producing ~2500 oz Au and Ag per year from heap leach operations until returning to standby in 2023. Ore grades reportedly run from about 0.9 to 2 g/t Au. Earliest estimates by Dumont cited 54,000 oz contained Au and a similar amount of Ag, which was upgraded to 90,000 to 120,000 oz by Desert Hawk. The operation could possibly be expanded to other larger stockwork zones along the deposit trend (e.g., Rainbow Hill); however, given the low grades it seems unlikely this system will ever be a significant gold producer.

The critical mineral potential of the low-sulfidation system is considered low. Beryllium is the most obvious candidate. The average Be grade of the proven and probable reserves at Spor Mountain is 2460 ppm Be, far exceeding even the highest grades intersected in drilling at Gold Hill. The proven and probable reserves at Spor Mountain, which has been in constant production since 1968, sits at over 42 million lbs beryllium and a custom mill in Delta, Utah, produces beryllium hydroxide from Spor Mountain ore that is shipped for further processing (Materion, 2023). Given the grade, robust reserves, processing, and infrastructure at the Spor Mountain site it seems

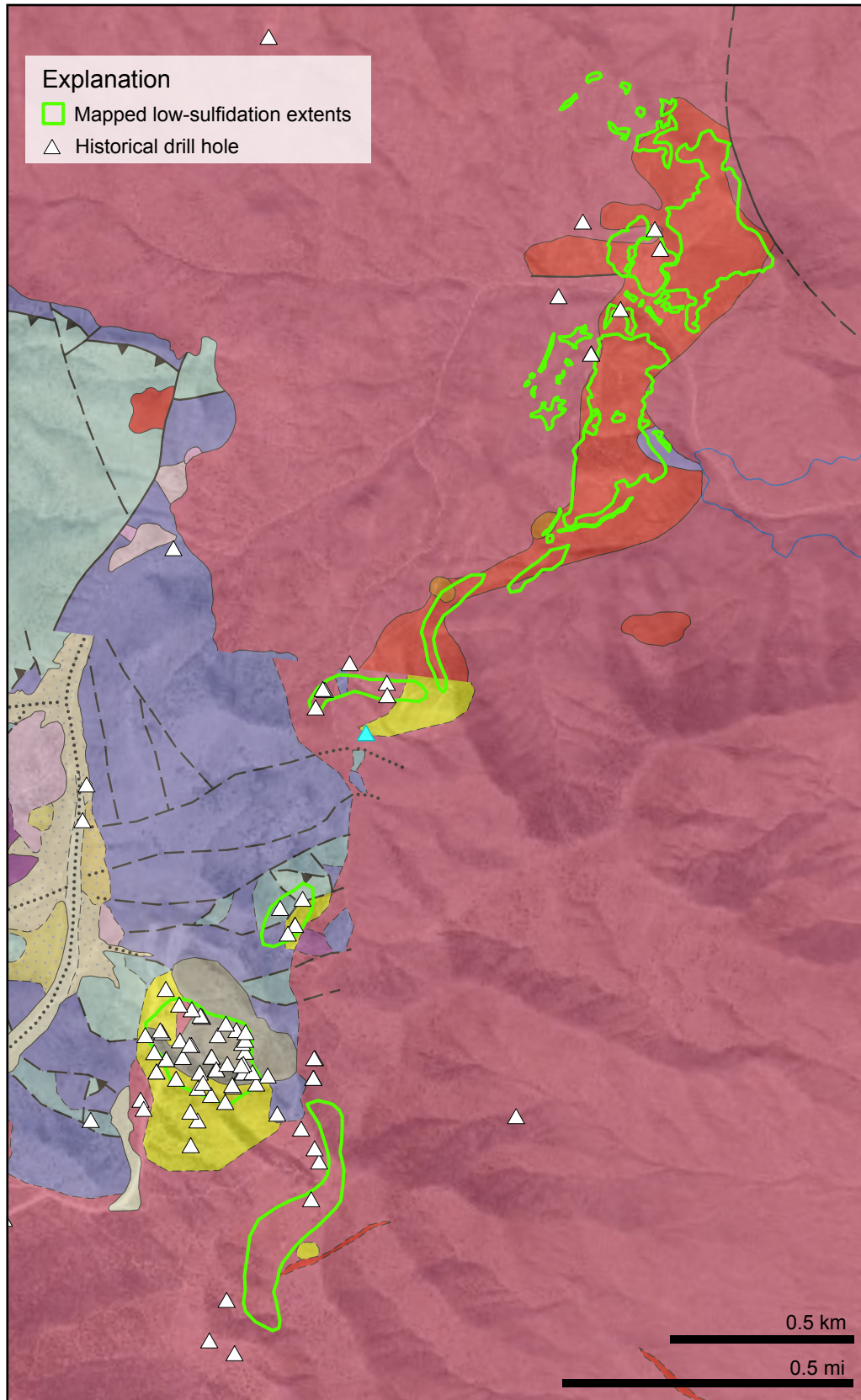


Figure 20. Mapped extents and historical drilling of the low-sulfidation epithermal system. Geology as in Figure 4, location of low-sulfidation system in Figure 2. Mapping of the low-sulfidation system based on mapping from Griffiths (1965), Newmont, and this study.

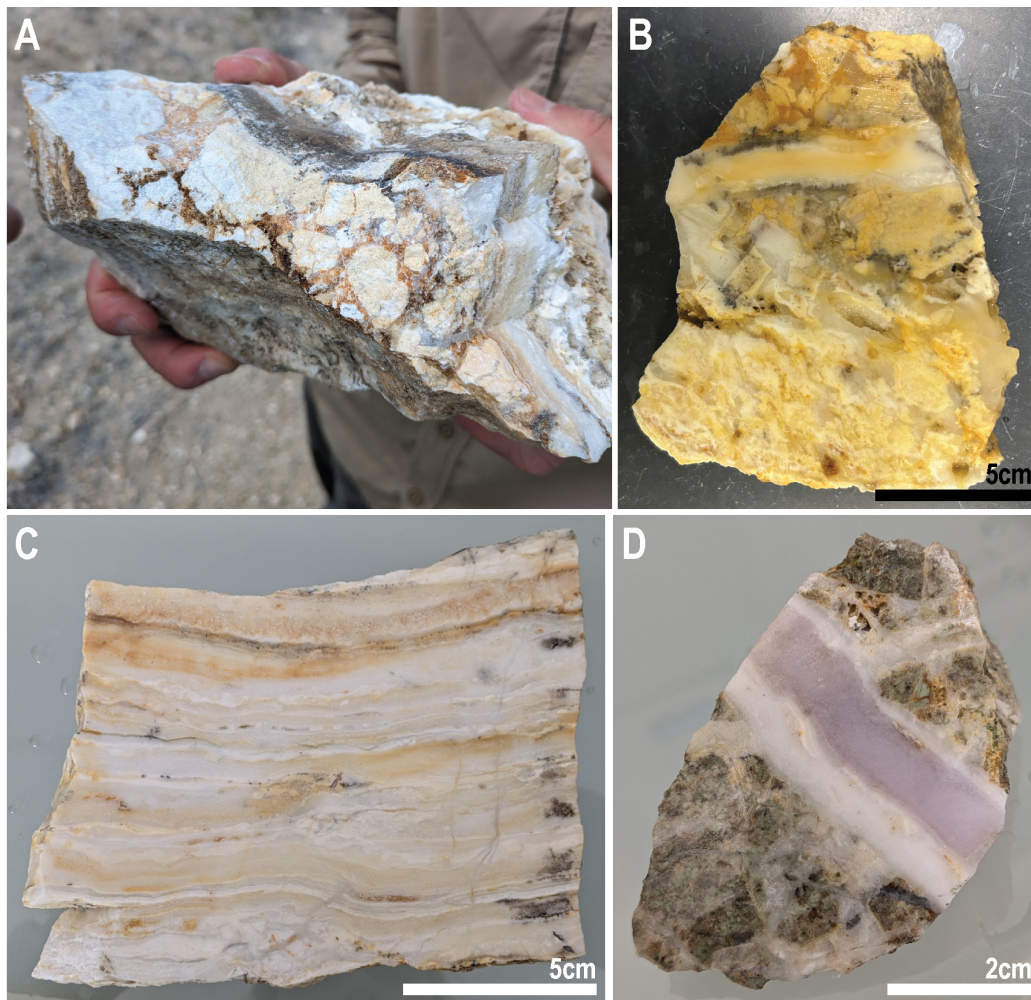


Figure 21. Textures from the low-sulfidation epithermal system. **A)** Hand sample of brecciated quartz monzonite that has been silicified and veined. **B)** Cut section through (A) showing the complex brecciation textures and zoning within the silicification around quartz monzonite clasts and in the vein. Photo courtesy of Eytan Bos Orent. **C)** Cut hand sample showing intense quartz-calcite colloform banding. **D)** Purple amethyst vein within quartz vein cross-cutting propylitically altered and silicified quartz monzonite.

extremely unlikely the beryllium enrichment at Gold Hill is economically significant. Low-sulfidation epithermal systems can be prospective for Sb and Te (Hofstra and Kreiner, 2020), though neither shows significant enrichment at Gold Hill.

Sediment-Hosted Gold Deposits

Much of the modern exploration (1980s and onward) at Gold Hill was focused on sedimentary-rock-hosted gold deposits, otherwise known as sediment-hosted gold deposits, distal disseminated deposits, or Carlin-type gold deposits. Though not all of these descriptions are directly equivalent in terms of ore genesis, they generally refer to deposits of very fine “invisible” (submicron) gold hosted in Paleozoic sedimentary strata. The gold deposits of the Carlin and Cortez trends in central Nevada are the archetypal examples of these deposits, and discovery of the Carlin trend in the 1960s spurred exploration for similar types of deposits across the Great Basin. Most sediment-hosted gold deposits in Nevada are hosted in Cambrian to Ordovician strata of the ancient shelf margin. In Utah, the Mercur deposit

in the Oquirrh Mountains demonstrates these deposits can also form in Mississippian to Pennsylvanian platform strata.

The first phase of sediment-hosted gold exploration at Gold Hill took place in the late 1980s to early 1990s and included exploration by Gold Fields, Superior Oil Company, HWP, ASARCO, and Coeur that did not yield any significant discovery (Table 3). Renewed interest by Dumont Nickel, Goldstack Resources, and Newmont in the 2000s to 2010s was driven by new models for sediment-hosted gold deposits and the discovery of the “off trend” Long Canyon deposit, located on the eastern flank of the Pequop Mountains, just 80 mi (125 km) northwest of Gold Hill (Smith et al., 2013). Newmont purchased the Long Canyon deposit in 2011 for \$2.2 billion.

Exploration interest in sediment-hosted gold deposits at Gold Hill was driven by the presence of a well-developed structural plumbing network within the Ochre Mountain Limestone. This formation was targeted as the favorable unit for mineralization because it is considered a western correlative

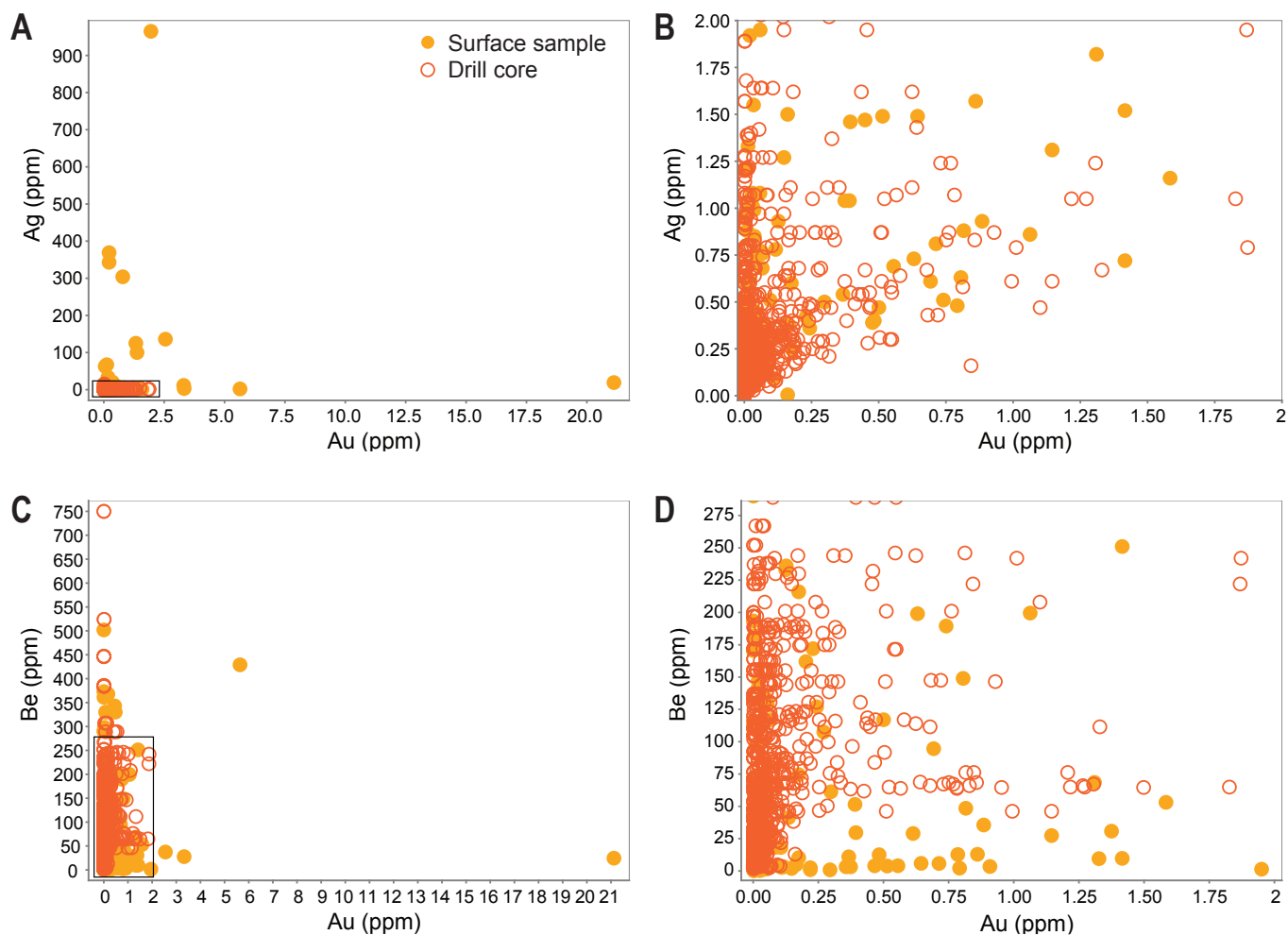


Figure 22. Au, Ag, and Be geochemistry from surface and drill hole samples around the Kiewit mine. **A)** Au vs. Ag showing full extents of the data. **B)** Au vs. Ag zooming into the highest density data cluster. **C)** Au vs. Be showing full extents of the data. **D)** Au vs. Be zooming in the highest density data cluster.

of the Great Blue Limestone, which hosts the Mercur deposit. A general feature of sediment-hosted gold deposits in the Great Basin is Paleozoic continental slope to shelf edge carbonate host rock, typically silty or “dirty” limestone grading to calcareous siltstone. In a review of historical exploration documents there was no mention of primary targets in the Ely Limestone (or Oquirrh Group) as a potential host rock. The Ely Limestone is correlative to the Butterfield Peaks and Bingham Mine Formations in the Oquirrh Mountains which hosts the skarn mineralization associated with the Bingham Canyon porphyry deposits.

The exploration models for sediment-hosted gold deposits at Gold Hill centered on the concept of higher grade, steep to subvertical feeder zones along faults or shear zones supplying metals to lower grade, subhorizontal strata-bound deposits. The models were supported by surface alteration such as jasperoid development, barite veins, and boxwork silicification with limonite, as well as geochemical results delineating patchy weak gold, arsenic, and mercury anomalies (Figure 23). The Ochre Springs area was the most heavily explored. Drilling by Superior Oil Company defined a 35-ft-thick (10

m) zone of gold enrichment (averaging >1 g/t Au) at 300 ft (90 m) depth, restricted to a structurally favorable zone. However, the resource was deemed subeconomic with little room for expansion. Other areas such as Cane Springs, Trail Gulch, and Rattler were also explored with no significant results.

Given the historically extensive exploration, there seems to be little potential for the discovery of a significant sediment-hosted gold deposit within the Gold Hill district. One possible explanation is the proximity of significant Tertiary magmatism, in the form of the Eocene granite stock in the north of the district. Although sediment-hosted gold deposits in Nevada, which formed ~40 Ma (Smith et al., 2013), occur in proximity to Jurassic-age intrusions (the >3 Moz Fourmile deposit being only ~2 mi (3 km) south of the Jurassic Mill Canyon intrusion), they are not associated with large bodies of younger intrusions. Many deposits are spatially associated with Cretaceous-age and younger dikes (e.g., Cortez Hills; Henry et al., 2023), but not large stocks. Although the relationship between magmatism and sediment-hosted gold deposits remains contested (e.g., Emsbo et al., 2003; Muntean and Einaudi, 2011), the crustal level indicated by the exposure of the Eocene stock and

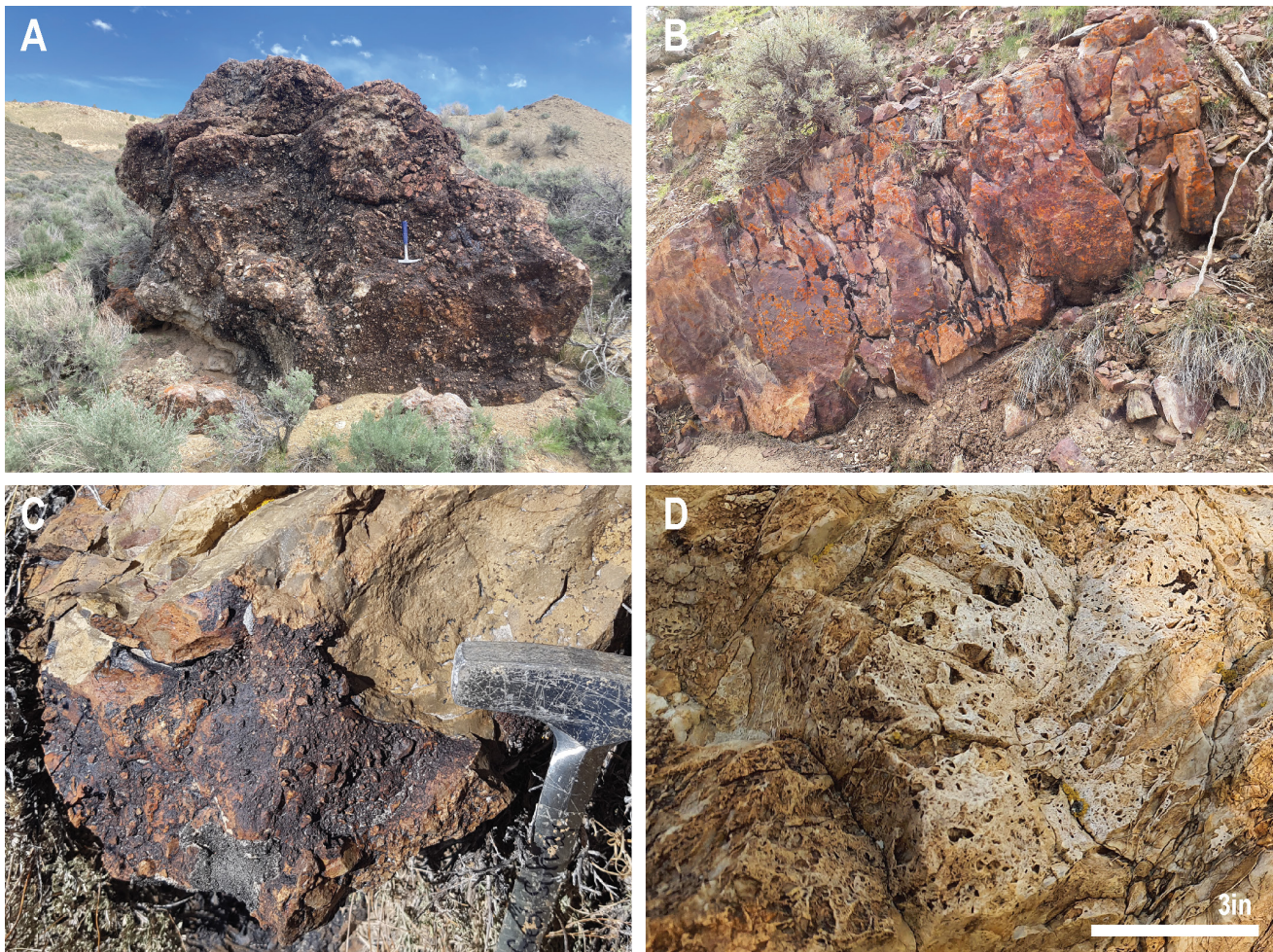


Figure 23. Examples of jasperoid and silicification textures. **A)** Brecciated jasperoid. **B)** Incipient bedding-controlled jasperoid alteration in limestone. **C)** Contact between black brecciated jasperoid and tan limestone. **D)** Boxwork silica alteration in tan limestone.

proximity to the stock itself may indicate Gold Hill is not the correct setting for formation of sediment-hosted gold deposits.

Arsenic and antimony are the critical minerals associated with sediment-hosted gold deposits (Hofstra and Kreiner, 2020), and though values of >2500 ppm As were recorded by exploration geologists, the anomalous arsenic values are patchy and unlikely to form any economic deposit.

Iron-Oxide Copper Gold (IOCG) Deposits

IOCG mineral systems are a class of magmatic-hydrothermal deposits typically associated with Cu and Au mineralization and oxidizing, saline ore fluids that produce large sodic(-calcic) alteration zones. The term IOCG can be used to consider a wide classification of iron-oxide-dominated deposits, for example deposits within the Yerington district in Nevada have at times been classified as IOCGs, despite being more widely recognized as a porphyry mineral system (Williams et al., 2005; Groves et al., 2010). IOCG mineral systems are capable of producing many of the same deposit types as porphyry systems, such as skarns, and many of these mineral systems ex-

ist on a continuum with one another. However, here the term IOCG is used *sensu stricto*, as in Groves et al. (2010).

IOCG-style alteration was recognized particularly around the Yellow Hammer deposit, though has been noted to occur commonly in the district by previous geologists, even where not identified as such (e.g., pyroxene-rich Jpqm phase of Burwell [2018]). Sodic(-calcic) to potassic(-calcic) alteration in the Jurassic quartz monzonite occurs as small, pervasive zones along structures and typically has albite-actinolite-epidote-potassic feldspar±chlorite±diopside assemblage (Figure 24). Some zonation to these alteration assemblages is likely, but detailed mapping of the alteration variations was outside the scope of this study. The sodic(-calcic) alteration is magnetite destructive which, if present over a large area, could contribute to magnetic lows in aeromagnetic data. The presence of apatite, tourmaline, and allanite are in line with the mineralogy associated with IOCG alteration and mineralization. Previous exploration geologists observed that skarn alteration in the intrusive units was characterized by quartz dissolution to produce garnet, suggesting the hydrothermal fluid was silica-undersaturated and may have had input from other fluid sources (Caleb King, personal communication).



Figure 24. Outcrop and hand sample photos of IOCG-style alteration and mineralization. **A)** Albite, K-feldspar, and actinolite alteration along a vein in quartz monzonite. **B)** Outcrop of quartz monzonite showing zoned alteration along fractures. **C)** Chlorite and actinolite alteration in quartz monzonite on fractures with minor epidote matrix alteration. **D)** Quartz-tourmaline mineralization.

The input of a non-magmatic hydrothermal fluid is in agreement with the IOCG system model, which is characterized by highly saline ore fluids (Groves et al., 2010). The salinity of the ore fluids is via incorporation of an external brine component (e.g., basinal fluids) or interaction with evaporite-bearing wallrock. In terms of external brine incorporation, previous authors have suggested IOCG systems may be able to incorporate brines from contemporaneous sources via thermal circulation (Barton and Johnson, 1996). Contemporaneous with the Jurassic pluton, evaporitic units were forming in the Carmel Formation at the southern end of the Arapien basin, which extended north towards Gold Hill (Doelling et al., 2013). Contemporaneous with the Eocene granite, the White Sage For-

mation was a lacustrine system, though there is no evidence for evaporite minerals (Dubiel et al., 1996). However, even if contemporaneous saline sources were available and given the intrusions in Gold Hill are shallowly emplaced by magmatic standards (Burwell, 2018; White, 2023), they were still more than 1 mile (1.6 km) below the surface during time of emplacement. Thermal convection and density contrast between saline and non-saline fluids has been demonstrated in some districts (e.g., Yerington) to circulate fluids 3 to 4 km so it is feasible for contemporaneous external brine sources to have played a role in the magmatic-hydrothermal system at Gold Hill (Carten, 1986; Barton and Johnson, 1996). More study is needed to delineate the source and degree of interaction of potential brines.

Interaction with an evaporitic host rock is a more feasible mechanism for creating highly saline ore fluids at Gold Hill. The Paleozoic sequence is not known to host conventional evaporitic units in the Mississippian to Pennsylvanian section; however, the Delle Phosphatic Member (Delle) is a basal member of the Woodman Formation, and although it has not been directly observed in Gold Hill it is a viable unit to occur. The Delle is not an evaporite, having formed in a shallow, possibly brackish setting from highly productive waters that may have been periodically anoxic (Jewell et al., 2000). The phosphate-rich horizon in the Delle is characterized by thin beds of peloidal phosphorite, and phosphorite sediments can have a variable mineralogy, including apatite + fluorapatite + dolomite + calcite + quartz + clays ± halite ± gypsum ± iron oxides ± siderite ± pyrite ± carnotite (Mosier, 1996; Jewell et al., 2000). There is little detail on the mineralogy of the Delle phosphorites in particular so it is unclear if they would have been able to provide the Na and Cl needed for an IOCG system. The Delle is known to occur within the Woodman Formation underlying the Ochre Mountain Limestone at Gold Hill hence is a viable unit to have undergone fluid-rock interaction.

In the Permian section, stratigraphically above the current level of exposure at Gold Hill, the Arcturus Group is known to contain gypsum-bearing evaporites in the Loray Formation (Bissell, 1964). Because this unit is stratigraphically above Gold Hill it is difficult to assess if it would have been capable of interacting with the magmas or fluids. It is mentioned here as a possibility to be considered in future research. It is also possible that evaporitic units are under represented in modern stratigraphy due to being soluble and readily deformed, particularly in a district like Gold Hill that has had such extreme faulting that would likely have utilized weak units and attenuated them (see Chainman Shale discussion above).

In terms of mineral vectoring for IOCG-related deposits in Gold Hill, sodic(-calcic) alteration in the IOCG model is deeper and more distal from ore, and is also notably extensive in economic deposits (Groves et al., 2010; Runyon et al., 2019). IOCG mineralization is temporally but not necessarily spatially associated with major magmatic intrusions. In Gold Hill, these factors suggest the current level of exposure is below the level of expected economic IOCG mineralization, which would have been eroded off. The interpretation here, given the lack of a pervasive alteration footprint and direct magmatic association, is that the alteration and mineralization assemblages observed did not result from an IOCG system *sensu stricto*, but rather are associated with porphyry mineral systems that may have interacted with external brines or evaporitic wall rocks to mimic IOCG style alteration. As noted above, deposits such as Yerington in Nevada have been interpreted both as an IOCG and as porphyries, demonstrating the overlap between the mineral systems (Groves et al., 2010). In terms of critical mineral potential, because of the similarity between IOCG and porphyry mineral systems, there is no variation between the critical mineral potential depending on which model is favored. Bi, Te, and Sb have all been identified as anomalous at Gold Hill,

but the deposits are small and metallurgically complex, making economic exploitation of the deposits unlikely.

Porphyry Molybdenum Deposits

Porphyry molybdenum deposits, also known as Climax-type porphyries due to the archetypal Climax deposit in Colorado, are a class of porphyry system enriched in molybdenum over copper with potential secondary enrichment in metals such as W and Sn. Porphyry Mo deposits are responsible for 95% of global Mo production (John and Taylor, 2016). Utah is known to host several porphyry Mo deposits, such as the Pine Grove porphyry in Beaver County. No explicit indications of a porphyry Mo system are present at Gold Hill, but there has been interest in the potential of a system based on the presence of the Goshute Wash dike swarm, which intrudes the Jurassic pluton on the eastern flank. The dikes range in width from 1 to 50 ft (0.3–165 m) with a mode of 15 to 25 ft (5–7 m). The largest dikes can be traced for several thousand feet; most are 500 to 1500 ft (150–450 m) along strike. The potential for a porphyry Mo system at Gold Hill was best summarized by Krahulec (2017) and his work forms the basis of this assessment, supplemented by additional mapping, geochronology, and geochemistry of the dikes carried out in this study.

The earliest interest in these dikes came from AMAX exploration in the late 1970s and early 1980s. The Goshute Wash dike swarm comprises multiple individual dike strands generally trending southeast with unknown dips (Figure 25). One of the most commonly outcropping dikes has a high-silica rhyolite chemistry, which is considered a favorable indicator for porphyry Mo systems. Geochemical results showed high Nb, Rb, and Rb/K₂O signatures, indicating an evolved magmatic signature, and encouraged AMAX to drill three rotary holes with core tails around Goshute Wash to final depths of ~2400 to 2600 ft (730–800 m). The holes intersected weak propylitic alteration in the Jurassic quartz monzonite pluton, and stronger alteration was associated with chloritic quartz-carbonate veins ± pyrite, quartz-pyrite veins, and quartz-only veins. Minor molybdenite was logged in only one vein. The quartz monzonite was cut by several dike compositions, which are also observed at surface.

Four compositions of dikes are reported in the Goshute Wash dike swarm. The first was reported by AMAX geologists but was not observed during this study. These dikes are described as the oldest in the dike swarm and trend northeast, as opposed to the dominant swarm orientation trending northwest. These dikes, termed quartz dikes by AMAX geologists, were described as flow-banded and aphanitic, comprising quartz and feldspar phenocrysts, and locally exhibiting strong argillic to sericitic alteration with disseminated pyrite.

One of the most abundant dike compositions recognized at the surface is a rhyolite porphyry dike comprising a light gray to green aphanitic matrix with phenocrysts of quartz, K-feldspar,

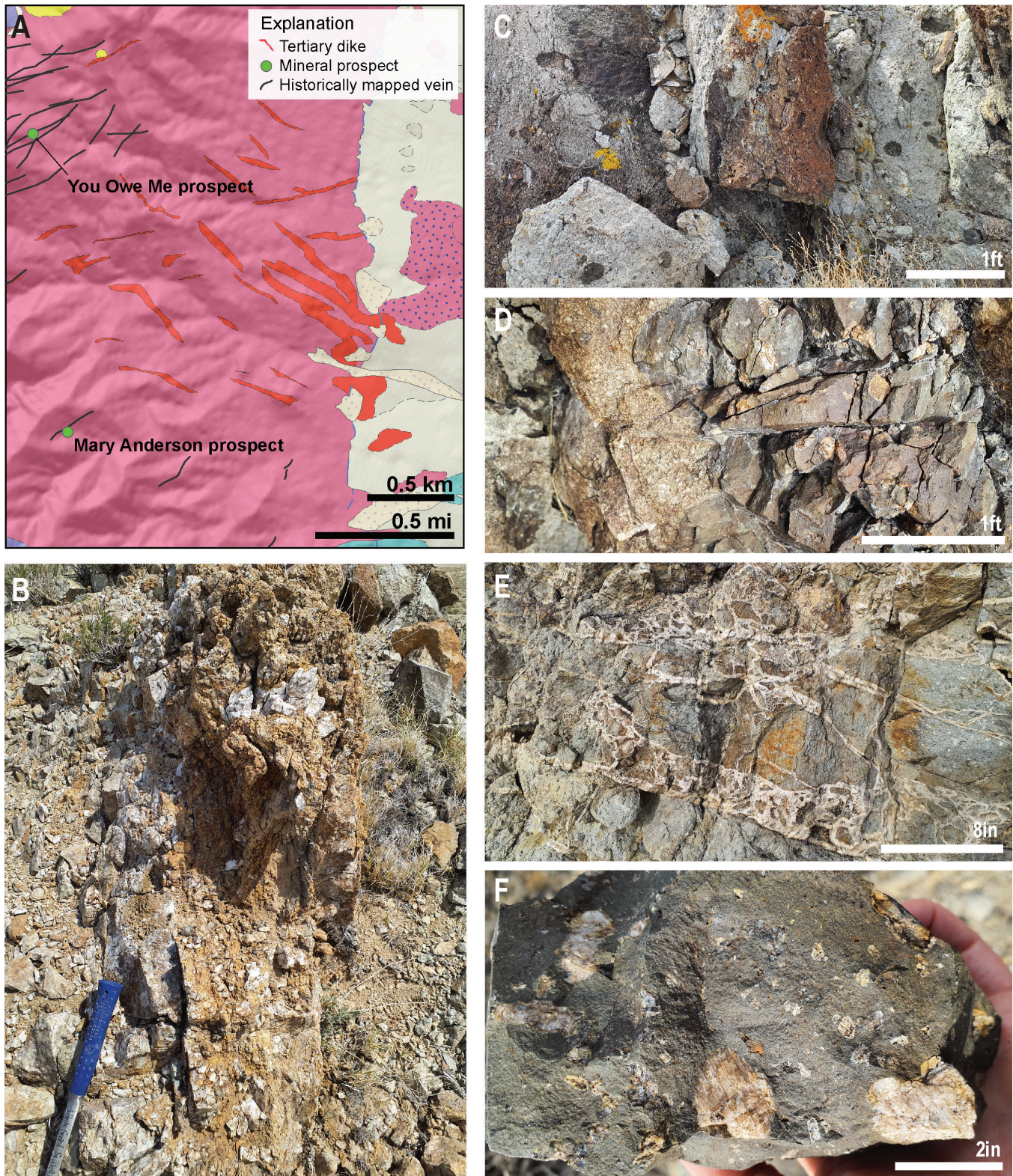


Figure 25. Goshute Wash dike swarm and examples of dike textures. **A)** Map of the Goshute Wash dike swarm (“Tertiary dike” on map), dike type undifferentiated. Location and geology as in Figure 4. **B)** Brecciated bull quartz vein cutting rhyolite porphyry dike. **C)** Rounded enclaves of the andesite porphyry dike in the rhyolite porphyry dike. **D)** Andesite porphyry dike intruding into rhyolite porphyry dike. **E)** Coarse-grained, pyramidal quartz veins cutting the rhyolite porphyry dike. **F)** Unusually large feldspar phenocrysts in the andesite porphyry dike.

and plagioclase (Figure 25) with local sericitic to argillic alteration. These are the high-silica dikes that encouraged exploration for a porphyry Mo system. U-Pb dating of zircon from this dike composition yielded an age of 16.23 ± 0.26 Ma (Mills et al., 2023). Two samples of this dike composition were collected in Mills et al. (2023), one of which demonstrates the relative enrichment in K_2O (4.8%), Nb (103 ppm), Sn (15 ppm), Rb (447 ppm), and W (12.4 ppm) as well as Rb/ K_2O and Nb/Zr values in the range of both the Henderson (Colorado) and Pine Grove (Utah) porphyry Mo deposits (Stegen, 2016).

The other most abundant dike composition in the Goshute Wash swarm is andesite porphyry (Figure 25). These dikes have a dark gray to black aphanitic matrix with large phenocrysts to megacrysts of plagioclase and K-feldspar, which form crossed twins in places. The compositions of these dikes range from andesite to trachyandesite to trachydacite. The relationship between the rhyolite porphyry and the andesite porphyry dikes is uncertain and could not be determined from field relationships, either by AMAX geologists or in this study. In areas, the andesite porphyry appears to cut the rhyolite porphyry, suggesting the rhyolite porphyry is older; however, there are inclusions of what appears to be the andesite porphyry in the rhyolite porphyry, suggesting the opposite (Figure 25). The conclusion reached in this study and by AMAX geologists is that these dikes are contemporaneous. A modern U-Pb age on the andesite porphyry dike composition would confirm this hypothesis. There are also clear mingling relationships between the andesite porphyry dike and the Jurassic pluton.

The final dike composition is volumetrically less abundant in outcrop and was not recognized as a separate composition of dike by AMAX geologists, who classified it as a phenocryst-poor endmember of the andesite dike. Mills et al. (2023) classified this dike as a distinct trachybasalt dike lithology. This composition of dike is dark gray to black and comprises an aphanitic matrix with no recognized phenocrysts. It occurs as thin slivers along the margins of the rhyolite and andesite porphyry dikes. Further field investigations in this study yielded individual outcrops where the trachybasalt and andesite porphyry compositions are transitional, which suggests the original AMAX interpretation that the trachybasalt dike is a phenocryst poor endmember of the andesite porphyry dike is accurate. The magmatic processes forming phenocryst-rich and -poor endmembers remain unclear, though it is likely that both the trachybasalt and andesite porphyry dikes are Miocene given the association with the rhyolite porphyry dike described above.

Geochemical results from the dikes did not indicate any anomalous Mo, W, Pb, or Zn values, but moderate F (1000 to 3600 ppm) and Sn (25 to 128 ppm) were present (Krahulec, 2017); it is unclear if these results are from surface sampling or drill core, though it is assumed they are related to the

rhyolite porphyry dike composition. Historical surface sampling yielded highly anomalous (up to 1000 ppm) Mo and Sn values from the You Owe Me and Mary Anderson prospects (Figure 25). Interestingly, the You Owe Me prospect occurs on the easternmost extent of the Clifton vein swarm (discussed above). The veins host Ag(-Au-Cu) mineralization and enrichment in Mo, Sn, Bi, Pb, and As, which is a unique metallogenic profile in the Clifton vein swarm. The Mary Anderson prospect is located south of the Clifton vein swarm, though it is still a polymetallic vein deposit following the same northeast trend with Au-Ag-Pb(-Cu-Sn) mineralization and As, Bi, and Sb enrichment. The trends of the veins (northeast-southwest) and the dikes (northwest-southeast) intersect at the You Owe Me prospect.

Several small quartz-dominated veins were observed in the Goshute Wash area. No mineralization was observed in association with these veins. Some of the largest outcroppings of rhyolite porphyry dikes are crosscut by a dense vuggy quartz vein network, which is a different style of veining than that found in the Clifton vein swarm and not interpreted to be related (Figure 25). Krahulec (2017) proposed that the ridge architecture west of the dike swarm suggests the area had been domed by underlying intrusive activity, though this hypothesis remains untested. The presence of a dense dike swarm with strong structural fabric hosted within an older intrusion is an intriguing aspect for mineral prospectivity; however, more work is needed to evaluate the explicit potential for a porphyry Mo system. The critical mineral potential of porphyry Mo systems includes W, Sn, Re, REE, and Sc (Hofstra and Kreiner, 2020).

Porphyry Copper Deposits

Interest in the potential for a porphyry copper deposit in Gold Hill has been a focus of exploration since at least the 1990s. Porphyry copper deposits are one of the most heavily explored for deposit types in modern exploration due to their large size, bulk mineable ore, and global occurrence. Porphyry deposits account for ~60% of global Cu production (John and Taylor, 2016; Tabela et al., 2021), as well as considerable Au and Ag. The recent attention to critical minerals and an increasingly electrified infrastructure (electric vehicles, renewable energy source, battery storage technology, etc.) has spurred exploration for porphyry copper deposits globally, which are known to produce multiple critical minerals as byproducts such as Te, Pd, and Pt (e.g., Mills and Rupke, 2023).

Porphyry copper deposits (differentiated here from porphyry molybdenum deposits and porphyry gold deposits) form from hydrous, oxidized, calc-alkaline magmas in continental subduction zone settings. Stepwise magma chambers form in the crust, undergoing progressive physical and chemical enrichment processes that ultimately lead to the formation of a parental magma chamber in the upper crust that is able to generate multiple enriched stocks that emplace at 2–5 km depth

and drive the low grade, high tonnage disseminated copper ore that is characteristic of porphyry copper deposits (Sillitoe, 2010; Chiaradia and Caricchi, 2022). Economic porphyry copper deposits are typically associated with multiple magmatic pulses and multiple cycles of fluid release, though the overall mineralization event takes place in less than 2 myr (Chiaradia and Caricchi, 2022). Deposits are characterized by disseminated copper sulfides, primarily chalcopyrite, as well as enrichment in metals such as Au, Mo, and Ag. Porphyry copper deposits are a standalone deposit type, but also are an expression of the overall porphyry copper mineral system, which encompasses porphyry copper and related deposits such as skarns, epithermal deposits, etc. (Sillitoe 2010; Hofstra and Kreiner, 2020).

Utah is known to host porphyry copper deposits, the most notable being the world-class Bingham Canyon deposit, as well as the Stockton and Southwest Tintic porphyries (Krahulec, 2014; Krahulec, 2018). Bingham, like Gold Hill, is located along the Uinta-Cortez axis, which is the basement suture of Precambrian and Proterozoic terranes that is thought to influence much of the Phanerozoic structural and magmatic development along the suture zone (Clark, 2020). A well documented, metal-enriched magmatic pulse swept across western Utah and eastern Nevada during the Eocene, associated with the rollback of the subducted Farallon plate and upwelling of asthenosphere interactions with enriched subcontinental lithospheric mantle. The regional setting of Gold Hill along many of the same structural and magmatic controls as Bingham Canyon has driven interest in the district.

One of the preconditions for forming porphyry copper deposits is active and long-lived magmatic activity in the mid crust, which may indicate a large reservoir of magma that is capable of supplying the enrichment needed to form an economic deposit (Chiaradia and Caricchi, 2022). Gold Hill has three defined magmatic pulses as well as a staggering array of minor magmatic phases that have not been adequately dated, characterized, or mapped. For example, drilling in the 1980s for sediment-hosted gold deposits intersected a previously unknown (and still undated) quartz porphyry sill along a thrust fault. Quartz-feldspar, porphyritic latite, and trachyte dikes/sills have subsequently been mapped in the area (Robinson, 1993) and a porphyritic latite dike was mapped at surface in the Ochre Springs valley that is noted as having weak propylitic alteration (Krahulec, 2017). Burwell (2018) noted the presence of a small diorite intrusion north of the Eocene stock and a granite dike cutting the north end of the Jurassic quartz monzonite, both dated at 40 Ma, as well as a monzonite dike on the northeastern extent of the Jurassic pluton dated at 17 Ma, close in age to the 16 Ma Goshute dike swarm. A multitude of other minor intrusive phases have been reported in the district including aplite, andesite, and latite dikes, where no mapping, geochemistry, or age controls exist. Clearly, the Gold Hill district has been a locus for multiple diverse magmatic events.

Two other conditions for the formation of an economic porphyry copper deposit are hydrothermal fluid and metals, for which there is evidence of both at Gold Hill. In addition to producing the most As and W in the state, Gold Hill produced over 3.5 million lbs of Cu, nearly 11 million lbs of Pb, 26,000 oz of Au, and over 800,000 oz of Ag, all from high-grade, relatively small and scattered deposits. The distribution of such high grades, even though they occur in small pockets, suggests metal-rich systems driving the formation of the deposits. Hydrous intrusions are typically thought of as having a large alteration halo, because the classic telescoped model developed for porphyry exploration was in Tertiary volcanics, which are relatively porous and allow hydrothermal fluids to permeate extensively (e.g., Halley et al., 2015). However, in carbonate and structurally complex terranes the exsolution of fluids is more likely to be fracture controlled, resulting in vein arrays as opposed to large halos. As with the metal endowment, Gold Hill has evidence for extensive veining across a considerable areal extent that indicates well-developed hydrothermal sources.

At Gold Hill, ages are lacking to decipher the paragenesis of veining in a larger district context. However, in many deposits, polymetallic veins are described as a late cross-cutting phase overprinting earlier skarn and/or replacement mineralization (e.g., quartz-tetrahedrite vein cutting massive arsenic mineralization in the Gold Hill mine [Nolan, 1935]). The age of veins relative to the mineralization they cross-cut has become an important exploration vectoring tool for porphyry deposits. For example, younger high-sulfidation veining in the pit of the Escondida mine in Chile led to the discovery of the deeper and younger Escondida Este and Escondida Pampa orebodies. The Escondida deposits were known to have formed between 38 and 36 Ma; however, dating of high sulfidation veins in the pit yielded ages of 36 to 34 Ma, suggesting the veins represented a shallow expression of a deeper magmatic-hydrothermal system (Hervé et al., 2012). Using younger cross-cutting veins as a vectoring tool has become an exploration strategy in other mature porphyry districts, such as Bingham Canyon. The temporal and spatial succession of deposit types related to evolving hydrothermal fluids was recognized as early as Nolan (1935) and has traditionally been attributed to a single evolving magmatic-hydrothermal source. Given modern studies of porphyry systems show not only lateral but vertical zonation from multiple blind intrusions (e.g., Al Furquan et al., 2022), it seems unlikely that all of the various overprinting styles and phases of mineralization observed around the Jurassic pluton would be related to only a single magmatic-hydrothermal source. It is reasonable to hypothesize that some deeper fluid source likely exists.

The Clifton vein swarm is the best example of high-density veining in the district. However, this interpretation is based on historical mapping of the veins, as re-mapping the vein swarm was out of scope for this project and is a focus for future research. The Clifton veins form a uniquely specific and discrete vein extent that is not present elsewhere in

the district. Accurate geochronology, better mapping, and characterization of the structural controls on these veins could indicate whether an unrecognized magmatic-hydrothermal system drove the formation of these veins, and potentially other blind mineralization. Previous drilling in the Clifton vein swarm noted propylitic alteration, assumed to be pervasive, and quartz-carbonate veins down to a considerable depth (Lee, 2004). The presence of pervasive propylitic alteration in the Jurassic pluton would align with the telescoped alteration model for porphyry deposits and provides another piece of evidence of a possible blind system in the district.

There is also potential for further exploration under cover in the west of the district. The geology underlying the Clifton Flat area is poorly understood, though it is likely that the Gold Hill Wash fault continues into Clifton Flat and may represent a deeply penetrating structure with potential to tap or localize a magmatic-hydrothermal system. A geophysical anomaly and mild surface alteration led Kenecott to drill 10 holes targeting porphyry mineralization just west of Clifton Flat in the 1990s. Little is known about the target and outcome of drilling, though Dumont conducted soil sampling over the area in the 2000s and was motivated to drill a follow up hole, though the hole was executed improperly and no mineralization was intercepted (Lee, 2004). Lastly, surprisingly little work has been done on the Eocene stock in Gold Hill, particularly given its similarity in age to Bingham and the presence of other Eocene magmatic activity in the district (small diorite intrusion, granite dike [Burwell, 2018]). The Eocene is the most likely period to have produced a porphyry copper deposit, given the delamination of the subducting slab and upwelling of metal-rich asthenosphere. Clearly, the stock was not the only expression of Eocene magmatism in the district, and given the array of structural features that could control the ascent and emplacement of magma, a blind Eocene magmatic-hydrothermal system is a possibility.

Overall, evidence for eras of prolonged magmatic activity, metal enrichment, hydrothermal transportation across large distances, and overprinting mineralization and alteration styles all suggest potential for a deeper magmatic-hydrothermal system in Gold Hill. Given the character of the polymetallic veins and of the propylitic alteration at depth in drill holes, a porphyry copper deposit is a likely magmatic-hydrothermal system. Detailed mapping, characterization (geochemical and petrologic), and dating of magmatic units and polymetallic veins in the district are needed to further refine a model for blind porphyry mineralization.

Supergene Processes

A feature often referred to in detailed deposit descriptions from Gold Hill but rarely discussed as a discrete mineralizing event is the oxidation of sulfide ore. The oxidation of ore is often referred to as part of the supergene process, which creates supergene (also known as secondary or oxide) deposits that can be significant ore resources. Supergene deposits

comprise oxidized ore that may be concentrated on the order of two to ten times original concentrations, particularly with respect to copper, and hence are a significant aspect of deposit metallogeny and economics (Reich and Vasconcelos, 2015). Gold is not concentrated by supergene processes, but when hosted in pyrite (refractory ore), oxidation makes the gold more amenable to heap leaching, thus making low-grade deposits economic (e.g., Goldstrike deposit, southwest Utah; Willden, 2006).

The supergene process is characterized by the leaching, transport, and reprecipitation of metallic components in an ore deposit by surficial hydrologic processes (Sillitoe, 2005). Supergene deposits are usually the last stage of a deposit's paragenesis and form during a temporally and genetically separate event to the original sulfide ore that formed at depth in the crust (referred to as hypogene ore). Hypogene deposits are uplifted or exhumed to surficial levels where the deposit intersects the groundwater table. Oxidation takes place in the vadose zone, in the capillary fringe above the water table, and creates a vertically zoned profile of oxidation. Multiple stacked supergene profiles can form in areas where deposits remain at or near the surface and the water table is periodically depressed, allowing oxidation of new ore horizons.

The shallowest expression of a supergene deposit is an iron-oxide leached cap, under which supergene "blankets" of enriched ore can form. Supergene minerals, also known as secondary minerals, can form as massive ore bodies, in veins or on fractures, rimming and/or replacing individual mineral grains, or as exotic deposits migrated away from the source ore. Secondary minerals in copper deposits of the western U.S. are often chrysocolla and chalcocite, though in many historical districts (including Gold Hill) the term "copper pitch," "black copper," or tenorite is used to describe a black aphanitic copper ore comprising oxidized Cu, Fe, and Mn minerals. Similar to skarn alteration, oxidation can be a volume reduction reaction, hence producing large crystals with open space growth textures, such as botryoidal malachite (Leveille and Stegen, 2012; Kahou et al., 2021). Common oxidation minerals at Gold Hill include scorodite (As-bearing); plumbojarosite, cerussite, anglesite (Pb-bearing); hemimorphite (Zn-bearing); chrysocolla, malachite, azurite, chalcocite (Cu-bearing); and powellite (W-bearing) as well as exotic species like austinite, juanitaite, and zálesítite that have been of interest to mineral collectors for many decades.

The hypogene ore at Gold Hill was likely exhumed and exposed to meteoric waters in the Eocene to Miocene timeframe, consistent with other major supergene events in the western U.S., such as in Arizona (Leveille and Stegen, 2012). This event is bracketed on the older end by the emplacement of the Eocene stock at 40 Ma, since several of the deposits associated with the stock are oxidized. The variable depth of oxidation in the U.S. and Gold Hill arsenic mines is suggested to relate to the pre-supergene formation of impermeable jasperoid zones.

No dating exists on the jasperoids to further constrain the oxidation event. Clearly, topographic changes have occurred through time, as evidenced by slivers of volcanic units only preserved in Rodenhouse or Gold Hill Wash, which are interpreted to have been topographic lows during volcanic deposition. Dating of the volcanics in the district is an area of active research, and a recent Eocene age was obtained for a welded tuff unit of limited extent exposed along the northeast margin of Clifton Flat near Gold Hill Wash (Mills et al., 2023; Don Clark, Utah Geological Survey, written communication, 2024). Given the similarity of this age to the Eocene stock, no further constraint on the oxidation event can be gleaned. Direct dating of the supergene event at Gold Hill would be a challenge, as most direct dating on supergene deposits has been conducted on alunite (e.g., Cook, 1994). Supergene deposits that form over an enriched hypogene deposit are dominated by kaolinite, and alunite may also form under arid to semiarid conditions (Sillitoe, 2005). Supergene deposits tend to be characterized by smectite where sulfides are oxidized in situ. Gold Hill appears to be a mix of these settings, where oxidation of sulfides was in situ, but these oxidized deposits still overlie enriched sulfide ore (e.g., the arsenic replacement deposits). Additionally, it is unclear if Gold Hill would have been situated in an arid enough environment to favor the formation of alunite. The potential for direct dating of the supergene processes via alunite should be considered on a deposit by deposit basis, though this is an area of active research (Nathan Carey, Arizona Geological Survey, written communication, 2024).

Given the intense structural convolutions in Gold Hill, the lateral extents and depths of an oxidation profile may be a complex feature to decipher on a district scale. Groundwater often flows to fault zones via topography-driven flow since fault zones commonly form valleys and topographic depres-

sions, e.g., Gold Hill Wash and Rodenhouse Wash. In an active fault setting, the interaction with groundwater becomes more complex due to the relatively high permeability of active fault zones resulting from the concentration of stress and fault slip and the potential for induced mechanical flow (Sibson et al., 1975; Gudmundsson, 2000; Fronzi et al., 2021). Low- and high-angle normal faults are mapped in Gold Hill and interpreted to be post-Eocene stock emplacement (Robinson, 1993), but there is no further age control on these features. In most deposits at Gold Hill, the oxidation appears to have occurred as in situ sulfide oxidation with relatively little transport of metals prior to reprecipitation. At the U.S. mine the interface between oxidized scorodite and arsenopyrite sulfide is relatively sharp, indicating the scorodite ore has likely formed where the original extent of the arsenopyrite sulfide body existed. A quartz-tetrahedrite vein in the U.S. mine was oxidized and copper locally transported in the upper zone of the ore body (Nolan, 1935). At Yellow Hammer mine, green copper oxide rims clasts of quartz monzonite in a massive tourmaline matrix, and green copper oxides have redeposited along the c-axis of the large bladed actinolite sheafs, which are altered to sericite (Figure 26). Notably, the molybdenite at Yellow Hammer still appears relatively fresh, attributed to molybdenum's lack of mobility in supergene processes (Sillitoe, 2005).

Ultimately, the supergene processes at Gold Hill can be important on the individual deposit level, and thus are an important consideration for the metallurgy around economic viability. However, based on field observations and historical exploration literature, leaching and transport of metal-enriched fluids was insignificant and is unlikely to have created a “supergene blanket” that often forms a viable economic ore body on its own.

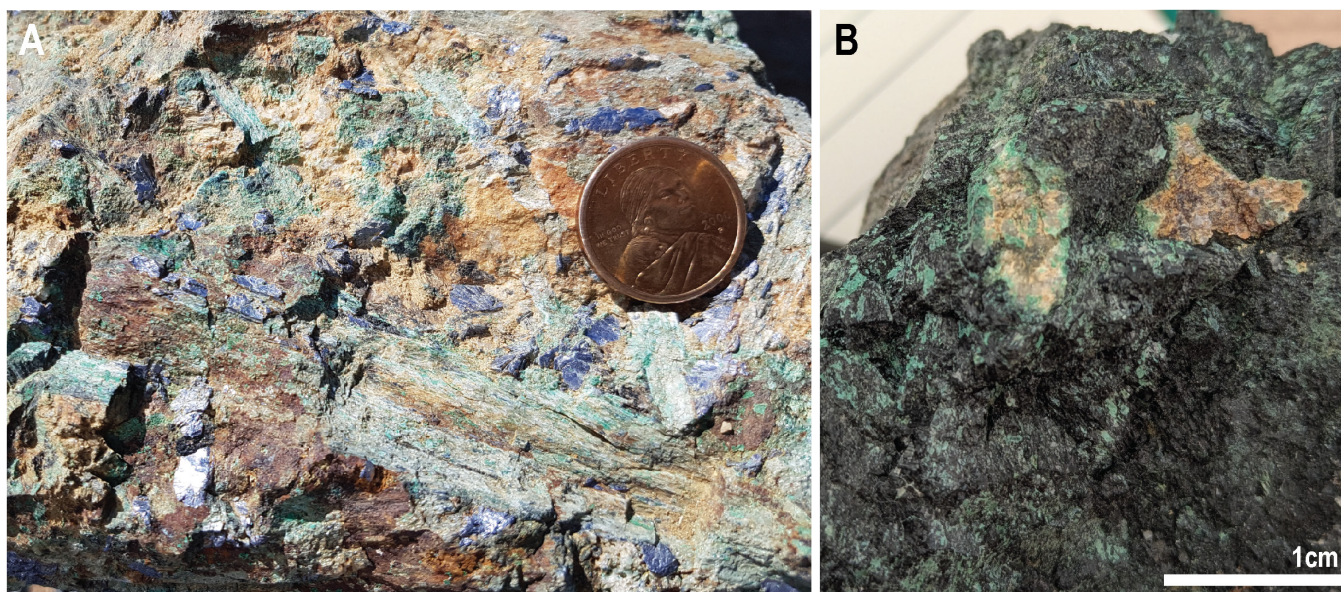


Figure 26. Examples of supergene oxidation at the Yellow Hammer mine. **A)** Green copper oxide mobilizing along the c-axis of altered actinolite sheafs with large blebs of silvery molybdenite. **B)** Green copper oxide mobilized to create a mantle around clasts of altered quartz monzonite in massive tourmaline.

Exploration Considerations and Future Work

As detailed in the sections above, many questions remain about the structural architecture and formation of the Gold Hill district: the nature, distribution, duration, and source of magmatic events; the number of mineralization eras; and the potential for deeper mineralization. Below is a summary of relevant future research questions related to the geological framework of Gold Hill, as well as a number of considerations on the mineral exploration potential, including critical mineral potential, of the district.

Research Questions

- **Multi-stage magmatism:** Abundant evidence for multi-stage magmatic evolution at Gold Hill exists and a focused effort to map, date, and characterize the diversity of magmatic bodies is needed. For example, the Eocene stock is often considered the summation of Eocene magmatism in the district, but there are diorite bodies along the margin of the stock and granite dikes cutting the Jurassic pluton also dated as Eocene (Mills et al., 2023; Burwell, 2018). The Eocene stock is cut by a mafic body that, by the established geochronological dates, is older than the stock itself, indicating a need for reconsideration (King and Burwell, 2016). Four recorded types of dikes occur in the Miocene-age Goshute dike swarm. Dating only exists on the rhyolite porphyry dike, and the quartz dike described by previous exploration geologists was not recognized in this study. The diversity of magmatism in the district requires a more detailed assessment, particularly to evaluate the potential for unrecognized magmatic-hydrothermal mineral systems in the district.
- **Magmatic emplacement:** The structural controls on the emplacement of the three defined stages of magmatism are poorly constrained. The Jurassic pluton has a distinct remnant magnetic feature striking perpendicular to the main structural fabric of the district but no compelling explanation has been proposed for this feature. The Eocene stock occurs at the intersection of two significant district faults and has been suggested to represent multiple individual but compositionally homogenous stocks (Robinson, 1993). The Miocene dike swarm has an unexplained strong northwest-southeast trend and is the opposite orientation to the most distinct vein swarm mapped in the district. Structural controls clearly play a significant role on the emplacement of all stages of magmatism; however, the exact relationship of these controls to magmatic emplacement and their implications for regional tectonics and mineralization have yet to be defined.
- **Formation of Clifton Flat and the Gold Hill Wash fault:** The origin of the Gold Hill Wash fault is not well understood, despite its potential control on the emplacement of the Eocene stock and role in the formation of Clifton Flat. Clifton Flat is a unique, structurally bound basin in

the district, but has had no focused research or exploration. It may represent a target area for buried mineralization, particularly deeper extensions of the magmatic-hydrothermal system that created the Clifton vein swarm.

- **Jasperoids:** The occurrence of jasperoid ridges is one of the most distinct aspects of the surface topography at Gold Hill and jasperoids have been recognized as exploration vectors or as potential controls in many deposits in the district; however, no focused characterization of the jasperoids is available. Many different styles and compositions of jasperoids have been recognized, and fault surfaces with slickensides are commonly observed within the jasperoid bodies. The faulting may represent post-jasperoid fault movement which could help constrain timing, though the jasperoids are theorized by some researchers to have formed syn-faulting. At a minimum, a comprehensive mapping, textural, and geochemical characterization of the jasperoids would begin to tie these distinct features into a holistic district interpretation. Recent advances have been made in dating of jasperoids using the (U-Th)/He system (Huff et al., 2020) and may present an option to gain absolute age constraints on the jasperoids in the district.
- **Volcanics:** Until relatively recently, little attention has been given to the volcanic units in the district. Recent mapping (Mills et al., 2023) improved the separation of volcanic units but further geochemical characterization and geochronological constraints are needed. Early results in this area indicate that at least one of the volcanic units was broadly coeval with the Eocene stock (Don Clark, Utah Geological Survey, written communication, 2024), which has implications for the crustal architecture in the district that now exposes a stock at the same elevation as subaerial volcanic units. A better understanding of volcanics of the same age is an essential aspect to understanding the magmatic framework, paleotopography, and structural evolution of the district.

Exploration Considerations

- **District mineral zonation:** Zonation of pathfinder elements, alteration halos, and metallogenic signatures has been a tool of choice for explorationists for decades. Many of these models are based on zonations observed around magmatic-hydrothermal systems in younger volcanics, and are not transferable to the Paleozoic carbonate terrane of the Basin and Range due to the geochemical buffering of carbonates and the relatively impermeable strata. Additionally, these models assume relatively little post-mineral structural modification and, in many cases, relatively little structural control on hydrothermal fluid flow (e.g., pervasive fluid flow in permeable host rocks versus structurally controlled fluid flow in impermeable host rocks). At Gold Hill and many other mining districts in the Basin and Range, all of these factors

(well developed pre-mineral structural fabric, impermeable host rocks, and post-mineral structural dismemberment/rotation) come together to render traditional zoned models inapplicable. Additionally, these models generally only consider one metallogenic event, whereas Gold Hill demonstrably has at least three discrete metallogenic events. Much effort has been put in by previous researchers to determine a district-wide zonation, but the limited age control and structural complexities have not yielded useful results, and other applications of mineral systems analysis are likely more relevant.

- **Structural plumbing:** As noted by Nolan (1935) and other researchers and explorationists in the district, the intense faulting of the Paleozoic basement has created a structural network well suited to the transportation of ore-bearing fluids. The structural plumbing in the district is possibly overdeveloped, meaning that there is no effective trap for fluids to concentrate in large volumes, e.g., lacking the “pressure-cooker” effect of Sil-litoe (2010). The level of faulting and fracturing in the district may be the reason for many small, high-grade deposits as opposed to fewer large deposits. Although the high-grade deposits were valuable for historical mining, modern mining typically requires larger tonnages to account for the high upfront costs of establishing mining operations. Though Gold Hill has many small, high-grade vein, skarn, and carbonate replacement deposits, none are on par with the size of major vein and carbonate replacement deposits in districts like Park City and Tintic, where an economic porphyry copper deposit has yet to be discovered. Gold Hill deposits have notably high grades, but their small size and intense structural control suggest that a mineralized porphyry system may yet remain at depth.
- **Structural inheritance and dismemberment:** As has been delineated throughout this report, the structural architecture of Gold Hill is extremely complex and multi-generational. Structural inheritance from the Mesozoic deformation contributed to the architecture of new and reactivated structures during Cenozoic extension. However, it is also important to factor in the impact of the Ferguson detachment fault, where the hanging wall of the detachment mobilized eastward along the Chainman Shale towards Gold Hill. The detachment caused intense deformation in Gold Hill against, around, or over the large, rigid Jurassic pluton. The Ferguson detachment not only created another generation of deformation overprinting Jurassic and Eocene mineralization, but also may have detached shallow expressions of mineralization from deeper mineralized sources. Without factoring in the effects of the detachment fault, vectoring from shallow indicators or pathfinders risks missing source targets. During Basin and Range era extension (post-dating the detachment faulting), large normal faults dismembered and rotated

the geology and previous mineralization even further, while also creating a structural host site for the younger low-sulfidation epithermal system. The importance of understanding each of these eras of structural deformation cannot be overstated in terms of minerals exploration and reconstructing the district.

- **Cross-cutting vein mapping and dating:** Many of the skarn and replacement deposits in the district note younger cross-cutting veins with differing mineralogy, e.g., a quartz-tetrahedrite vein cross-cutting the arsenic replacement ore at U.S. mine. These veins are thought to be a late phase of the deposit but generally related to the same event. However, the Gold Hill deposits have little to no age constraints, and the assumption that the veins are related to the same mineralizing event overlooks the potential that veins may be a shallow, distal expression of deeper magmatic-hydrothermal activity. The presence of younger veins cross-cutting porphyry mineralization has been used as a successful exploration vector to deeper mineralization, such as at Escondida Este (Hervé et al., 2012). The importance of recognizing overprinting mineralization, versus different expressions of the same mineralization event, is key to understanding the potential for deeper mineralization in Gold Hill and emphasizes the need for detailed mapping of the veins and cross-cutting relationships informed by absolute age dating.
- **Clifton vein swarm:** The Clifton vein swarm has an anomalous vein density, spatial footprint, and structural fabric compared to the rest of the Gold Hill district. The historical mapped extent of the vein swarm, which was not verified in this study, is on par with the polymetallic vein swarm at Bingham Canyon (Tomlinson et al., 2021). The veins are characteristic “fissure veins,” meaning they are strongly structurally-controlled and thicknesses vary significantly along strike; however, several veins hosted high-grade mines, including the Monaco mine with copper grades up to 10% Cu. Despite the size of the vein swarm and locally high grades, the Clifton vein swarm has received relatively little exploration focus or consideration as a vector for mineralization. Geochronology, detailed mapping, and mineralogical characterization is needed. The Clifton vein swarm represents the best exploration potential in the district for vectoring to a major magmatic-hydrothermal deposit, particularly given the proximity to shallow basin fill in Clifton Flat that could provide cover for a deeper source deposit.

SUMMARY AND CONCLUSIONS

The Gold Hill district is a structurally complex, multi-generational magmatic-hydrothermal mineral district hosted in Paleozoic carbonate bedrock in the eastern Great Basin. Gold

Hill is the largest past-producer of W and As in Utah, and a notable past-producer of Pb, Cu, Au, Ag, and Zn. Known mineralizing events include skarn, replacement, and vein deposits related to a Jurassic quartz monzonite pluton; skarn and vein deposits related to an Eocene granite stock; and a Late Miocene low-sulfidation epithermal system that has been evaluated for Au and Be potential. Minerals exploration in the district has also pursued sediment-hosted gold deposits associated with the Mississippian and Pennsylvanian carbonate units, porphyry molybdenum deposits associated with the mid-Miocene Goshute Wash dike swarm, and porphyry copper potential across the district.

This study highlights three questions about the framework geology in the district and the implications for mineral deposit formation. First, the emplacement of the Jurassic pluton, one of the largest geological bodies in the district, is poorly understood with respect to tectonic regime and fault controls during emplacement. Additionally, a remnant magnetic feature cuts west-northwest across the northern end of the pluton, perpendicular to the structural fabric of the district, which currently has no explanation. Given the size of the pluton within the district, the rheological variation with the surrounding Paleozoic bedrock, and the mineral deposits associated with the pluton, a better understanding of the pluton's structure is clearly needed to understand its role in subsequent district evolution and mineralization. Second, the Chainman Shale is a regionally significant unit that has been severely attenuated within Gold Hill and likely acted as a lubricating unit during Jurassic compressional deformation, creating a complex architecture of Paleozoic carbonates and structural pathways for ore fluids in later mineralizing events. Additionally, the Tertiary Ferguson detachment fault slipped along the Chainman Shale, creating another era of deformation in Gold Hill and disconnecting the geology above and below the Chainman. Further structural analysis to constrain Chainman-centered deformation in the Jurassic and Tertiary and implications for mineral systems is needed. Third, Clifton Flat is a notable basin within the Paleozoic bedrock of the district but has received little research attention in terms of formation and has had no known exploration for buried mineralization. The eastern margin of Clifton Flat is bounded by the Gold Hill Wash fault, which also controls the emplacement of the Eocene stock farther north. Despite its significance for basin formation and magmatic emplacement, the timing and kinematic history of the Gold Hill Wash fault is poorly understood.

The most promising potential for undiscovered mineral deposits in Gold Hill are polymetallic veins that cross-cut skarn and replacement mineralization and may be an indicator of deeper magmatic-hydrothermal mineralization, and the Clifton vein swarm. The Clifton vein swarm is a structurally consistent, high density, aerially extensive set of fissure veins that locally host high-grade Pb, Ag, and Cu deposits. The historically mapped extent and scale of the Clifton vein swarm is on par with the polymetallic vein swarm at Bingham Canyon, which is interpreted as intermediate sulfidation veins associated with the Bingham porphyry copper system. Although geochronol-

ogy, mapping, and characterization of the Clifton vein swarm is needed, the potential for the vein swarm to vector towards deeper porphyry copper mineralization is considered the highest priority exploration target in the district.

The critical mineral potential of known deposits in the district is considered low, as the deposits are high grade but low tonnage and have complex metallogeny. The arsenic replacement deposits (Gold Hill mine and U.S. mine) are the highest potential given that ore is known to remain, but these are underground deposits which further complicate the economics of any mining operation. The W-bearing skarns associated with the Jurassic pluton (e.g., Yellow Hammer, Reaper) are likewise small, mostly mined out, and too mineralogically complex for economic development. The W skarns around the Eocene granite are understudied and currently considered too small to be economic. However, the mineralogy of these deposits is less complex and there may be some unidentified upside potential. Beryllium enrichment in the low-sulfidation epithermal system has been identified since the 1960s, but the grades are an order of magnitude lower than those found at Spor Mountain, which has a remaining mine life of at least 75 years. The low-sulfidation epithermal system is not highly enriched in Au or Ag, so mining Be as a byproduct is also not economic. The most prospective critical mineral target in the district is the porphyry copper potential associated with the Clifton vein swarm, since porphyry copper deposits are known to be capable of producing various critical minerals as byproducts.

ACKNOWLEDGMENTS

This report was funded by the U.S. Geological Survey Earth Mapping Resource Initiative grant G20AC00168-01. Support from Warren Day in developing the project is greatly appreciated. Don Clark and Andrew Rupke (UGS) are co-authors on the Clifton quadrangle 7.5' map (Mills et al., 2023) that was also completed under this grant, and their insight into how the framework geology informed mineralization is greatly appreciated. Conversations with Don Clark on the regional setting have been phenomenally helpful. Don is currently leading a STATEMAP-funded intermediate-scale mapping project in this area. Nathan Carey (Arizona Geological Survey) and Simon Jowitt (University of Nevada Reno) provided invaluable insight on the paragenesis of Jurassic skarns that greatly helped understanding the potential for cross-cutting relationships. This work draws strongly on previous researchers and mineral exploration geologists who worked in the Gold Hill district, notably Ken Krahulec (retired UGS) and Jamie Robinson. Newmont Gold Corp. contributed geophysical, geochemical, and drilling data in support of this project which greatly enhanced understanding of the district, and the efforts of Jim Essman and Scott Briscoe are greatly appreciated. Caleb King (Bronco Creek Exploration) provided valuable insight into many of the structural controls on various mineral systems in the district and on IOCG deposits. Private landowners in

the Gold Hill area allowed access for sampling and mapping, which is deeply appreciated. Several previous and current UGS staff assisted in the geochemical sampling for this program and thanks is given to Kayla Smith, Wil Hurlbut, Bear Jordan, and Taylor Boden for their support. Reviews by Don Clark, Caleb King, Nathan Carey, Jim McVey, Andrew Rupke, and Stephanie Carney greatly improved the quality of this report.

REFERENCES

- Al Furqan, R., Watanabe, Y., Arribas, A., Leys, C., Echigo, T., Putri, R.A., and Sevirajati, R., 2022, Chemical and short-wave infrared characteristics of white mica associated with the Gajah Tidur porphyry copper system at the deep Grasberg Cu-Au-(Mo) deposit, Indonesia: *Resource Geology*, v. 72.
- Allmendinger, R.W., and Jordan, T.E., 1981, Mesozoic evolution, hinterland of the Sevier orogenic belt: *Geology*, v. 9, p. 308–313.
- Allmendinger, R.W., and Jordan, T.E., 1984, Mesozoic structure of the Newfoundland Mountains, Utah—Horizontal shortening and subsequent extension in the hinterland of the Sevier belt: *Geological Society of America Bulletin*, v. 95, no. 11, p. 1280–1292.
- Allmendinger, R. W., 1992, Chapter 13—Thrust and fold tectonics of the western United States exclusive of the accreted terranes, in Burchfiel, B. C., Lipman, P., and Zoback, M. L., editors, *The Cordilleran orogen—Conterminous U. S.*: Boulder, Colorado, Geological Society of America, 583 p.
- Arehart, G.B., Chryssoulis, S.L., and Kesler, S.E., 1993, Gold and arsenic in iron sulfides from sediment-hosted disseminated gold deposits—Implications for depositional processes: *Economic Geology*, v. 88, no. 1, p. 171–185.
- Armstrong, R.L., 1968, Sevier orogenic belt in Nevada and Utah: *Geological Society of America Bulletin*, v. 79, no. 4, p. 429–458.
- Armstrong, R.L., 1970, Geochronology of Tertiary igneous rocks, eastern Basin and Range Province, western Utah eastern Nevada and vicinity, U.S.A.: *Geochimica et Cosmochimica Acta*, v. 34, p. 205–232.
- Bailey, G.B., 1974, The occurrence, origin, and economic significance of gold-bearing jasperoids in the central Drum Mountains, Utah: Stanford, California, Stanford University, Ph.D. dissertation, 319 p.
- Ballantyne, J.M., and Moore, J.N., 1988, Arsenic geochemistry in geothermal systems: *Geochimica et Cosmochimica Acta*, v. 52, no. 2, p. 475–483.
- Barton, M.D., Girardi, J.D., Kreiner, D.C., Seedorff, E., Zurcher, L., Dilles, J.H., Haxel, G.B., and Johnson, D.A., 2011, Jurassic igneous-related metallogeny of southwestern North America, in Steiner, R.C., Pennell, B., editors, *Great Basin evolution and metallogeny: Geological Society of Nevada, 2010 Symposium*, Geological Society of Nevada, Reno, Nevada, p. 373–396.
- Barton, M.D., and Johnson, D.A., 1996, Evaporitic-source model for igneous-related Fe oxide-(REE-Cu-Au-U) mineralization: *Geology*, v. 24, p. 259–262.
- Barton, M.D., and Young, S., 2002, Non-pegmatitic deposits of beryllium—Mineralogy, geology, phase equilibria and origin, in Grew, E.S., editor, *Beryllium—Mineralogy, petrology, and geochemistry: Reviews in Mineralogy and Geochemistry*, v. 50, p. 591–691.
- Beinlich, A., Barker, S.L.L., Dipple, G.M., Hansen, L.D., and Megaw, P.K.M., 2019, Large-scale stable isotope alteration around the hydrothermal carbonate-replacement Conico de Mayo Zn-Ag deposit, Mexico: *Economic Geology*, v. 14, no. 2, p. 375–396.
- Bell, A.S., and Simon, A., 2011, Experimental evidence for the alteration of the Fe³⁺/ΣFe of silicate melt caused by the degassing of chlorine-bearing aqueous volatiles: *Geology*, v. 39, no. 5, p. 499–502, <https://doi.org/10.1130/G31828.1>.
- Beranek, L.P., Link, P.K., and Fanning, C.M., 2016, Detrital zircon record of mid-Paleozoic convergent margin activity in the northern U.S. Rocky Mountains—Implications for the Antler orogeny and early evolution of the North American Cordillera: *Lithosphere*, v. 8, no. 5, p. 533–550.
- Bereskin, S.R., McLennan, J.D., Chidsey, T.C. Jr., and Nielsen, P.J., 2015, Hydrocarbon reservoir potential of the Mississippian Chainman Shale, western Utah: *Utah Geological Survey Miscellaneous Publication 15-4*, 81 p., <https://doi.org/10.34191/MP-15-4>.
- Best, M.G., Christiansen, E.H., de Silva, S., and Lipman, P.W., 2016, Slab-rollback ignimbrite flareups in the southern Great Basin and other Cenozoic American arcs—A distinct style of arc volcanism: *Geosphere*, v. 12, no. 4, p. 1097–1135.
- Bissell, H.J., 1964, Patterns of sedimentation in Pennsylvanian and Permian strata of part of the eastern Great Basin, in Merriam, D.F., editor, *Symposium on cyclic sedimentation: Kansas Geological Survey, Bulletin 169*, p. 43–56.
- Bowman, J.R., 1998, Stable-isotope systematics of skarns, in Lentz, D.R., editor, *Mineralized intrusion-related skarn systems: Mineralogical Association of Canada Short Course*, v. 26, p. 99–145.
- Brodbeck, M., McClenaghan, S.H., Kamber, B.S., and Redmond, P.B., 2022, Metal(loid) deportment in sulfides from the high-grade core of the Bingham Canyon porphyry Cu-Mo-Au deposit, Utah: *Economic Geology*, v. 117, no. 7, p. 1521–1542.
- Burisch, M., Gerdes, A., Walter, B.F., Neumann, U., Fettel, M., and Markl, G., 2017, Methane and the origin of five-element veins—Mineralogy, age, fluid inclusion chemistry and ore forming processes in the Odenwald, SW Germany: *Ore Geology Reviews*, v. 81, p. 42–60.

- Burwell, J., 2018, Alteration and associated mineralization in the Gold Hill Jurassic pluton, Tooele County, Utah: Tucson, University of Arizona, M.S. thesis, 186 p.
- Butler, B.S., Loughlin, G.F., and Heikes, V.C., 1920, Ore deposits of Utah: U.S. Geological Survey Professional Paper 111, 672 p., 7 plates.
- Camillari, P.A., and Chamberlain, K.R., 1997, Mesozoic tectonics and metamorphism in the Pequop Mountains and Wood Hills region, northeastern Nevada—Implications for architecture and evolution of the Sevier orogeny: Geological Society of America Bulletin, v. 109, p. 74–94.
- Candela, P.A., and Bouton, S.L., 1990, The influence of oxygen fugacity on tungsten and molybdenum partitioning between silicate melts and ilmenite: Economic Geology, v. 85, no. 3, p. 633–640.
- Carey, N.J., 2022, Age and genesis of W-Mo-Cu mineralization, Gold Hill, Utah: Las Vegas, University of Nevada Las Vegas, M.S. thesis, 158 p.
- Carten, R.B., 1986, Sodium-calcium metasomatism—Chemical, temporal, and spatial relationships at the Yerington, Nevada, porphyry copper deposit: Economic Geology, v. 81, p. 1495–1519.
- Cashman, P.H., and Sturmer, D.M., 2021, Paleogeographic reconstruction of Mississippian to Middle Pennsylvanian basins in Nevada, southwestern Laurentia: Palaeogeography, Palaeoclimatology, Palaeoecology, v. 584, no. 110666, <https://doi.org/10.1016/j.palaeo.2021.110666>.
- Chamberlain, A.K., 1981, Biostratigraphy of the Great Blue Formation, in Hamblin, W.K., and Gardner, C.M., eds., Brigham Young University Geology Studies, v. 28, no. 3, p. 9–17.
- Chang, Z., 2021, Skarn—Zoning patterns and controlling factors [abs.]: Indonesian Society of Economic Geologists (MGEI) Proceedings 13th Annual Convention, Jakarta, 14–15 December.
- Chang, Z., and Meinert, L.D., 2008, Zonations in skarns—complexities and controlling factors [abs.]: Proceedings of the PACRIM Congress, November 2008, Gold Coast, Queensland, Australia November 24–26, 2008.
- Chang, Z., Shu, Q., and Meinert, L.D., 2019, Skarn deposits of China: Society of Economic Geologists Special Publication, no. 22, p. 189–234.
- Chiaradia, M., and Caricchi, L., 2022, Supergiant porphyry copper deposits are failed large eruptions: Communications Earth & Environment, v. 3, no. 107, <https://doi.org/10.1038/s43247-022-00440-7>.
- Chorney, R., 1943, Scheelite and mineral association at the Reaper mine, Gold Hill, Utah: Salt Lake City, University of Utah, M.S. thesis, 56 p.
- Christensen, O.D., 1975, Metamorphism of the Manning Canyon and Chainman Formations: Stanford, California, Stanford University, Ph.D. dissertation, 166 p.
- Clark, D.L., 2020, The Uinta-Tooele structural zone—what’s in a name?: Utah Geological Survey Survey Notes, v. 52, no. 2, p. 4–5, <https://doi.org/10.34191/snt-52-2>.
- Colgan, J.P., and Henry, C.D., 2009, Rapid middle Miocene collapse of the Mesozoic orogenic plateau in north-central Nevada: International Geology Review, v. 51, no. 9–11, p. 920–96.
- Cook, H.E., and Corboy, J.J., 2004, Great Basin Paleozoic carbonate platform—Facies, facies transitions, depositional models, platform architecture, sequence stratigraphy, and predictive mineral host models: U.S. Geological Survey Open-File Report 2004-1078, 135 p.
- Cook, S.S., 1994, The geological history of supergene enrichment in the porphyry copper deposits of southwestern North America: Tucson, University of Arizona, Ph.D. dissertation, 163 p.
- Cox, D.P., 1986, Descriptive model of polymetallic veins, in Cox, D.P., and Singer, D.A., editors, Mineral deposit models: U.S. Geological Survey Bulletin 1693, p. 125–129.
- Crawford, A.L., and Chorney, R., 1944, The tungsten pipe of the Reaper mine: Utah Academy of Science, Arts, and Letters, v. 19–20, p. 143–149.
- Day, W.C., 2019, The Earth Mapping Resources Initiative (Earth MRI)—Mapping the Nation’s critical mineral resources (ver. 1.2, September 2019): U.S. Geological Survey Fact Sheet 2019–3007, 2 p., <https://doi.org/10.3133/fs20193007>.
- Dasch, M.D., 1969, Antimony and other minor metals, in Mineral and water resources of Utah: Utah Geological and Mineral Survey Bulletin 73, p. 135–144, <https://doi.org/10.34191/B-73>.
- DeCelles, P.G., 2004, Late Jurassic to Eocene evolution of the Cordilleran thrust belt and foreland basin system, western U.S.A.: American Journal of Science, v. 304, p. 105–168.
- DeCelles, P.G., and Coogan, J.C., 2006, Regional structure and kinematic history of the Sevier fold-and-thrust belt, central Utah: Geological Society of America Bulletin, v. 118, p. 841–864.
- Di Fiori, R.V., Long, S.P., Fetrow, A.C., Snell, K.E., Bonde, J.W., and Vervoort, J.D., 2021, The role of shortening in the Sevier hinterland within the U.S. cordilleran retroarc thrust system—Insights from the Cretaceous Newark Canyon Formation in central Nevada: Tectonics, v. 40, 31 p.
- Dickinson, W.R., 2006, Geotectonic evolution of the Great Basin: Geosphere, v. 2, no. 7, p. 353–368.
- Doelling, H.H., Sprinkel, D.A., Kowallis, B.J., and Kuehne, P.A., 2013, Temple Cap and Carmel Formations in the Henry Mountains basin, Wayne and Garfield Counties, Utah, in Morris, T.H., and Resselar, R., editors, The San Rafael Swell and Henry Mountains basin—Geologic centerpiece of Utah: Utah Geological Association Publication 42, p. 279–318.

- Dubiel, R.F., Potter, C.J., Good, S.C., and Snee, L.W., 1996, Reconstructing an Eocene extensional basin—The White Sage Formation, eastern Great Basin, *in* Beratan, K.K., editor, Reconstructing the history of Basin and Range extension using sedimentology and stratigraphy: Geological Society of America Special Paper 303.
- Dumont Nickel Inc., 2005, Annual report 2005: TSX Venture Exchange stock filing, March 31, 2005.
- Dupuis, C., and Beaudoin, G., 2011, Discriminant diagrams for iron oxide trace element fingerprinting of mineral deposit types: *Miner Deposita* 46, p. 319–335, <https://doi.org/10.1007/s00126-011-0334-y>.
- Eggleston, T., Reid, D., and Colquhoun, W., 2019, AntaKori project, Cajamarca Province, Peru: Ni 43-101 Technical Report prepared for Regulus Resources Inc., 191 p.
- Einaudi, M.T., Hedenquist, J.W., and Inan, E.E., 2003, Sulfidation state of fluids in active and extinct hydrothermal systems—Transitions from porphyry to epithermal environments: *Society of Economic Geologists Special Publication* 10, p. 285–314.
- Einaudi, M.T., Meinert, L.D., and Newberry, R.J., 1981, Skarn deposits: *Economic Geology*, 75th Anniversary Volume, p. 317–391.
- Elison, M.W., 1995, Causes and consequences of Jurassic magmatism in the northern Great Basin—Implications for tectonic development: *Geological Society of America Special Paper* 299, 19 p.
- El-Shatoury, H.M., and Whelan, J.A., 1970, Mineralization in the Gold Hill mining district, Tooele County, Utah: *Utah Geological and Mineralogical Survey Bulletin* 83, 44 p., <https://doi.org/10.34191/B-83>.
- Emsbo, P., Hofstra, A.H., Lauha, E.A., Griffin, G.L., and Hutchinson, R.W., 2003, Origin of high-grade gold ore, source of ore fluid components, and genesis of the Meikle and neighboring Carlin-type deposits, northern Carlin trend, Nevada: *Economic Geology*, v. 98, p. 1069–1100.
- Erickson, A.J.Jr., 1974, The Uinta-Gold Hill trend—An economically important lineament, *in* Hodgson, R.A., Gay, S.P.Jr., and Benjamins, J.Y., editors, *Proceedings of the First International Conference on the New Basement Tectonics*: Utah Geological Association, no. 13, p. 126–138.
- Everett, F.D., 1961, Tungsten deposits in Utah: U.S. Bureau of Mines Information Circular 8014, 44 p.
- Ferre, E.C., Galland, O., Montanari, D., and Kalakay, T.J., 2012, Granite magma migration and emplacement along thrusts: *International Journal of Earth Sciences (Geologisch Rundsch)*, v. 101, p. 1673–1688.
- Fontboté, L., and Bendezú, R., 2009, Cordilleran or Butte-type veins and replacement bodies as a deposit class in porphyry systems: 10th Biennial Society of Geology Applied to Ore Deposits Meeting, Townsville, Australia, *Proceedings*, p. 521–523.
- Fronzi, D., Mirabella, F., Cardellini, C., Caliro, S., Palpacelli, S., Cambi, C., Valigi, D., and Tazioli, A., 2021, The role of faults in groundwater circulation before and after seismic events—Insights from tracers, water isotopes and geochemistry: *Water*, v. 13, no. 11, 1499, <https://doi.org/10.3390/w13111499>.
- Griffitts, W.R., 1965, Recently discovered beryllium deposits near Gold Hill, Utah: *Economic Geology*, v. 60, p. 1298–1305.
- Groves, D.I., Bierlein, F.P., Meinert, L.D., Hitzman, M.W., 2010, Iron oxide copper-gold (IOCG) deposits through Earth history—Implications for origin, lithospheric setting, and distinction from other epigenetic iron oxide deposits: *Economic Geology*, v. 105, p. 641–654.
- Gruen, G., Heinrich, C.A., and Schroeder, K., 2010, The Bingham Canyon porphyry Cu-Mo-Au deposit II—Vein geometry and ore shell formation by pressure-driven rock extension, *in* Krahulec, K., and Shroeder, K., editors, *Tops and bottoms of porphyry copper deposits—The Bingham and Southwest Tintic districts, Utah*: *Society of Economic Geologists Guidebook Series*, v. 41.
- Gudmundsson, A., 2000, Active fault zones and groundwater flow: *Geophysical Research Letters*, v. 27, no. 18, p. 2993–2996.
- Halley, S., Dilles, J.H., and Tosdal, R.M., 2015, Footprints—Hydrothermal alteration and geochemical dispersion around porphyry copper deposits: *SEG Discovery*, v. 100, p. 1–17.
- Henry, C.D., John, D.A., Leonardson, R.W., McIntosh, W.C., Heizler, M.T., Colgan, J.P., and Watts, K.E., 2023, Timing of rhyolite intrusion and Carlin-type gold mineralization at the Cortez Hills Carlin-type deposits, Nevada, USA: *Economic Geology*, v. 118, no. 1, p. 57–91.
- Hervé, M., Sillitoe, R.H., Wong, C., Fernández, P., Crignola, F., Ipinza, M., and Urzúa, F., 2012, Geological overview of the Escondida porphyry copper district, northern Chile, *in* Hedenquist, J.W., Harris, M., and Camus, F., editors, *Geology and genesis of major copper deposits and districts of the world—A tribute to Richard H. Sillitoe*: *Society of Economic Geologists Special Publication*, v. 16, p. 55–78.
- Hess, F. L., 1924, Molybdenum deposits—A short review: *U.S. Geological Survey Bulletin* 761, 35 p.
- Hofstra, A.H., and Kreiner, D.C., 2020, Systems-deposits-commodities-critical minerals table for the Earth Mapping Resources Initiative (ver. 1.1, May 2021): U.S. Geological Survey Open-File Report 2020–1042, 26 p., <https://doi.org/10.3133/ofr20201042>.
- Horton, J.D., and San Juan, C.A., 2016, Prospect- and mine-related features from U.S. Geological Survey 7.5- and 15-minute topographic quadrangle maps of the United States (ver. 10.0, May 2023): U.S. Geological Survey data release, <https://doi.org/10.5066/F78W3CHG>.

- Huff, D.E., Holley, E., Guenther, W.R., and Kaempfer, J.M., 2020, Fe-oxides in jasperoids from two gold districts in Nevada—Characterization, geochemistry, and (U-Th)/He dating: *Geochimica et Cosmochimica Acta*, v. 286, p. 72–102.
- Jewell, P.W., Silberling, N.J., and Nichols, K.M., 2000, Geochemistry of the Mississippian Delle phosphatic event, eastern Great Basin, U.S.A.: *Journal of Sedimentary Research*, v. 70, no. 5, p. 1222–1233.
- John, D.A., 2006, Geology and mining history of the Park City mining district, central Wasatch Mountains, Utah, *in* Bon, R.L., Gloyd, R.W., and Park, G.M., editors, *Mining districts of Utah: Utah Geological Association Publication 32*, p. 67–93.
- John, D.A., and Ballantyne, G.H., 1997, Geology and ore deposits of the Oquirrh and Wasatch Mountains, Utah: *Society of Economic Geologists Guidebook Series*, v. 29.
- John, D.A., and Taylor, R.D., 2016, By-products of porphyry copper and molybdenum deposits, *in* Verplanck, P.L., and Hitzman, M.W., editors, *Rare earth and critical elements in ore deposits: Society of Economic Geologists Reviews in Economic Geology*, v. 18, p. 137–164.
- Jones, C.H., Sonder, L.J., and Unruh, J.R., 1998, Lithospheric gravitational potential energy and past orogenesis—Implications for conditions of initial Basin and Range and Laramide deformation: *Geology*, v. 26, no. 7, p. 639–642.
- Jones, A.J., Sturmer, D.M., Bidgoli, T.S., Dietsch, C., and Moeller, A., 2021, Sediment routing and provenance of shallow to deep marine sandstones in the late Paleozoic Oquirrh Basin, Utah: *Palaeogeography, Palaeoclimatology, Palaeoecology*, v. 578, no. 110582, <https://doi.org/10.1016/j.palaeo.2021.110582>.
- Kahou, Z.S., Duchêne, S., Brichau, S., Campos, E., Estrade, G., Poujol, M., Kathirgamar, J., Testa, H., Leisen, M., Choy, S., de Parseval, P., Riquelme, R., and Carretier, S., 2021, Mineralogical and chemical characterization of supergene copper-bearing minerals—Examples from Chile and Burkina Faso: *Ore Geology Reviews*, v. 11, <https://doi.org/10.1016/j.oregeorev.2021.104078>.
- Kalakay, T.J., John, B.E., and Lageson, D.R., 2001, Fault-controlled pluton emplacement in the Sevier fold-and-thrust belt of southwest Montana, USA: *Journal of Structural Geology*, v. 23, p. 1151–1165.
- Ketner, K.B., 1998, The nature and timing of tectonism in the western facies terrane of Nevada and California—An outline of evidence and interpretations derived from geologic maps of key areas: *U.S. Geological Survey Professional Paper 1592*, 19 p.
- King, C.A., and Burwell, J., 2016, Report on the igneous petrology and U-Pb ages of igneous rocks from Gold Hill and Ferber Flats geochronology of the igneous rocks: Unpublished report by the University of Arizona, Tucson, Arizona, 16 p.
- Krahulec, K., 2014, Discovery of the Stockton porphyry copper system, Stockton mining district, Tooele County, Utah, *in* Ganske, R., Schroeder, K., and Krahulec, K., editors, *Uncovering the Bingham and Stockton Cu-Mo-Au porphyries: Society of Economic Geologists Guidebook Series*, v. 41.
- Krahulec, K., 2015, Tertiary intrusion-related copper, molybdenum, and tungsten mining districts of the Eastern Great Basin, *in* Pennell, W.M., and Garside, L.J., editors, *New concepts and discoveries: Geological Society of Nevada 2015 Symposium*, p. 219–250.
- Krahulec, K., 2017, Mineral resource potential of the Gold Hill mining district, Tooele County, Utah: Utah Geological Survey contract deliverable prepared for the Utah School and Institutional Trust Lands Administration, 63 p., 2 appendices.
- Krahulec, K., 2018, Utah mining districts: Utah Geological Survey Open-File Report 695, 195 p., 1 plate, scale 1:1,000,000, <https://doi.org/10.34191/OFR-695>.
- Langenheim, V.E., Vazquez, J.A., Schmidt, K.M., Guglielmo, G., Sweetkind, D.S., 2021, Influence of pre-existing structure on pluton emplacement and geomorphology—The Merrimac plutons, northern Sierra Nevada, California, USA: *Geosphere*, v. 17, no. 2, p. 455–478.
- Large, R.R., Danyushevsky, L., Hollit, C., Maslennikov, V., Meffre, S., Gilbert, S., Bull, S., Scott, R., Emsbo, P., Thomas, H., Singh, B., and Foster, J., 2009, Gold and trace element zonation in pyrite using a laser imaging technique—Implications for the timing of gold in orogenic and carlin-style sediment-hosted deposits: *Economic Geology*, v. 104, no. 5, p. 635–668.
- Large, S.J.E., 2018, The magmatic to hydrothermal evolution of porphyry Cu-Au deposits—A zircon perspective: Ph.D. thesis, Eidgenössische Technische Hochschule Zürich, 133 p.
- Lee, F., 2004, Report on the Clifton-Gold Hill property, Gold Hill mining district, Tooele County, Utah, USA: unpublished consultant's report for Dumont Nickel Inc., 101 p.
- Lemmon, D.M., 1969, Tungsten, *in* *Mineral and water resources of Utah: Utah Geological and Mineralogical Survey Bulletin 73*, p. 121–124, <https://doi.org/10.34191/B-73>.
- Lentz, D.R., 2005, Mass-balance analysis of mineralized skarn systems—Implications for replacement processes, carbonate mobility, and permeability evolution, *in* Mao, J., and Bierlein, F.P., editors, *Mineral deposit research—Meeting the global challenge: Proceedings of the Eighth Biennial SGA Meeting Beijing, China, 18–21 August 2005*, p. 421–424.
- Leveille, R.A., and Stegen, R.J., 2012, The southwestern North America porphyry copper province, *in* Hedenquist, J.W., Harris, M., and Camus, F., editors, *Geology and genesis of major copper deposits and districts of the*

- world—A tribute to Richard H. Sillitoe: Society of Economic Geologists Special Publication, v. 16, <https://doi.org/10.5382/SP.16.15>.
- Liu, H., Chen, Y., Wang, B., Faure, M., Erdmann, S., Martelet, G., Scaillet, B., and Huang, F., 2020, Role of inherited structure on granite emplacement—An example from the Late Jurassic Shibeï pluton in the Wuyishan area (South China) and its tectonic implications: *Tectonophysics*, no. 779, <https://doi.org/10.1016/j.tecto.2020.228394>.
- Long, S.P., 2015, An upper-crustal fold province in the hinterland of the Sevier orogenic belt, eastern Nevada, U.S.A.—A cordillera valley and ridge in the Basin and Range: *Geosphere*, v. 11, no. 2, p. 404–424.
- Long, S.P., 2019, Geometry and magnitude of extension in the basin and range province (39°N), California, Nevada, and Utah, U.S.A.—Constraints from a province-scale cross section: *Geological Society of America Bulletin*, v. 131, no. 1–2, p. 99–119.
- Long, S.P., Blackford, N.R., Lee, J., and Soignard, E., 2024, Crustal thermal architecture, structural reconstructions, field relationships, and geophysical data rule out deep structural burial of the footwall of the Northern Snake Range metamorphic core complex (Nevada, USA): *Tectonics*, no. 43, 48 p.
- Mabey, D.R., Zeitz, I., Eaton, G.P., and Kleinkopf, M.D., 1978, Regional magnetic patterns in part of the Cordillera of the western United States, *in* Smith, R.B., and Eaton, G.P., editors, *Cenozoic tectonics and regional geophysics of the western Cordillera*: Geological Society of America Memoir 153, p. 93–106.
- Manske, S.L., and Paul, A.H., 2002, Geology of a major new porphyry copper center in the Superior (Pioneer) district, Arizona: *Economic Geology*, v. 97, no. 2, p. 197–220.
- Materion, 2023, 2022 Annual Report: Online, <https://investor.materion.com/financials/annual-reports-and-proxies/default.aspx>, accessed May 2023.
- Megaw, P.K.M., Ruiz, J., and Titley, S.R., 1988, High-temperature, carbonate-hosted Ag-Pb-Zn(Cu) deposits of northern Mexico: *Economic Geology*, v. 83, p. 1856–1885.
- Meinert, L.D., 1992, Skarns and skarn deposits: *Geoscience Canada*, v. 19, no. 4, p. 145–162.
- Meinert, L.D., 1995, Compositional variation of igneous rocks associated with skarn deposits—Chemical evidence for a genetic connection between petrogenesis and mineralization, *in* Thompson, J.F.H., editor, *Magma, fluids, and ore deposits*, Mineralogical Association of Canada Short Course Series, v. 23, p. 401–418.
- Meyer, C., Shea, E.P., and Goddard, C.C., Jr., 1968, Ore deposits at Butte, Montana, *in* Ridge, J.D., editor, *Ore deposits of the United States, 1933–1967*, the Granton-Sales Volume, 2: New York, American Institute of Mining, Metallurgical, and Petroleum Engineers, p. 1373–1416.
- Miller, D.M., and Allmendinger, R.W., 1991, Jurassic normal and strike-slip faults at Crater Island, northwestern Utah: *Geological Society of America Bulletin*, v. 103, p. 1239–1251.
- Miller, D.M., and Hoisch, T.D., 1995, Jurassic tectonics of northeastern Nevada and northwestern Utah from the perspective of barometric studies: *Geological Society of America Special Paper* 299, 28 p.
- Miller, D.M., Wooden, J.L., and Wright, J.E., 1989, Mantle-derived Late Jurassic plutons emplaced during possible regional extension of the crust, northwest Utah and northeast Nevada [abs.]: *Geological Society of America Abstracts with Programs*, v. 21, no. 5, p. 117.
- Mills, S.E., and Rupke, A., 2023, Critical minerals of Utah, second edition: *Utah Geological Survey Circular* 135, 47 p., <https://doi.org/10.34191/C-135>.
- Mills, S.E., Rupke, A., and Clark, D.L., 2023, Interim geological map of the Clifton quadrangle, Tooele County, Utah: *Utah Geological Survey Open-File Report* 752DM, 22 p., 2 plates, scale 1:24,000, <https://doi.org/10.34191/OFR-752DM>.
- Mochnacka, K., Oberc-Dziedzic, T., Mayer, W., Pieczka, A., Goralski, M., 2009, New insights into the mineralization of the Czarnów ore deposit (West Sudetes, Poland): *Geologica Sudetica*, v. 41, p. 43–56.
- Mohammad, A.T., and El Kazzaz, Y.A., 2022, Geometry and growth of syn-tectonic plutons emplaced in thrust shear zones—Insights from Abu Ziran pluton, Egypt: *Journal of Structural Geology*, v. 162, 22 p.
- Montanari, D., Corti, G., Sani, F., Del Ventisette, C., Bonini, M., and Moratti, G., 2010, Experimental investigation on granite emplacement during shortening: *Tectonophysics*, v. 484, p. 147–155.
- Moore, W.J., and McKee, E.H., 1983, Phanerozoic magmatism and mineralization in the Tooele 1x2-degree quadrangle, Utah: *Geological Society of America Memoir* 157, p. 183–190.
- Morley, C.K., von Hagke, C., Hansberry, R.L., Collins, A.S., Kanitpanyachoen, W., and King, R., 2017, Review of major shale-dominated detachment and thrust characteristics in the diagenetic zone—Part I, meso- and macroscopic scale: *Earth-Science Reviews*, v. 173, p. 168–228.
- Mosier, D.L., 1996, Descriptive model of upwelling type phosphate deposits, *in* Cox, D.P., and Singer, D.A., editors, *Mineral deposit models*, U.S. Geological Survey Bulletin 1693.
- Muntean, J.L., and Einaudi, M.T., 2001, Porphyry-epithermal transition—Maricunga Belt, Northern Chile: *Economic Geology*, v. 96, no. 4, p. 743–772.
- Musumeci, G., Mazzarini, F., Corti, G., Barsella, M., and Montanari, D., 2005, Magma emplacement in a thrust ramp anticline—The Gavorrano granite (northern

- Apennines, Italy): *Tectonics*, v. 24, no. TC6009, <https://doi.org/10.1029/2005TC001801>.
- Nakano, T., and Ishihara, S., 2003, Geochemical characteristics of the Akiyoshi limestones, Japan, and their bearing on exploration for blind skarn deposits: *Resource Geology*, v. 53, no. 1, p. 29–36.
- Newberry, R.J., Allegro, G.L., Cutler, S.E., Hagen-Levelle, J.H., Adams, D.D., Nicholson, L.C., Weglarz, T.B., Bakke, A.A., Clautice, K.H., Coulter, G.A., Ford, M.J., Myers, G.L., and Szumigala, D.J., 1997, Skarn deposits of Alaska, *in* Goldfarb, R.J., and Miller, L.D., editors, *Mineral Deposits of Alaska: Society of Economic Geologists Monograph Series*, v. 9.
- Nolan, T.B., 1935, The Gold Hill mining District, Utah: U.S. Geological Survey Professional Paper 177, 172 p., 3 plates, geological map scales 1:62,500 (plate 1) and 1:24,000 (plate 2), structure map (plate 3).
- Perry, L.I., and McCarthy, B.M., 1977, Lead and zinc in Utah, 1976: Utah Geological and Mineralogical Survey Open-File Report 22, 525 p., <https://doi.org/10.34191/OFR-22>.
- Presnell, R.D., 1998, Structural controls on the plutonism and metallogeny in the Wasatch and Oquirrh Mountains, Utah, *in* John, D.A., and Ballantyne, G.H., editors, *Geology and ore deposits of the Oquirrh and Wasatch Mountains, Utah: Society of Economic Geologists Guidebook Series*, v. 29, p. 1-9.
- Radtke, A.S., 1985, Geology of the Carlin gold deposit Nevada: U.S. Geological Survey Professional Paper 1267, 120 p.
- Reich, M., and Vasconcelos, P.M., 2015, Geological and economic significance of supergene metal deposits, *in* Reich, M., and Vasconcelos, P.M., editors, *Supergene metal deposits: Elements Magazine*, v. 11, no. 5, p. 305–310.
- Roberts, R.J., Crittenden, M.D.Jr., Tooker, E.W., Morris, H.T., Hose, R.K., and Cheney, T.M., 1965, Pennsylvanian and Permian basins in northwestern Utah, northeastern Nevada, and south-central Idaho: *Bulletin of the American Association of Petroleum Geologists*, v. 49, no. 11, p. 1926–1956.
- Robinson, J.P., 1987, Late Cenozoic high- and low-angle normal faulting and related igneous events in Gold Hill, northern Deep Creek Mountains, western Utah, *in* Kopp, R.S., and Cohenour, R.E., editors, *Cenozoic geology of western Utah: Utah Geological Association publication* 16, p. 429–436.
- Robinson, J.P., 1990, Comprehensive study of the structural geology and regional tectonics of the Gold Hill area, southern Deep Creek Mountains, western Utah: Ithaca, Cornell University, Ph.D. thesis, 312 p.
- Robinson, J.P., 1993, Provisional geological map of the Gold Hill quadrangle, Tooele County, Utah: Utah Geological Survey Map 140, 16 p., 3 plates, scale 1:24,000, <https://doi.org/10.34191/M-140>.
- Robinson, J.P., 2005, Gold Hill, Utah—Polyphase, polymetallic mineralization in a transverse zone, *in* Gloyd, R.W., Park, G.M., Spangler, L.E., editors, *Utah Geological Association Publication* 32, 16 p.
- Robinson, J.P., 2016, The Kiewit gold deposit—A late Miocene (?) low-sulfidation gold-quartz stockwork, Gold Hill mining district, Tooele County, Utah, *in* Comer, J.B., Inkenbrandt, P.C., Krahulec, K.A., and Pinnell, M.L., editors, *Resources and geology of Utah's West Desert, Utah Geological Association Publication* 45, p. 43-58.
- Robinson, J.P., 2023, Provisional geological map of the Gold Hill quadrangle, Tooele County, Utah (GIS reproduction of UGS Map 140 [1993]): Utah Geological Survey Map 301DR, 16 p., 3 plates, scale 1:24,000, <https://doi.org/10.34191/M-301DR>.
- Rowley, P.D., 1998, Cenozoic transverse zones and igneous belts in the Great Basin, western United States—Their tectonic and economic implications: *Geological Society of America Special Paper* 323, 35 p.
- Runyon, S.E., Nickerson, P.A., Seedorff, E., Barton, M.D., Mazdab, F.K., Lecumberri-Sánchez, P., and Steele-MacInnis, M., 2019, Sodic-calcic family of alteration in porphyry systems of Arizona and adjacent New Mexico: *Economic Geology*, v. 114, p. 745–770.
- Scharrer, M., Sandritter, K., Walter, B.F., Neumann, U., Markl, 2020, Formation of native arsenic in hydrothermal base metal deposits and related supergene U6+ enrichment—The Michael vein near Lahr, SW Germany: *American Mineralogist*, v. 105, no. 5, p. 727–744, <https://doi.org/10.2138/am-2020-7062>.
- Seo, J.H., Guillong, M., and Heinrich, C.A., 2012, Separation of molybdenum and copper in porphyry deposits—The roles of sulfur, redox, and pH in ore mineral deposition at Bingham Canyon: *Economic Geology*, v. 107, p. 333–356.
- Shu, Q., Deng, J., Zhang, Z., Wang, Q., Niu, X., Xing, K., Sun, X., Zhang, Z., Zeng, Q., Zhao, H., and Yu, F., 2024, Skarn zonation of the giant Jiama Cu-Mo-Au deposit in southern Tibet: *Economic Geology*, v. 119, no. 1, p. 1–22.
- Sibson, R.H., Moore, J.M., Rankin, A.H., 1975, Seismic pumping—A hydrothermal fluid transport mechanism: *Journal of the Geological Society*, v. 131, no. 6, p. 653–659.
- Silberling, N.J., and Nichols, K.M., 2002, geologic map of the White Horse Pass area, Elko County, Nevada: Nevada Bureau of Mines and Geology Map 132, 1 plate, scale 1:24,000.
- Sillitoe, R.H., 2005, Supergene oxidized and enriched porphyry copper and related deposits: *Economic Geology*, 100th Anniversary Volume, p. 723–768.
- Sillitoe, R.H., 2010, Porphyry copper systems: *Economic Geology*, v. 105, p. 3–41.
- Simmons, S.F., White, N.C., and John, D.A., 2005, Geological characteristics of epithermal precious and base metal

- deposits: *Economic Geology*, 100th Anniversary Volume, p. 485–522.
- Simmons, W.B., Falster, A.U., and Freeman, G., 2020, The Plumbago North pegmatite, Maine, USA—A new potential lithium resource: *Mineralium Deposita*, v. 55, p. 1505–1510.
- Smith, M.T., Rhys, D., Ross, K., Lee, C., and Gray, J.N., 2013, The Long Canyon deposit—Anatomy of a new off-trend sedimentary rock-hosted gold discovery in north-eastern Nevada: *Society of Economic Geologists* v. 108, p. 1119–1145.
- Stacey, J.S., and Zartman, R.E., 1978, A lead and strontium isotopic study of igneous rocks and ores from the Gold Hill mining district, Utah: *Utah Geology*, v. 5, no. 1, p. 1–15.
- Stegen, R.J., 2016, Mineralization and alteration characteristics of the Pine Grove porphyry molybdenum deposit, Beaver County, Utah, in Comer, J.B., Inkenbrandt, P.C., Krahulec, K.A., and Pinnell, M.L., editors, *Resources and geology of Utah's West Desert*: Utah Geological Association Publication 45, p. 59–72.
- Stewart, J.H., Moore, W.J., and Zietz, I., 1977, East-west patterns of igneous rocks, aeromagnetic anomalies, and mineral deposits, Nevada and Utah: *Geological Society of America Bulletin*, v. 88, p. 67–77.
- Stokes, W.L., Hintze, L.F., and Madsen, J.H., Jr., 1961–1963, Geologic map of Utah: Utah Geological and Mineral Survey and University of Utah College of Mines and Mineral Industries, 1:250,000 scale, <https://doi.org/10.34191/Q-2thru5>.
- Su, S., Qin, K., Li, G., Olin, P., and Thompson, J., 2019, Cathodoluminescence and trace elements of scheelite—Constraints on ore-forming processes of the Dabaoshan porphyry Mo-W deposit, South China: *Ore Geology Reviews*, v. 115, p. 1–18.
- Subías, I., Fanlo, I., Mateo, E., Billström, K., Recio, C., 2010, Isotopic studies of Pb–Zn–(Ag) and barite Alpine vein deposits in the Iberian Range (NE Spain): *Geochemistry*, v. 70, no. 2, p. 149–158.
- Tabelin, C.B., Park, I., Phengsaart, T., Jeon, S., Villacorte-Tabelin, M., Alonzo, D., Yoo, K., Ito, M., and Hiroyoshi, N., 2021, Copper and critical metals production from porphyry ores and E-waste—A review of resource availability, processing/recycling challenges, socio-environmental aspects, and sustainability issues: *Resources, Conservation and Recycling*, v. 170, p. 105610.
- Titley, S.R., 1996, Characteristics of high temperature, carbonate-hosted replacement ores and some comparisons with Mississippi Valley-Type ores, in Sangster, D.F., Anderson, G.M., Garven, G., Hagni, R.D., Shelton, K.L., Coveney, R.M. Jr., Gregg, J.M., and Kesler, S.E., editors, *Carbonate-hosted lead-zinc deposits—75th Anniversary Volume*: Society of Economic Geologists Special Publication, v. 4.
- Tomlinson, D.H. Jr., Christiansen, E.H., Keith, J.D., Dorais, M.J., Ganske, R., Fernandez, D., Vetz, N., Sorensen, M., and Gibbs, J., 2021, Nature and origin of zoned polymetallic (Pb-Zb-Cu-Ag-Au) veins from the Bingham Canyon porphyry Cu-Au-Mo deposit, Utah: *Economic Geology*, v. 116, no. 3, p. 747–771.
- U.S. Geological Survey, 2017, Mineral commodity summaries 2017: U.S. Geological Survey, 202 p., <https://doi.org/10.3133/70180197>.
- U.S. Geological Survey, 2023, Mineral commodity summaries 2023: U.S. Geological Survey, 210 p., <https://doi.org/10.3133/mcs2023>.
- Utah Geological Survey, 2023, Utah Mineral Occurrence System (UMOS) database, 2023 update: Utah Geological Survey Open-File Report 757, 11 p., <https://doi.org/10.34191/OFR-757>.
- Vogel, T.A., Cambray, F.W., and Constenius, K.N., 2001, Origin and emplacement of igneous rocks in the Wasatch Mountains, Utah: *Rocky Mountain Geology*, v. 36, no. 2, p. 119–162.
- Wang, X., Zheng, Y., Yu, P., Chen, X., Wu, Y., Huang, Y., Long, L., Shu, L., Chen, M., and Guo, L., 2024, Temperature as a major control on Cd enrichment in a skarn system—A case study of the Yiliu Pb-Zn-As deposit, south China: *Ore Geology Reviews*, v. 165, <https://doi.org/10.1016/j.oregeorev.2024.105920>.
- Welsh, J.E., and Bissell, H.J., 1979, The Mississippian and Pennsylvanian (Carboniferous) systems in the United States—Utah: U.S. Geological Survey Professional Paper 1110-Y, 35 p.
- Whelan, J.A., 1970, Radioactive and isotopic age determinations of Utah rocks: *Utah Geological and Mineralogical Survey Bulletin* 81, 57 p., <https://doi.org/10.34191/B-81>.
- White, E., 2023, Petrogenetic evolution during cordilleran orogenesis—Constraints from the North and South American cordilleras: College Station, Texas, Texas A&M University, Ph.D. dissertation, 662 p.
- White, N.C., and Hedenquist, J.W., 1990, Epithermal environments and styles of mineralization—Variations and their causes, and guidelines for exploration: *Journal of Geochemical Exploration*, v. 36, p. 445–474.
- Whitmeyer, S.J., and Karlstrom, K.E., 2007, Tectonic model for the Proterozoic growth of North America: *Geosphere*, v. 3, no. 4, p. 220–259.
- Willden, R., 2006, Goldstrike mining district, Washington County, Utah, in Bon R.L., Gloyd, R.W., and Park, G.M., editors, *Mining districts of Utah*: Utah Geological Association Publication 32, p. 458–476.
- Williams, P.J., Barton, M.D., Johnson, D.A., Fontbote, L., de Haller, A., Mark, G., Oliver, M.H.S., Marschik, R., 2005, Iron oxide copper-gold deposits—Geology, space-time distribution, and possible modes of origin: *Economic Geology*, v. 100, p. 371–405.

- Wones, D.R., 1989, Significance of the assemblage titanite + magnetite + quartz in granitic rocks: *American Mineralogist*, v. 74, p. 744–749.
- Wright, J.E., and Wooden, J.L., 1991, New Sr, Nd, and Pb isotopic data from plutons in the northern Great Basin—Implications for crustal structure and granite petrogenesis in the hinterland of the Sevier thrust belt: *Geology*, v. 19, p. 457–460.
- Wu, Y.F., Evans, K., Fisher, L.A., Zhou, M.F., Hu, S.Y., Fougereuse, D., Large, R.R., and Li, J.W., 2020, Distribution of trace elements between carbonaceous matter and sulfides in a sediment-hosted orogenic gold system: *Geochimica et Cosmochimica Acta*, v. 276, p. 345–362.
- Xu, X., Xu, X., Szmihelsky, M., Yan, J., Xie, Q., Steele-MacInnis, M., 2023, Melt inclusion evidence for limestone assimilation, calc-silicate melts, and “magmatic skarn”: *Geology*, v. 51, p. 491–495, <https://doi.org/10.1130/G50893.1>.
- Yonkee, W.A., Dehler, C.D., Link, P.K., Balgord, E.A., Keeley, J.A., Hayes, D.S., Wells, M.L., Fanning, C.M., and Johnston, S.M., 2014, Tectono-stratigraphic framework of Neoproterozoic to Cambrian strata, west-central U.S.—Protracted rifting, glaciation, and evolution of the North American Cordilleran margin: *Earth Science Reviews*, v. 135, p. 59–95.
- Yonkee, W.A., and Weil, A.B., 2015, Tectonic evolution of the Sevier and Laramide belts within the North American Cordillera orogenic system: *Earth Science Reviews*, v. 150, p. 531–593.
- Zhan, Q., Gao, X., Meng, L., Zhao, T., 2021, Ore genesis and fluid evolution of the Sandaozhuang supergiant W-Mo skarn deposit, southern margin of the North China Craton—Insights from scheelite, garnet and clinopyroxene geochemistry: *Ore Geology Reviews*, v. 139B, p. 1–20.
- Zucchetti, S.C., 1958, The lead-arsenic-sulfide ore deposit of Bacu Locci (Sardinia, Italy): *Economic Geology*, v. 53, no. 7, p. 867–876.
- Zuza, A.V., Thorman, C.H., Henry, C.D., Levy, D.A., Dee, S., Long, S.P., Sandberg, C.A., and Soignard, E., 2020, Pulsed Mesozoic deformation in the Cordilleran hinterland and evolution of the Nevadaplano—Insights from the Pequop mountains, NE Nevada: *Lithosphere*, v. 2020, no. 1, <https://doi.org/10.2113/2020/8850336>.

APPENDICES

APPENDIX A
Historical Drilling Compilation

Link to supplemental data:

https://ugspub.nr.utah.gov/publications/special_studies/ss-175/ss-175-a.zip

APPENDIX B

Surface Geochemistry

Link to supplemental data:

https://ugspub.nr.utah.gov/publications/special_studies/ss-175/ss-175-b.zip

APPENDIX C

Drillhole Geochemistry

Link to supplemental data:

https://ugspub.nr.utah.gov/publications/special_studies/ss-175/ss-175-c.zip

APPENDIX D

Geophysics Data

Link to supplemental data:

https://ugspub.nr.utah.gov/publications/special_studies/ss-175/ss-175-d.zip